ISSN 1173-5996

Performance of Gypsum Plasterboard Assemblies Exposed to Real Building Fires

by
Bevan Jones

Supervised by

Associate Professor Andrew Buchanan
Associate Professor Peter Moss
and
J T (Hans) Gerlich

Fire Engineering Research Report 01/4
March 2001

This report was presented as a project report as part of the M.E. (Fire) degree at the University of Canterbury

School of Engineering
University of Canterbury
Private Bag 4800
Christchurch, New Zealand

Phone 643 364-2250
Fax 643 364-2758
www.civil.canterbury.ac.nz

ABSTRACT

The performance of gypsum plasterboard assemblies is typically evaluated in accordance with standardised test methods such as BS476, AS1530 or ASTM E119. Standard time-temperature curves give good comparison between tested materials. However, they are generally less severe than a typical short duration compartment fire, they do not have a decay phase, and may be conservative for long duration fires. It is not common knowledge that test time-temperature relationships, such as ISO834, have not significantly changed since they were originally formulated in the early 1930's.

Full-scale compartment testing based on typical residential scenarios conducted as part of this study, revealed that temperatures within a compartment can far exceed those of standard time-temperature curves within several minutes of ignition.

Pilot-scale furnace testing to non-standard time-temperature curves has revealed that the performance of light framed gypsum plasterboard assemblies is highly dependent on the severity of the fire exposure. A system that has achieved a fire resistance rating of 60 minutes failed within 30 minutes to a fire exposure that would represent a moderate compartment fire.

Current fire engineering designs often use sophisticated evacuation models to calculate minimum escape times required for safe evacuation of occupants. These evacuation times typically fall in the range from 15 – 60 minutes. The suitability of protecting escape routes using barriers rated against a standard fire test is questioned.

SAFIR, a powerful finite element program, has been employed to predict the thermal behaviour of various gypsum plasterboard assemblies exposed to a range of non-standard fires. Results from the computer modelling are compared with several full and pilot scale furnace tests. It was found that the model calibrated to results from standard ISO834 furnace testing provided reasonable predictions of temperatures within assemblies exposed to a moderate fire. Temperature predictions of assemblies exposed to severe fires were poor.

ACKNOWLEDGEMENTS

The experimental program of this report was conducted at the fire research facilities of the Building Research Association of New Zealand (BRANZ), Wellington. Financial support was provided by the Foundation for Research, Science and Technology and Winstone Wallboards Ltd.

Completion of the project would not have been possible without the assistance of the following people and organisations:

I would like to thank my supervisors, Dr Andrew Buchanan and Dr Peter Moss of the University of Canterbury and Hans Gerlich of Winstone Wallboards Ltd for their inspiration, guidance and enthusiasm.

All of the staff at BRANZ were helpful, especially with provision of an office and access to resources. In particular I would like to thank Peter Whiting for welcoming me and making me feel at home during my time at BRANZ, Peter Collier for sharing his knowledge, experience and guidance, Merv, Rik and Brett for their help with testing.

Winstone Wallboards Ltd have been most generous with financial assistance and provision of materials for testing. With special mention to Peter Collins of the Christchurch branch for the provision of an office and for the on-site experience.

John Mason of Sinclair Knight Merz for his guidance and further development of his pre-processor in his own time so that I could proceed with the modelling.

The New Zealand Fire Service for allowing me to participate in the fire investigation course and compartment burns.

I would also like to thank Hamish and Gabrielle for allowing me to live in their lounge while I was studying at BRANZ, and Ashley Peterson for proof reading my work and advice throughout the year.

Last but foremost I would like to thank my girlfriend Narelle, and my family for their support, patience and understanding, as my time with them has been very limited for the past year.

TABLE OF CONTENTS

LIST OF FIGURES

LIST OF TABLES

1 INTRODUCTION

1.1 Background

Fire resistant barriers play an important role in maintaining building integrity and reducing the spread of fire from the room of origin to adjacent compartments. Building codes typically require compartments within a building to be separated by continuous fire rated barriers, such as drywall construction. Drywall construction is an efficient and cost effective method of achieving a flexible partition assembly within a commercial or residential building. The traditional method of drywall construction in New Zealand is with light timber framing (LTF) and sheet material linings. However, there has been an increasing demand in the commercial arena for prefabricated light steel frame systems (LSF).

The flexibility of drywall construction is the ability to specify the type and thickness of the linings and the framing configuration in order to achieve specific performance requirements. Such as appearance of the finished wall, impact resistance, water resistance, sound control or fire resistance while maintaining a light form of construction. Paper-faced gypsum plasterboard linings are most commonly used particularly when a fire resistance rating is required.

Rated fire barriers are designed to control the fire within the compartment of origin for an extended period of time, which is usually specified, to allow safe egress of building occupants. Additionally, the barriers may provide sufficient time for the fire service to extinguish the fire before it can spread to other compartments. The extent to which these barriers provide that protection is measured as the *fire-resistance rating.*

In New Zealand, the fire resistance of barriers is determined by physical testing or by seeking an opinion from a fire expert or laboratory. Present regulations require extensive testing both for initial acceptance and as a means of gathering data to support variations by opinion (Collier 2000). The testing of drywall construction is generally in the form of full-scale fire testing against standard time-temperature furnace conditions. Such standardised furnace tests will provide good comparative

data for systems tested under identical conditions. However, standard fire resistance tests do not accurately model the performance of a building element when exposed to certain types of realistic fires.

With the advent of performance-based codes and performance-based fire safety design, coupled with the cost and time requirements of full scale testing, there exists a need to advocate validated analytical models as a means of predicting the performance of light frame construction.

1.2 Aim of this Project

This project was undertaken as the initial stage in developing a commercially available software package to predict the thermal and structural behaviour of gypsum plasterboard assemblies with steel or timber framing exposed to a user defined time-temperature curve.

The three specific objectives were:

- To observe and evaluate the thermal behaviour of typical gypsum plasterboard wall assemblies subjected to standard and non-standard time-temperature curves.

- To evaluate the ability of the SAFIR program to model the performance of the tested systems.

- To compare realistic compartment fires with standard and non-standard furnace fires.

In order to achieve the above objectives the following were performed:

- Conduct a literature review on recent work in this field of study;
- Familiarisation of the computational program and input requirements;
- Review the thermal properties and parameters of relevant materials;

- Evaluate the behaviour of materials under elevated temperatures from both literature and experimental work;
- Calibrate the input variables within the model to provide comparative results with standard ISO834 experimental results;
- Evaluate the validity of predictions from the model when extended to non-standard fire conditions.

2 LITERATURE REVIEW

2.1 General

This section provides a brief overview of previous work performed by various researchers in this field of study. Literature was obtained from the School of Engineering library, University of Canterbury, and the building industry database at BRANZ.

2.2 Previous Work in this Field

2.2.1 Collier, P.C.R.

Collier (2000) developed a software package for predicting the likely fire resisting performance of non-loadbearing or loadbearing walls subjected to a standard fire resistance test, or real fire conditions.

Prediction of the performance of fire barriers employed finite difference techniques for heat conduction within linings and also for convection and radiation on the boundaries and cavity. A user-friendly interface was developed for input of the parameters, from the lining properties and dimensions, stud sizes, wall height and the stud material, either timber or steel. The ability of the user to input time-temperature relationships other than standard curves is also incorporated. Algorithms for the charring of timber and the reduction of steel strength and stiffness at elevated temperatures are included to determine a structural failure condition for the studs.

Collier's model provides reliable prediction of the thermal performance and insulation failure of cavity walls in both standard and real fires. The model is able to conservatively predict the structural performance of both steel and timber studs. However, beyond steel temperatures of approximately 400°C, measured and predicted values tend to diverge.

Collier also extended the software to predict the performance of cavity walls in a 3.6 m x 2.4 m x 2.4 m high compartment fire with wood pallets as fuel. It was found that the model performs similarly given that the actual time-temperature curve from the

room burn can be used as input. Using input time-temperature curves based on design fire principles indicated that for the one trial conducted, predicted fire exposure may be conservative.

Collier also reported that the moisture content of the gypsum had a noticeable effect on the enthalpy and therefore makes a significant difference to the predictions of structural and insulation failure.

2.2.2 Thomas, G.C.

Thomas (1997) used commercially available software packages to predict the thermal and structural behaviour of timber framed gypsum plasterboard assemblies. Time-temperature curves were obtained from COMPF-2, a compartment fire model developed by Brabrauskas and Williamson (1978a and 1979). Thomas used these curves as input for the heat transfer model TASEF (Sterner and Wickstrom 1990), which is a two-dimensional model designed for fire applications. To evaluate the structural performance of the heated wall/floor system, Thomas employed a general-purpose finite element program ABAQUS (Hibbit, Karlsson and Sorenson 1994).

Thomas used several full and pilot scale furnace tests conducted at BRANZ to calibrate his model. Two non-standard pilot-scale furnace tests where also performed to evaluate the models ability to predict the behaviour of an assembly subjected to non-standard fire conditions. He found that, through calibration of the thermal properties of materials within the model, TASEF was able to predict the evolution of temperature through an assembly exposed to the standard fire with reasonable accuracy.

Thomas' modelling also provided good prediction of temperatures within timber studs. However, there was insufficient data available to determine the accuracy of the temperature prediction within timber floor joists. For the first non-standard fire test resembling a fuel surface controlled fire, good predictions were obtained. However, the model made poor predictions of the assembly's behaviour when subjected to the second non-standard fire, which resembled a hydrocarbon pool fire.

Sensitivity studies performed by Thomas revealed that variation in the value of the heat transfer coefficients within a reasonable range on the fire side of the wall had little influence on the predictions of the model. Limitations of the model, such as its inability to predict ablation and moisture movement were overcome by manipulation of material properties.

Thomas also extended his modelling to prediction of temperature evolution through the walls and floors of a full-sized timber framed compartment, measuring 3.9 m by 3.8 m and 3.12 m high. Although temperature measurements were terminated before maximum compartment temperatures were reached. It was found that the model provided reasonably poor predictions of the actual temperature history through the building components.

2.2.3 Gerlich, J.T.

Gerlich (1995) used TASEF along with the calibrated thermal properties defined by Thomas, to develop a model for predicting the performance of loadbearing LSF systems exposed to fire. Gerlich modified existing methods of predicting the structural behaviour of cold-formed steel sections at ambient temperatures for elevated temperature conditions. To evaluate the performance of loadbearing LSF drywall systems, two standard ISO834 and one non-standard full-scale fire tests were conducted at BRANZ.

Gerlich found that his model could predict the performance of systems exposed to standard conditions with 80%-90% accuracy. However, agreement between predictions and results for the more severe "real" fire were much less accurate.

2.2.4 Clancy, P.

Clancy has produced several studies on the prediction of the behaviour of timber framed plasterboard systems. Clancy (1999) describes the complex two-dimensional thermal model ADIDRAS, which is capable of accurately predicting the thermal behaviour of LTF gypsum plasterboard systems, exposed to standard fire conditions.

Novel features inherent in ADIDRAS are:

1. Radiation analysis for cavities with re-entrant corners and smoke.
2. Simple modelling for the transfer of heat by the movement of moisture.
3. Modelling for the sloughing of individual sheets of gypsum plasterboard.
4. Implicit finite difference procedures that, for the analysis of thermal diffusion alone, are fast, numerically stable and independent of time step.

When coupled with the structural model developed by Young (2000), predictions of time to failure for loadbearing and non-loadbearing assemblies gave good agreement with eight full-scale furnace tests conducted for the purpose of his study and with results from experiments of other studies. Validation of the time to failure model has only been done for standard fire curves. Performance predictions under non-standard conditions have yet to be performed.

2.2.5 Forintek Canada Corporation

Mehaffy *et al* (1994) developed a simple two-dimensional computer model to predict heat transfer through gypsum board/wood stud walls exposed to fire. Predictions were validated with four reduced-scale and two full-scale furnace tests. Predictions for finish ratings, time to onset of charring of the studs and time for the failure of the assembly, due to heat transmission, were shown to be in reasonable agreement with results of standard furnace tests.

Takeda and Mehaffy (1998) describe the two-dimensional computer model WALL2D, for predicting heat transfer through uninsulated wood-stud walls protected by gypsum board. WALL2D's predictions for time-dependent temperature profiles in wood-stud walls were in good agreement with the results of both small and full-scale standard furnace testing. WALL2D is a further refinement of Mehaffy *et al's* (1994) work, which incorporates three sub-models describing heat transfer through gypsum boards, through wood studs and across the cavity. No validation of the model was performed in terms of predicting assembly behaviour in non-standard fires.

2.2.6 National Research Council Canada

Sultan (1996) describes a one-dimensional model for predicting heat transfer through uninsulated non-loadbearing steel-stud gypsum board wall assemblies. Two uninsulated non-loadbearing full-scale furnace tests were performed to validate model predictions. In order to reduce the complexity of the model Sultan based his mathematical model on several influential assumptions. Such as considering heat transfer in only one dimension across the cavity, and that the heat leaving the fire-exposed lining and entering the cavity was considered to be totally absorbed by the gypsum board surface on the opposite side of the cavity. The combination of many assumptions led to conservative predictions by Sultan's model.

Sultan *et al* (1999, 2000) extended the one-dimensional heat transfer model described in Sultan (1996), to predict the loadbearing performance of steel stud gypsum board assemblies with cavity insulation. Calibration of the input thermal properties within the model was performed in order to achieve reasonable predictions of the heat transfer across the assembly and to simulate structural performance exhibited in full-scale standard furnace testing.

2.2.7 Tratek – Swedish Institute for Wood Technology Research

Konig and Walleij (1999) describe a model that calculates the loadbearing capacity of timber framed wall and floor assemblies with cavity insulation subjected to standard fire exposure. The design model consists of a charring model giving a simplified rectangular cross section, and a mechanical model describing the strength and stiffness properties of the residual cross section. The design model presented by Konig and Walleij takes into account the different charring rates that exist during the time of protection provided by the lining, and during the post-protection phase after failure of the exposed lining. However, validation of the models predictions is not given, and it is assumed that this is still to be performed.

2.2.8 Cooper, L.Y.

Cooper (1997) developed GYPST, a FORTRAN subroutine to simulate the thermal response of steel-stud/gypsum board assemblies exposed to fire. Two full-scale standard furnace tests were performed to verify predictions from the model. Good comparisons were achieved between predicted and experimental results.

2.3 Findings

Although there has been significant research and model development in this field, it is a general conclusion that attempts by researchers to model the behaviour of gypsum plasterboard assemblies subjected to realistic building fires remains inconclusive. Several of these models previously mentioned have the capability to replace some fire resistance testing. However, with the implementation of performance-based design in many fire codes, there exists the need to provide a design tool that will allow the user to accurately predict the behaviour of assemblies exposed to realistic fire situations.

3 COMPUTATIONAL MODEL

The computational model employed in this study to predict the thermal behaviour of the tested gypsum plasterboard assemblies was SAFIR2001.

3.1 Computer Program

3.1.1 SAFIR

SAFIR is a special purpose computer program for the analysis of structures under ambient and elevated temperature conditions. The program, which is based on the Finite Element Method (FEM), can be used to study the behaviour of one, two and three-dimensional structures. The program (SAFIR) was developed at the University of Liège, Belgium, and is today viewed as the second generation of structural fire codes developed in Liège (Franssen *et al* 2000).

The FEM was originally developed as a numerical method for stress analysis. It was very quickly applied to heat transfer analysis, and is now used for fluid mechanics, bio-mechanics, hydraulics, and many other problems too complex to be solved analytically. The recent rapid growth in the power of desktop computers has enabled the FEM to evolve from a tool that was difficult to use, expensive, and rarely used by most engineers, to a tool that is now commonly used for analysis. The continuing increase of computing power can only widen the use of finite element analysis (Mason 2000).

As a finite element program, SAFIR accommodates various elements for different idealisation, calculation procedures and various material models for incorporating stress-strain behaviour. Two-dimensional finite elements used are triangular (3 node) or quadrilateral (4 node). Only linear elements may be used for thermal analysis. Three-dimensional elements available include solid elements (six or eight nodes), shell, beam, and truss elements.

There are a number of standard materials available in the program (most based on Eurocode 2 and 3), with thermal and mechanical properties for these materials generated automatically within the program code. In the original model one user-defined material could be selected with properties assigned by the user. However, for the purpose of this project the number of available user-defined materials was extended to five, due to the presence of multiple materials within a plasterboard assembly with temperature dependent properties that vary significantly from default properties within the program.

Two standard time-temperature distributions are incorporated into the program, ISO834 and ASTM E119. User-defined time-temperature distributions can also be specified, which allows interaction with the results from compartment fire models, such as CFAST, or the use of standard time-temperature distributions not included in the program (e.g. Eurocode parametric fires).

Within the section boundaries, the program models heat transfer by conduction. Heat transfer by convection and radiation are modelled at the boundaries. Internal cavities are permitted in two-dimensional analysis, with radiation and convection modelled along void boundaries. SAFIR98a only allowed heat transfer to be modelled through a completely closed void, totally surrounded by boundary elements. However, further modifications to the program by Franssen *et al* led to the ability to model heat transfer across an open void defined by an axis of symmetry at the cavity opening. This feature is now incorporated in SAFIR2001.

The SAFIR model is defined in a series of text files that can be created or edited with any standard text editor. The results of the analysis are presented in text files. Pre-processing and post-processing capability are available in separate programs. This process of creating input files can be tedious and prone to error, and there is no feasible means of checking and verifying the accuracy of the data. Therefore, the pre-processing program SAPPHIRE developed by Mason (2000) was employed to facilitate preparation of the input data files.

3.1.2 SAPPHIRE Pre-Processor

SAPPHIRE is an interactive program for the creation and modification of SAFIR data files for two-dimensional thermal analysis. Standard sections with a pre-defined mesh facilitate the creation of new SAFIR models. The standard sections available include steel I-sections, hollow core concrete slabs (Dycore), and profiled metal deck composite concrete slabs (Hi-Bond). Steel section libraries available include Australian, American, and European I-sections. These sections can have profile insulation or box insulation added. Dycore and Hi-Bond models include varying slab thickness.

A basic set of CAD-like tools allow the user to interactively manipulate the model, enabling refinement of the mesh, or allowing the user to quickly modify the standard models. When modifying the finite element mesh, the user can delete elements, sub-divide elements, and create new elements by copying existing elements or drawing new elements on the screen. Further development of the program by Mason during the course of this project provided a tool that allows the user to draw sections, save them in a library file and then input them as block sections into another input file. This feature is very useful for the development of cavity wall systems, as it allows the user to define their own library of steel/timber studs, and linings, which could then be combined to form an entire section.

Any existing two-dimensional thermal SAFIR98a data file can be opened in SAPPHIRE and further manipulated. Currently, input files for SAFIR2001 cannot be supported by SAPPHIRE due to the change in input file format for the later version of SAFIR. However, input files from SAPPHIRE can be easily modified so that they are recognised in SAFIR2001. Work to modify SAPPHIRE to accept both forms of input format is currently under way. The pre-processor can be used interchangeably with the other input methods, allowing the user to choose the method that is most convenient for that particular input task. For example, minor modifications to the data file may be made more conveniently with a text editor. Doing so does not prevent the user from subsequently editing the same file with SAPPHIRE.

SAPPHIRE allows the user to apply the ISO834 or ASTM E119 time-temperature curves to any selected element. SAFIR also supports a user-defined time-temperature curve. The pre-processor takes advantage of this by automatically generating time-temperature data for ISO834 fires with a linear decay phase and Eurocode parametric fires calculated from parameters provided by the user.

All materials supported by SAFIR are available within SAPPHIRE. Consultation with Mason during the project led to modification of the pre-processor to support five user-defined materials. The properties of these user-defined materials are plotted on screen as they are entered to facilitate confirmation of the data. Material properties can be applied to any selected element.

Other features such as zoom, pan, element and node number viewing aid the user when constructing and modifying sections. Figure 3-1 shows the main window of SAPPHIRE.

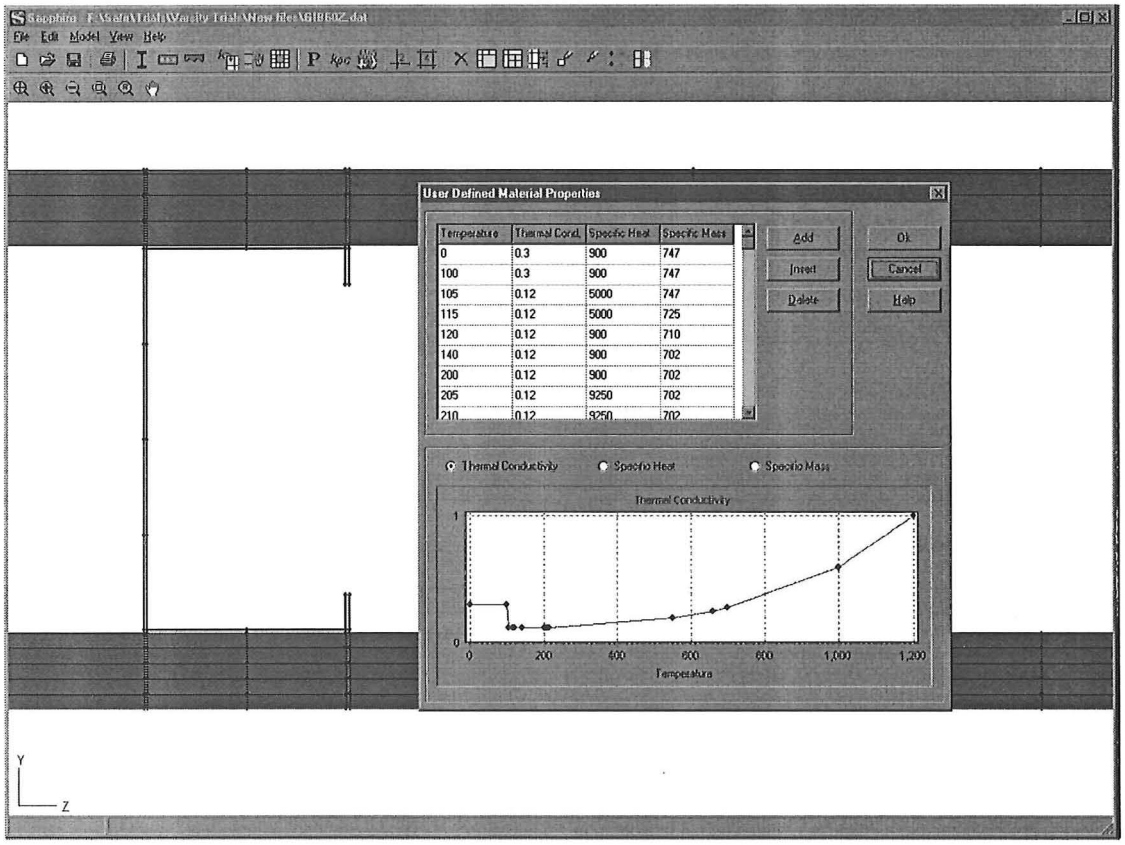

Figure 3-1: Main window of SAPPHIRE with properties window open.

3.1.3 DIAMOND Post-Processor

Diamond is a post-processing graphics package developed by the authors of SAFIR. The current version is DIAMOND2001. It allows the user to plot temperature contours from a two and three-dimensional analysis. DIAMOND can also support the results from a mechanical analysis of a member by plotting bending moments, deflections, etc. Temperature contours can be animated to show the evolution of temperature through the section with time. A chart function is also available to plot a nodal/elemental temperature history.

3.1.4 Input Parameters

3.1.4.1 Thermal Properties

For the thermal analysis of a section comprised of user-defined materials, SAFIR requires thermal properties that define the materials behaviour when exposed to elevated temperatures. These temperature dependent properties are density, ρ (kg/m^3), specific heat, c_p (J/kg.K), and thermal conductivity, k (W/m.K). Internally, SAFIR calculates the specific volumetric enthalpy, e (J/m^3), defined as:

$$e = \int_{T_0}^{T} \rho c_P dT \qquad \textbf{[3-1]}$$

This ensures that a peak in the specific heat is not missed if consecutive time steps lie before and after the peak.

3.1.4.2 Thermal Coefficients

Each material used to define the section requires a convective coefficient, h (W/m^2.K), for both the exposed and unexposed faces as well as a relative emissivity value for the exposed surface. Although these coefficients vary throughout the duration of exposure, SAFIR requires only a constant value that will represent the heat transfer characteristics of the materials surface for the duration of fire-exposure.

3.1.4.3 Assumptions

- The specific heat of air is typically three orders of magnitude lower than solid materials, so this is ignored in the model.
- It is also assumed that there is no flow of air into and out of the cavity.
- The temperature within the cavity is assumed to be uniform, and is determined by the total convective flux from the elements surrounding the cavity.
- Properties are assumed to be homogeneous throughout materials.

3.2 Assembly Description

The assemblies tested in this study are proprietary systems available from Winstone Wallboards Ltd. Other available systems are detailed in Winstone Wallboards Ltd (1997).

3.2.1 Steel Stud System

The steel stud assemblies are based on the two-way systems GBS30 and GBS60 (WWB Ltd 1997). These assemblies consist of 63 x 34 x 0.55 mm thick steel channel sections (described in Section 5.2.1), with a centre line spacing of 600 mm. One layer of 12.5 mm gypsum plasterboard is screwed at 300 mm centres to both sides of the stud, as shown by Figure 3-2.

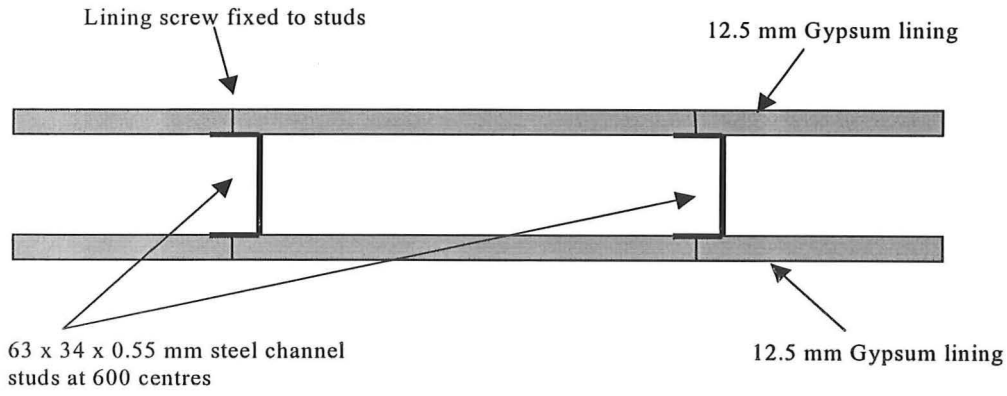

Figure 3-2: Description of steel stud assembly.

For the GBS30 system, 12.5 mm GIB® standard board is used, while GIB® Fyreline is used to line the GBS60 system.

3.2.2 Timber Stud System

Dummy studs used in the experimental phase of this project were constructed from New Zealand Radiata pine. The typical timber framing size used in light framed assemblies is nominal 94 x 44 mm wood members. A 500 x 63 x 44 mm dummy stud was used in the specimens of this study so that both steel and timber framing members could be tested in the same assembly. This reduced the number of required tests and exposed both types of framing to identical conditions. A schematic of the timber dummy stud positioned within the steel studs is given in Section 5.2.3.

3.3 Section Discretisation

3.3.1 Steel Stud Assembly

The modelled assembly consists of a steel stud with two 12.5 mm thick gypsum board linings extending 300 mm to either side of the stud centerline, as shown by Figure 3-3. Either end of the assembly is bound by an axis of symmetry, which allows calculation of heat transfer across the open void.

Due to the high variability of the thermal properties with temperature, of materials within the assembly, a very "fine" finite element mesh was initially assigned to the section, illustrated by Figure 3-3. This mesh consisted of 484 nodes forming 399 elements.

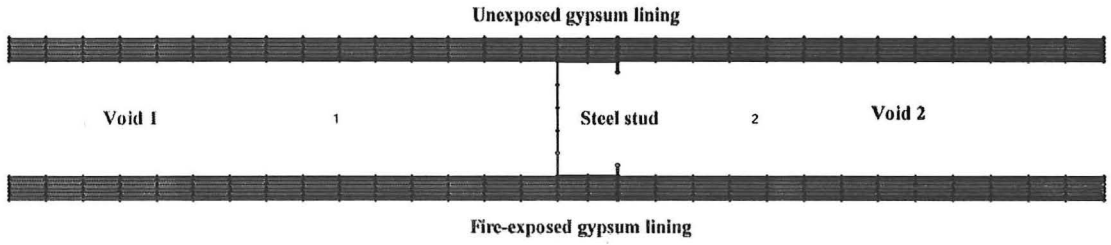

Figure 3-3: Finely discretised gypsum board/steel stud assembly.

However, run times for the "fine" section proved to be too long and output files were tedious to work with due to the large number of elements, so a "coarse" finite element mesh was used, shown by Figure 3-4. This section was defined by 185 nodes forming 140 elements.

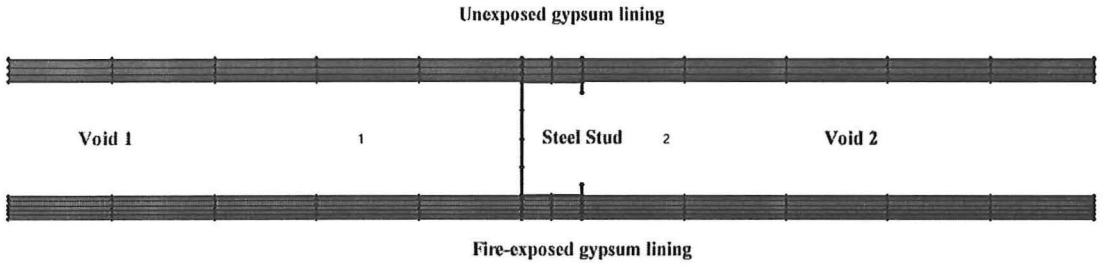

Figure 3-4: Coarsely discretised gypsumboard/steel stud assembly.

Figure 3-5 shows the discretisation of the steel section and lining in order to maintain continuity of the finite element mesh.

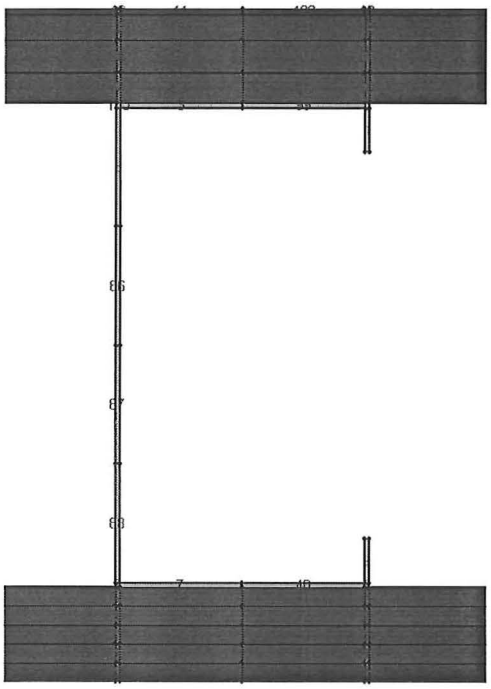

Figure 3-5: Close-up of gypsum board/steel stud assembly.

3.3.1.1 Timber Stud Assembly

The modelled timber stud assembly consisted stud with 300 mm of 12.5 mm gypsum plaster board either side of the centreline of the stud, as shown by Figure 3-6.

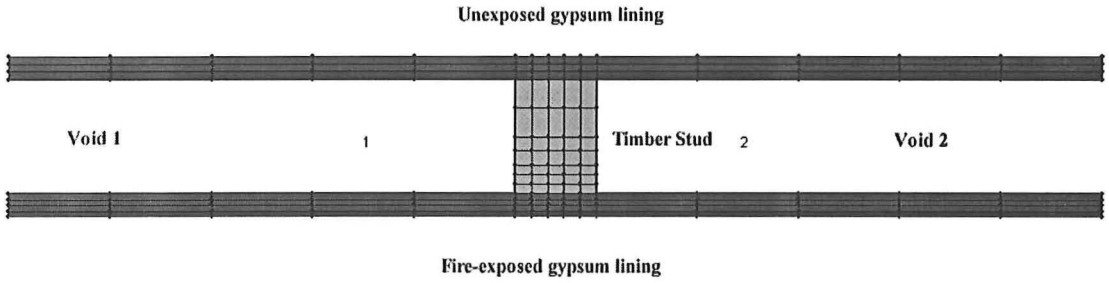

Figure 3-6: Coarsely discretised gypsum board/timber stud assembly.

Figure 3-7 shows the discretisation of the dummy stud and linings with numbering of the finite elements.

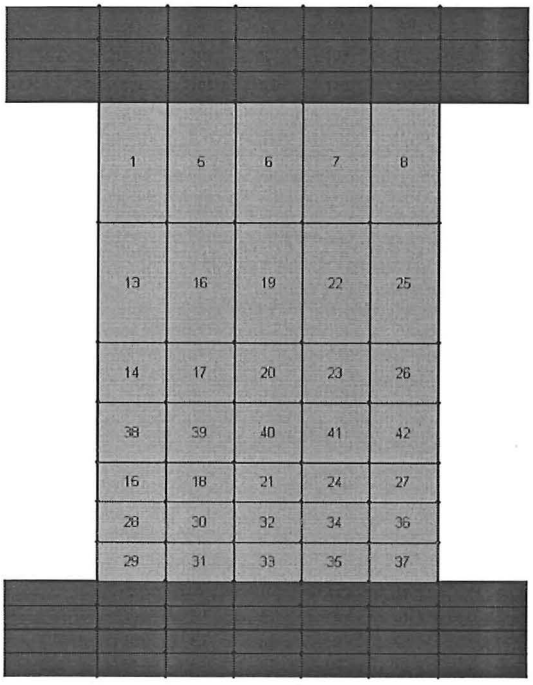

Figure 3-7: Close up of dummy stud/gypsum lining section.

The mesh for this assembly consisted of 180 nodes to form 140 elements. Generally the mesh in the fire-exposed lining was much finer than that of the unexposed lining because of the rapid changes in temperature within the exposed board. A much

coarser grid could be used in the unexposed lining because thermo-physical changes within the board are occurring over a much greater time scale. A similar approach has been adopted for the timber stud as shown by Figure 3-6, where the mesh gets coarser as distance from the exposed lining increases. Table 3-1 summarises the finite element mesh used for each assembly. Based on experience from the steel section, only one "coarsely" discretised assembly was used for the timber stud assembly.

Table 3-1: Element discretisation of Assemblies.

Section	Steel stud with "fine" mesh	Steel stud with "coarse" mesh	Wood stud with "coarse" mesh
Exposed lining	192	56	45
Stud	15	14	35
Unexposed lining	192	70	60
Total No. of Elements	399	140	140

3.4 Influence of Changes in Model on Results

3.4.1 Discretisation of Assembly

Results from the analysis of the 60 minute system with both the "course" and "fine" mesh is given in Figure 3-8, which shows that there is very little difference between the temperature predictions when a "fine" or "course" finite element mesh is applied to the modelled section. Although some deviation is observed between 20 and 30 minutes, this has no effect on the temperatures beyond 30 minutes, which are of more importance, as this is the region where failure of the assembly is expected. Therefore, use of the "coarsely" discretised section should accurately represent predictions from the model.

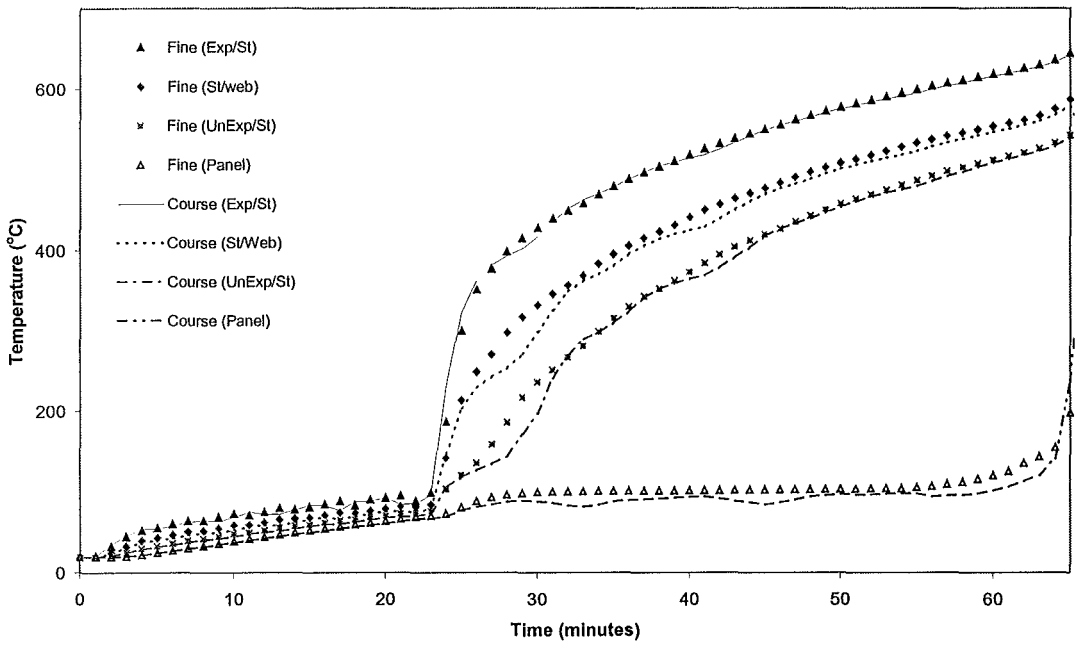

Figure 3-8: Comparison of predicted temperatures from a "course" and "fine" finite element mesh.

3.4.2 Thermal Coefficients

The locations in the assembly where temperatures have been derived are described in Figure 5-15.

3.4.2.1 Relative Emissivity

The relative emissivity of the fire-exposed gypsum board was varied between values of 0.6 to 1.0, with a value of 0.8 used in the modelling. Predicted temperatures given in Figure 3-9 are from modelling the 60 minute system. Figure 3-9 shows that the predicted temperatures of the cavity face of the exposed lining are mostly influenced by changes in the relative emissivity between temperatures of 100°C to approximately 500°C.

Deviation in temperature of the cavity face of the exposed lining due to variation of the relative emissivity is also reflected on the cavity face of the unexposed lining.

However, Figure 3-9 indicates that changes in the relative emissivity have negligible influence on temperatures of the ambient side of the assembly.

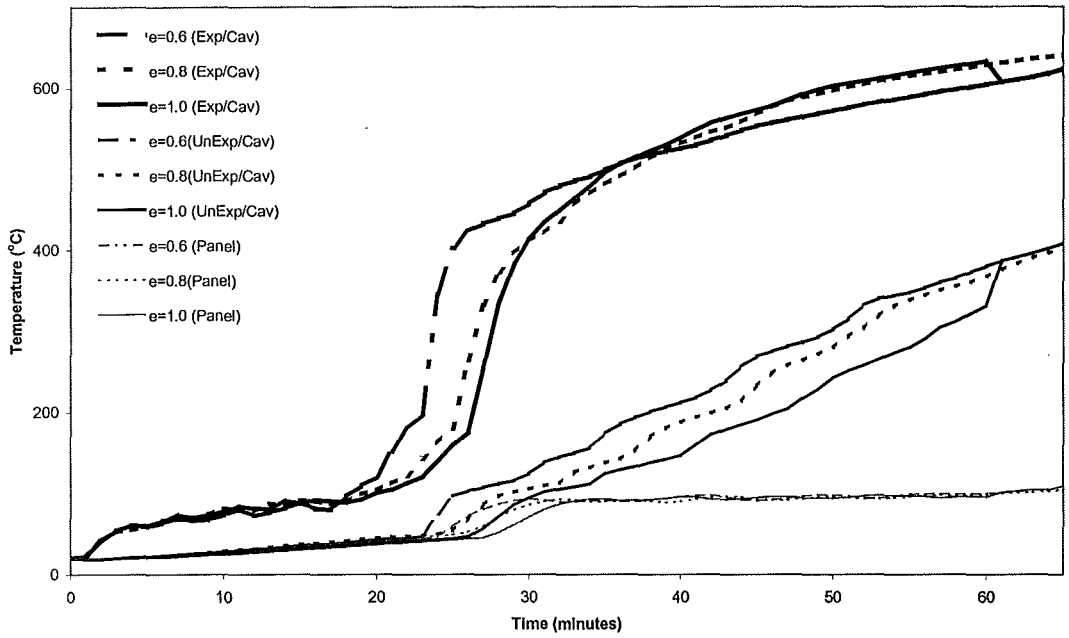

Figure 3-9: Temperature predictions for relative emissivity of 0.6, 0.8, and 1.0.

Therefore, variation of the relative emissivity of the exposed face may cause predicted temperatures within the cavity to vary. Temperatures of the unexposed face, which indicate thermal failure of the system, are relatively unaffected.

3.4.2.2 Convective Coefficient of the Exposed Face

The convective coefficient of the exposed face of the gypsum board lining was varied between 5 and 25 $W/m^2.K$, with 5 $W/m^2.K$ used in the modelling. The influence of variations in the value of the convective coefficient of the exposed face is negligible as shown by Figure 3-10.

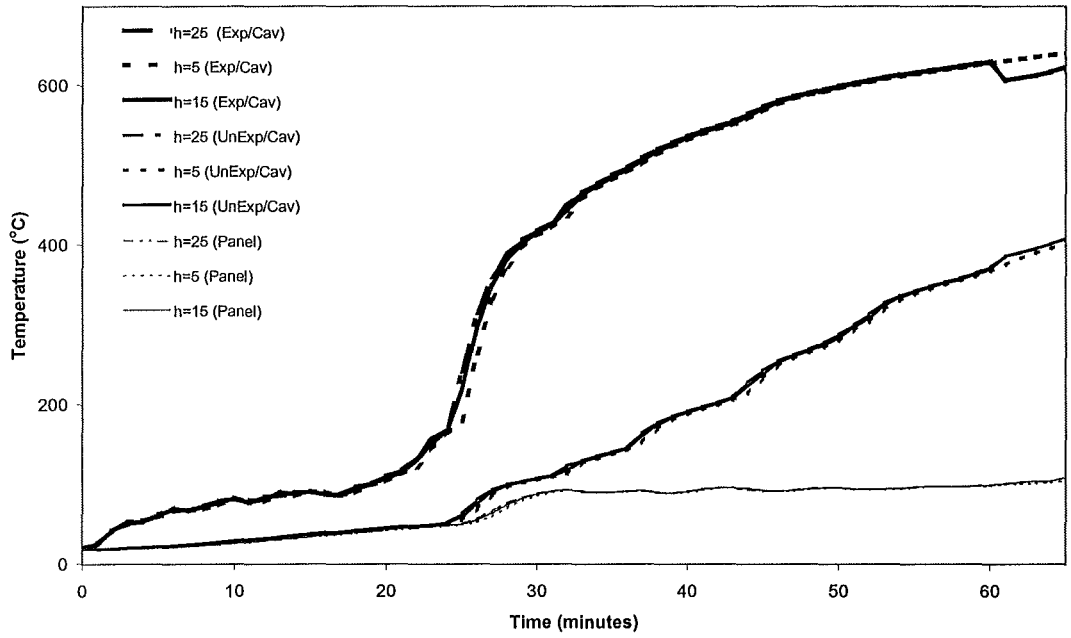

Figure 3-10: Predicted temperatures for convective coefficient values of 5, 15, and 25 W/m^2.K.

3.4.2.3 Convective Coefficient of the Unexposed Face

The convective coefficient of the unexposed face was varied between 5 and 25 W/m^2.K. A value of 12 W/m^2.K has been used in the modelling of the assemblies. Figure 3-11 shows that changing the value of the convective coefficient of the unexposed gypsum board face has negligible effect on the predicted temperatures.

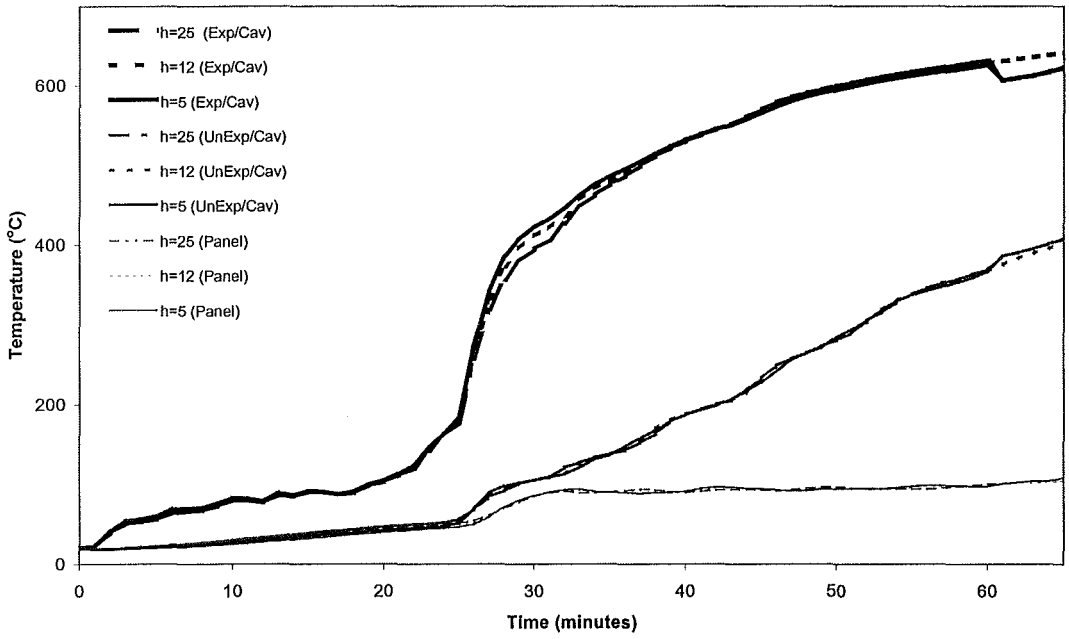

Figure 3-11: Predicted temperatures for convective coefficient values of 5, 12, and 25 W/m^2.K.

3.5 Limitations with Modelling

Although SAFIR is a very powerful finite element program, the program deficiencies and limitations exist in its ability to model gypsum plasterboard assemblies, and are given in the following:

3.5.1.1 Time Step

Both gypsum and wood have large changes in the value of specific heat over a short range of temperature, relating to vaporisation of moisture within the material structure. These peaks in the relationship for specific heat with temperature require very small time steps for the model in order to take account of their influence. If the time step is too large the user may run the risk of missing these peaks entirely, resulting in inaccurate output from the model. However, the consequence of decreasing the time step, so as to ensure accurate predictions, is that the model will require a substantial duration to complete calculations.

Although SAFIR has the option of allowing the user to specify different time steps throughout the iteration time, what magnitude of time step and where in the calculation to use that time step is purely an iterative process. If the time steps used for the calculation are too large, then numerical instability will occur within the model, and the calculation will cease. This iterative process to maintain numerical stability can take minutes or several days, depending on the complexity of the model and how the calculation loop progresses before it stops. This phenomenon had a large influence on the progress of this section of the study. Since each time the thermal properties were calibrated within the model, several runs were required to define the correct sequence of time steps to achieve a complete calculation. Hence, results from modelling the timber stud assembly have not been included. It is possible to allocate a very small time step for the whole calculation duration. However, this creates the problem of excessive run times.

Table 3-2 gives a typical time step format required to ensure that a complete run up to 3900 seconds is achieved.

Table 3-2: Typical time step format for SAFIR calculation.

Time step (secs)	Calculation time (secs)
0.01	500
0.05	1200
0.2	2400
0.5	3900

3.5.1.2 Run Time

As mentioned previously, the run time is highly dependent on the time steps assigned throughout the duration of the calculation. The complexity of the structure being analysed and the computer speed were also major influences on the calculation run time. Initially, the model was run on a Pentium 1 computer with 64MB of RAM and 120MHz processing speed. It took approximately three to four days for this computer to complete a calculation using the "finely" discretised section. Calculating the same

section on a Pentium 3 computer with 128MB of RAM and 500MHz processing speed required a run time of just under two days. However, a run time of approximately two days was still too excessive, so a much coarser mesh was applied to the section. This reduced the run times on a Pentium 3 computer to approximately 6 hours.

3.5.1.3 Input

As with any computer program, the output is only as good as the input. In the case of SAFIR, input is in the form of text files, which can be cumbersome and very time consuming to prepare. Although, pre-processors developed by the authors of SAFIR are available, these are of little use, as they do not support gypsum or wood based materials. As mentioned previously, the pre-processor SAPPHIRE, developed by Mason (2000) was used to construct the input files for analysis within SAFIR2001. However, because an independent author developed SAPPHIRE, changes to SAFIR, as in the new version SAFIR2001, are not necessarily reflected in SAPPHIRE. Resulting in compatibility problems between the two programs.

SAFIR2001 was required for this study because it allows the user to define up to five user-defined materials, while SAPPHIRE was used to prepare the input files. However, SAPPHIRE currently supports only SAFIR98a files, and therefore could not be directly calculated by SAFIR2001 without further modification of the text file. This proved to be a cumbersome exercise.

3.5.1.4 Output

The post-processor, DIAMOND, is only able to support output files from SAFIR. Therefore the user must seek alternative methods of output presentation if comparisons with test data, or other forms of data are to be performed. The author employed an Excel spreadsheet to modify output data to a manageable form that could be compared with test data. This also took considerable time to prepare.

Therefore, a need exists to develop a user-friendly interface for SAFIR, which incorporates both pre and post-processing capabilities.

3.5.1.5 Moisture Movement

Heat transfer within gypsum and wood is highly dependent on the moisture content of the material. The user has the ability to account for moisture content within the material by modifying the respective specific heat curve in the model. However, modelling moisture movement across the cavity is a more complex problem, which is not considered in SAFIR. This phenomenon is generally neglected due to its complexity, and because it only influences the heat transfer across the cavity at temperatures below 120°C (Thomas 1997).

3.5.1.6 Ablation

Ablation is the process when consecutive thin layers of gypsum shed from the lining. This has the effect of reducing the cross-sectional thickness of the gypsum lining, therefore, increasing the heat flux across the lining. SAFIR does not allow the user to remove elements from the section to simulate ablation, and therefore, must be taken account for in the thermal properties of the lining.

3.5.1.7 Shrinkage

Shrinkage and cracking of the lining is typically taken account for by increasing the thermal conductivity of the lining once dehydration has occurred. However, another phenomenon occurs within the assembly due to moisture movement within materials, shrinkage of timber studs. This creates a void between the lining and the stud, altering the form of heat transfer into the stud. SAFIR does not currently allow the user to modify the dimensions of elements during a calculation. A possible way of accounting for this effect is to pre-define a gap between the stud and lining, assigning it with the properties of wood initially, and then alter the properties to that of air once shrinkage is expected to have occurred. Further investigation of this phenomenon and its influence on modelling results will be left for recommended study.

4 TEMPERATURE EFFECTS

4.1 General

Light frame construction can have excellent fire behaviour, provided that it is well constructed from the correct materials. Both real fires and fire tests have shown that gypsum plasterboard linings can prevent fire spread and protect the load bearing light steel or light timber frame for the duration of the fire.

4.2 Properties of Gypsum Plasterboard at Elevated Temperatures

Gypsum plasterboard linings are commonly used to provide fire resistance in framed construction. Pure Gypsum consists of calcium sulphate with free water at equilibrium moisture content of approximately 3%, and chemically combined water of crystallisation (approximately 20%) (Gerlich 1995). Its chemical formula is $CaSO_4.2H_2O$ (calcium sulphate di-hydrate). Other materials exist in small quantities, such as glass fibre and vermiculite within the various proprietary products in order to improve their durability and performance when exposed to elevated temperatures.

When gypsum board lining is heated during a fire, temperatures on the exposed face will increase steadily until about 100°C is reached. At this time there will be a delay in the evolution of temperature through the gypsum core while the water of crystallisation is driven off. As the heating continues, the 100°C temperature plateau will progress slowly through the board, until the entire board has been dehydrated. The length of this plateau is a function of the lining thickness, density and composition.

The process of removing the chemically bound water is called 'calcination', resulting in loss of strength and shrinkage of the sheet material. During heating, gypsum plaster undergoes two endothermic decomposition reactions. The first dehydration reaction occurs at approximately 100 – 120°C when the calcium sulphate di-hydrate is converted to calcium sulphate hemihydrate as shown by the following reaction.

$$CaSO_4.2H_2O \rightarrow CaSO_4.{}^1/_2H_2O + {}^3/_2H_2O \quad \text{[4-1]}$$

There is some discrepancy to when the second dehydration reaction occurs. Sultan (1996) reported that the remaining dehydration occurs at approximately 600°C. However, Andersson and Jansson (1987) and Groves (1958) estimate the second reaction occurs between 210°C and 300°C. The second dehydration reaction occurs when calcium sulphate hemihydrate is converted to calcium sulphate anhydrate as shown by the following reaction.

$$CaSO_4.{}^1/_2H_2O \rightarrow CaSO_4 + {}^3/_2H_2O \quad \text{[4-2]}$$

The paper facings, which contain the core material and provide tensile strength to the plasterboard linings, is burned away after temperatures reach approximately 300°C.

Additives such as vermiculite and glass-fibre reinforcing enhance the fire resistance of gypsum plasterboard. Vermiculite expands when heated, which will partly counteract the shrinkage of the gypsum core. Glass-fibre reinforcing will attempt to bridge any shrinkage cracks that occur and will enhance the integrity of the board during the calcination process, and after the loss of paper facings. Glass-fibres also delay the ablation of the exposed surface and therefore slows down the calcination process as the calcined board is forming a protective insulating layer (Gerlich 1995).

4.2.1 Thermal Properties

4.2.1.1 General

The gypsum plasterboard used in the experimental phase of this project is New Zealand GIB® standard and GIB® Fyreline, both manufactured by Winstone Wallboards Ltd (Winstone Wallboards 1997). The New Zealand boards are based on the equivalent American boards, regular, Type X, and special purpose Type C (Gypsum Association 1994). GIB® standard board is similar to the American regular board while GIB® Fyreline is similar to Type C (Buchanan *et al* 1997).

Regular or standard board is not required to have any fire resistant rating, so it usually has a low-density gypsum core with no reinforcing except the external paper. The

low density arises from air entrainment during manufacture. Regular gypsum displays poor fire resistance performance compared to Type X or special purpose boards. The board tends to crack and fall off the wall or ceiling when the paper face is consumed and the gypsum core starts to dehydrate (Buchanan 2000).

Type X is a generic fire resistance board that is rated to provide 45 or 60 minutes protection to a load bearing wood or steel frame with a lining thickness of 12.7 or 15.9 mm, respectively. All Type X boards contain some glass-fibre reinforcing and may have other additives to improve fire performance (Buchanan 2000).

Special purpose boards (GIB® Fyreline, Type C) are often manufactured in non-standard thicknesses and formulations to meet special market requirements for fire resistance or other performance. These types of boards generally have a higher content of glass-fibre, more core additives, and greater gypsum core density. Thermal properties, at ambient temperature, published by gypsum board manufacturers around the world are given in Table 4-1, which has been adopted, from Clancy (1999).

Table 4-1: Thermal properties of gypsum plasterboard at ambient conditions from various sources.

Country	Reference	Density (kg/m^3)	Specific Heat (J/kg.K)	Conductivity (W/m.K)
New Zealand	Winstone Wallboards ltd			
	-GIB® Fyreline	730-880		
	-Standard	690		
Australia	Boral (1997) Firestop	810		0.17
Australia	CSR Gyprock (1997)			0.18
Canada	Westrock Heavy, regular	578	600	0.2
Canada	Mehaffy (1994)-Type C	732	950	0.24
	-Type X	648	950	0.24
Canada	Sultan (1996)-Type X	698	1500	0.25
United Kingdom	British Gypsum Glasroc	1000		0.288
United Kingdom	British Gypsum Fireline	800		0.2
United Kingdom	Knauf Plasterboards	800		0.2
Europe	Konig *et al* (2000)			
	Nordic -Type F	825		0.25
	-Type GN (regular)	700		0.25
United States	Gypsum Assoc. (1993)			0.16

Samples of the gypsum plasterboard linings used in the experiments of study were measured and weighed to determine their ambient density, values are given in Table 4-2. Samples were then oven dried at a constant temperature of 55°C to establish their equilibrium free moisture content, which is defined in Section 4.2.3.

Table 4-2: Ambient density of 12.5 mm gypsum plasterboard used in testing.

Test Specimen	Density (kg/m^3)
FP2879 (Standard)	700
FP2880 (Standard)	700
FP2881 (GIB® Fyreline)	747
FP2882 (GIB® Fyreline)	745
FP2922 (Standard)	670

Generally the density values given in Table 4-2 are in good agreement with those reported by Winstone Wallboards Ltd in Table 4-1.

4.2.1.2 Density

Table 4-1 indicates that the reported ambient density of gypsum plasterboard ranges from 578 to 1000 kg/m^3. Variations in board density result from different moisture contents and entrained air within the gypsum core. Both of these factors play an important role in the fire resisting performance of gypsum plasterboard. Variations in product composition and testing methods used by researchers to determine the thermal properties of gypsum board are depicted in Figure 4-1, where different studies of similar plasterboards have provided variations in the evolution of density with increasing temperature.

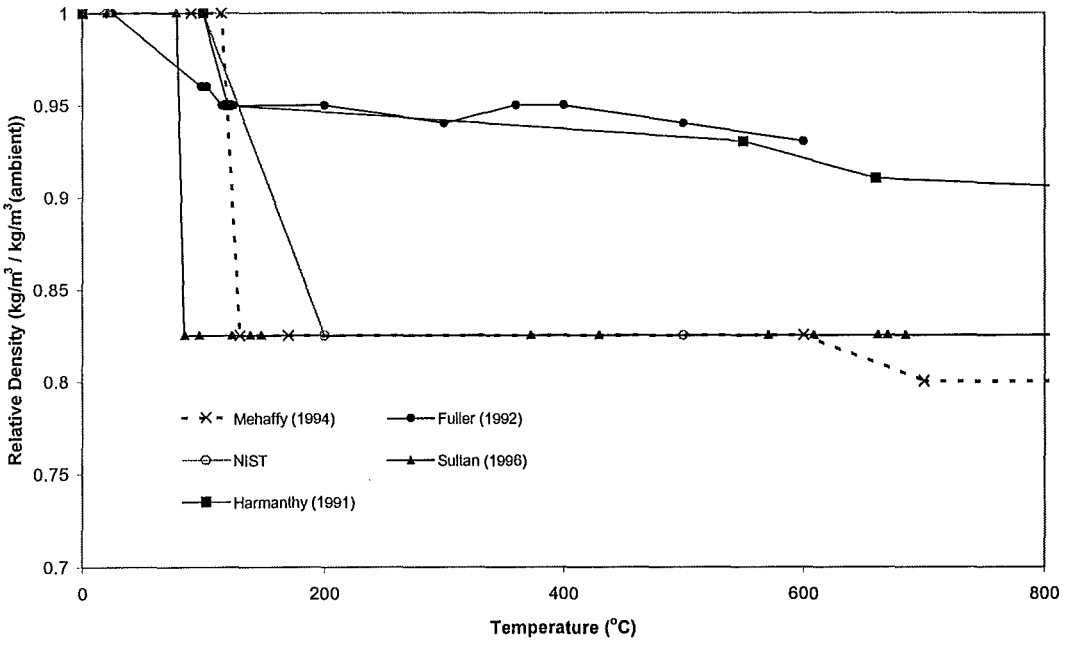

Figure 4-1: Density of gypsum plaster relative to ambient density, versus temperature.

Mehaffy *et al* (1994), Sultan (1996), and NIST (1980) report similar findings for the change in density with temperature for Type X and Type C gypsum boards. Figure 4-1 shows the large decrease in the density at approximately 100°C where the first dehydration reaction occurs. Of these three researchers only Mehaffy *et al* reports the second dehydration reaction, indicated by the drop in relative density at approximately 600°C. Default thermal properties for both Type X and Type C gypsum within the SAFIR software are from research performed by Cooper (1997), which was based on the work of Sultan (1996).

Harmanthy (1991) and Fuller *et al* (1992) also report changes in density with temperature for Type X and C gypsum boards. However, their studies have found values that differ somewhat to those of and Sultan Mehaffy *et al,* although Harmanthy does report a drop in the density at 600°C. The evolution of density with increasing temperature proposed by Harmanthy has been adopted for this project, based on the knowledge that Thomas (1997), Gerlich (1995), and Collier (2000) used similar values and achieved good results from modelling.

4.2.1.3 Specific Heat

Values for the specific heat of gypsum plasterboard measured at ambient conditions range from 600 to 1500 J/kg.K as shown by Table 4-1. Similar to the change in density with temperature, there is large variation between the reported values for specific heat with temperature from different studies of similar gypsum boards. Figure 4-2 shows that there is good agreement agmonst researchers that the first dehydration reaction occurs at approximately 100°C. However, there is inconsistency between studies on where the second dehydration reaction occurs.

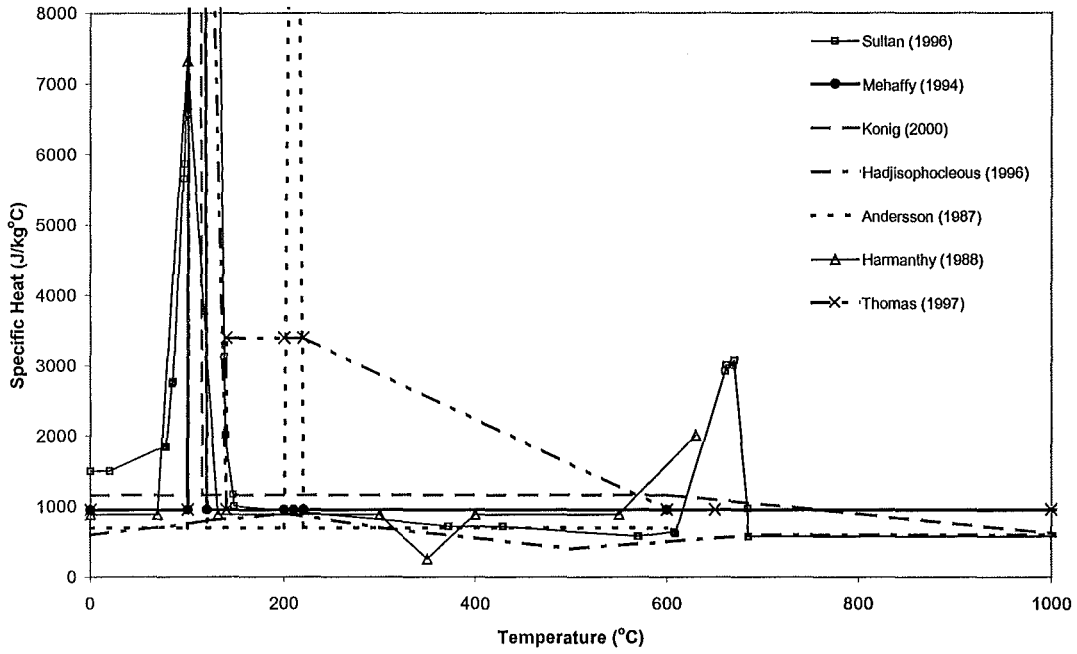

Figure 4-2: Specific heat of gypsum board reported by various studies.

Sultan (1996) reports peaks in the evolution of specific heat for Type X gypsum board of 18500 and 3070 J/kg.K at 125°C and 670°C, respectively. Harmanthy (1988) provides a peak of 7320 J/kg.K at 100°C and although Harmanthy gives measurements up to only 630°C, a peak of 2000 J/kg.K indicates similar findings to that of Sultan. Although not shown on Figure 4-2 Fuller *et al* (1992) reported similar findings to Sultan and Harmanthy, with a first peak of 16600 J/kg.K at 103°C and indicated that a second peak of 1700 J/kg.K occurred at 600°C. Mehaffy *et al* (1994) only measured specific heat up to 200°C and did not record a second peak. Their studies report a peak of 49950 J/kg.K at 110°C, with an ambient value of 980 J/kg.K

extrapolated for increasing temperatures. Hadjisophocleous (1996) did not report any spikes in the specific heat of gypsum plaster.

Andersson and Jansson (1987) provide values of specific heat obtained from measurements of Nordic gypsum plasterboard. They report peaks of 52200 and 19200 J/kg.K occurring at 110°C and 210°C, respectively. Thomas (1997) studied the values reported by Mehaffy *et al*, Andersson *et al*, and Harmanthy. The specific heat used by Thomas in the software modelling were similar to that of Andersson *et al* with a peak of 52450 J/kg.K at 110°C. However, in order to maintain numerical stability within the modelling, Thomas accounted for the second peak with high baseline values after the initial peak at 110°C. Konig and Walleij (2000) define values for specific heat based on the research of Harmanthy, Mehaffy *et al*, Andersson *et al*, and Thomas. They report apparent values with a peak 46300 J/kg.K at 105°C and neglect a second peak, which provided good results from numerical modelling.

4.2.1.4 Thermal Conductivity

As shown by Figure 4-3 there is consistent agreement between researchers on the thermal conductivity of gypsum plasterboard up to 400°C. At which point reported values from each study deviate considerably. It is known that several researchers such as Mehaffy *et al* (1994), Thomas (1997), and Sultan *et al* (2000) have adopted significantly greater conductivities than those measured at temperatures exceeding 400°C to allow for the inclusion of heat transfer through cracks.

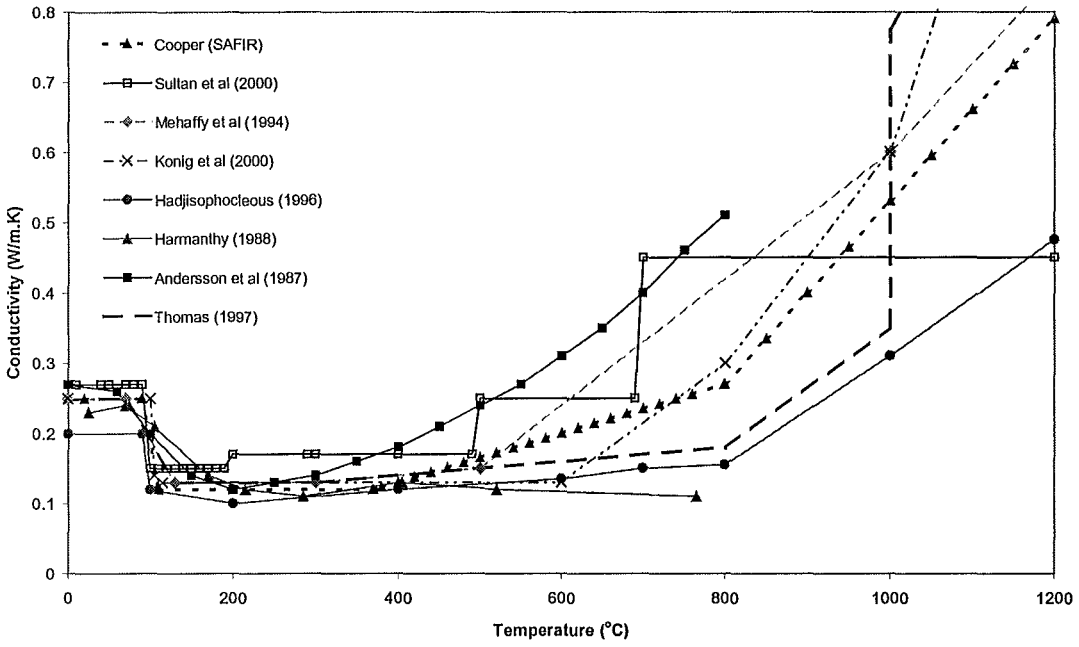

Figure 4-3: Thermal conductivity of gypsum board reported by various studies.

Cooper (1997) defined the default values for thermal conductivity of gypsum board within the SAFIR software, which originate from work performed by Sultan (1996) on Type X and Type C boards. Sultan (2000) defines apparent thermal conductivity values that provided good comparison between theoretical and experimental results. Mehaffy *et al* (1994) extrapolated a conductivity curve from measurements conducted at the National Research Council Canada (NRCC) on Type X and C gypsum board. Harmanthy (1988) provides values up to 750°C, but did not record any increase in thermal conductivity beyond 400°C. Andersson *et al* (1987) report high conductivity values from measurements conducted on European manufactured boards.

Thomas (1997) used values derived from Mehaffy *et al* for Type X gypsum board, extrapolated to 1000°C. To account for ablation, Thomas modified the conductivity curve to 0.775 W/m.K at 1000°C reaching 2.3 W/m.K at 1500°C. However, none of the test specimens reported or used by Thomas indicate that the gypsum lining exceeded 800°C and it is unlikely that the gypsum lining would have remained intact beyond this temperature as indicated by Sultan (1996), Carne (1995), and Goncalves *et al* (1996). Konig *et al* (2000) used a similar approach to that of Mehaffy *et al* and Thomas, and used calibrated values for the conductivity of Nordic Type F and Type

GN gypsum boards. Conductivity values reported by Hadjisophocleous (1996) are generally lower than those from other studies, this difference may be due to variations in cracking within gypsum boards from different manufacturers as noted by Goncalves *et al* (1996).

4.2.1.5 Specific Volumetric Enthalpy

The enthalpy of gypsum board is given by the area under the specific heat multiplied by the density versus temperature curve defined by [4-3].

$$E(T) = \int_{T_A}^{T} C_P(T')\rho(T')dT' \qquad \textbf{[4-3]}$$

Where E(T) is the enthalpy in $J/m^3.K$ at temperature T, $C_P(T')$ is the specific heat (J/kg.K) at temperature T', and $\rho(T')$ is the density (kg/m^3) at temperature T'. T' is the dummy variable of integration and T_A is the ambient temperature. To provide a comparison between various studies, curves depicted in Figure 4-4 are based on an ambient density of 474 kg/m^3.

Although there is still a certain degree of variation between different studies, Figure 4-4 shows that the inconsistencies present in the reported values of specific heat in Figure 4-2 are smoothed by the summation of area under the respective curves.

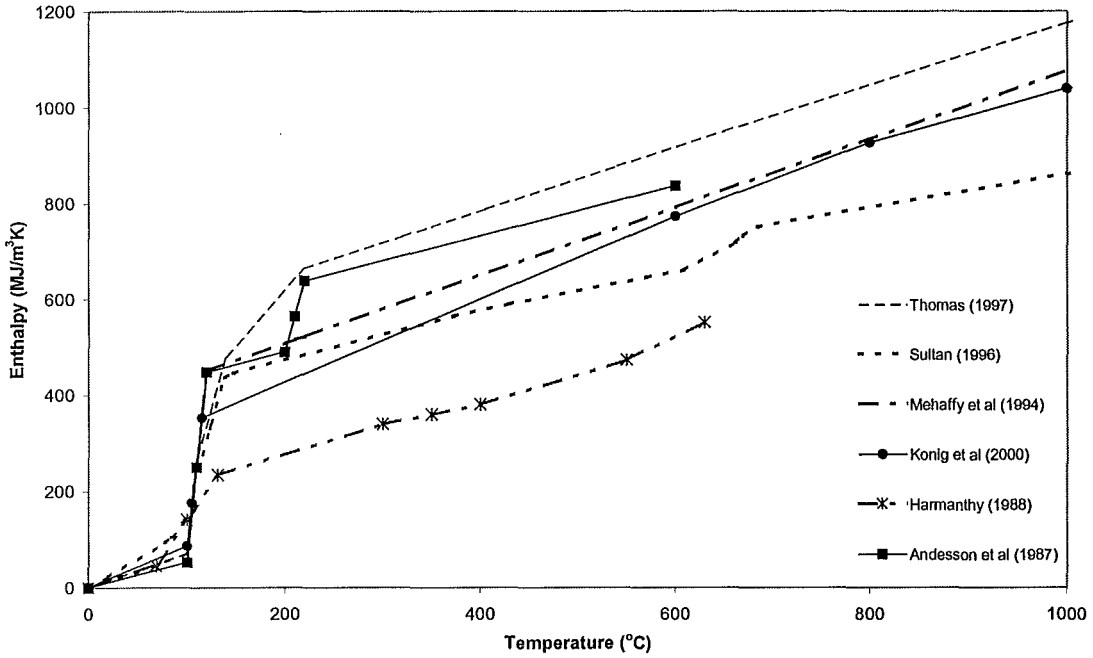

Figure 4-4: Comparative enthalpy of gypsum plasterboard from various sources.

Thomas (1997) used a smoothed version of his calculated enthalpy curve, which was based upon the findings of Andersson *et al* (1987). Values reported by Mehaffy *et al* are similar to Andersson and Janssen's values, except they exclude the second steep rise in enthalpy due to the second dehydration reaction at approximately 210°C. The thermal properties of gypsum board used in the study by Konig *et al* (2000) were based upon those measured by Mehaffy *et al* (1994), which is indicated by similar enthalpy curves. Sultan (1996) based his enthalpy curve upon the properties of Type C gypsum board, which are present in the default thermal properties of gypsum board in the SAFIR software. The second peak in the specific heat values reported by Sultan give rise to the step in the enthalpy curve at approximately 600°C. The values of Harmanthy (1988) are significantly lower than those of other studies, due to the low reported peak in the specific heat curve at 100°C.

4.2.1.6 Relative Emissivity and Coefficient of Convection of Gypsum Plasterboard

The emissivity of the exposed gypsum board should be dependent on the state of the thermal degradation of its surface (Clancy 1999). However, the difficulty is in determining the evolution of surface emissivity with temperature. In SAFIR a relative emissivity coefficient is used to represent the surface emissivity of the board at all temperatures. A similar approach is adopted for the coefficient of convection for both the exposed and unexposed surfaces.

Franssen (1999) conducted a review of the heat transfer coefficients reported from the works of Gerlich *et al* (1996), Thomas *et al* (1994), Sultan (1996), and Cooper (1997). His recommended values of 0.8 for the relative emissivity and 5 $W/m^2.K$ for both convection coefficients are based upon those of Gerlich *et al* and Thomas *et al.* Clancy (1999) reviewed the works of Thomas *et al* (1996 and 1997), Sterner and Wickstrom (1990), and Mehaffy *et al* (1994). Clancy found that results from modelling were insensitive to surface emissivity values in the range of 0.6-0.9, which was also found by Thomas (1997). Clancy adopted a low value of 2 $W/m^2.K$ for the convective coefficient of the exposed gypsum surface and a value of 12 $W/m^2.K$ for the unexposed surface. He states that although there are substantial differences given by various researchers, these variations are not expected to significantly affect the time of failure due to the dominance of radiant heat transfer over convective.

For the purpose of this report values of 0.8, 5 $W/m^2.K$, and 12 $W/m^2.K$ have been used for the relative surface emissivity and convective coefficients of the exposed and unexposed surfaces, respectively.

4.2.2 Shrinkage, Crazing and Sloughing of Gypsum Plasterboard

Shrinkage is a mechanical characteristic of gypsum plaster, which has a significant influence on heat transfer through walls lined with gypsum plasterboard. Mehaffy *et al* (1994) studied the temperature dependence of the shrinkage of two Canadian plasterboard's, Type X with a density of 648 kg/m^3 and Type C (732 kg/m^3) as depicted by Figure 4-5. It was found that the special purpose Type C gypsum core

experienced less shrinkage than the general purpose Type X core throughout the temperature range studied.

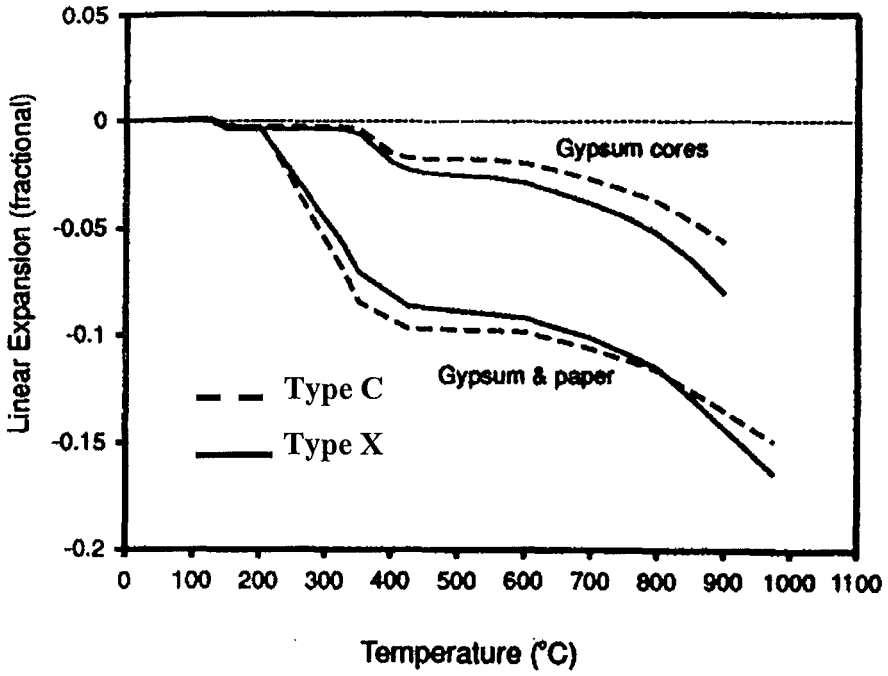

Figure 4-5: Linear shrinkage of gypsum plasterboard thickness with temperature (Mehaffy 1994).

In addition to shrinkage of the core, the thickness of the board is also reduced due to the combustion of the paper lining in the range of 200°C to 350°C. It is presumed that the in-plane shrinkage of fire rated boards is similar. However, research performed by Goncalves *et al* (1996) reports that the concentration of fibre reinforcing within gypsum board can vary up to 30% with direction, indicating that in-plane shrinkage may vary with board direction.

Figure 4-5 shows that some shrinkage of the gypsum core commences at low fire temperatures between 200°C and 400°C, whereas significant shrinkage of the board does not become apparent until high temperatures are reached. Shrinkage has inconsistent effects on heat transfer. Shrinkage reduces thickness, which inturn reduces the resistance to heat transfer. However, shrinkage also increases density, which increases the resistance to heat transfer. The overall shrinkage of gypsum linings is prevented in the construction of walls because they are attached and

restrained against movement by fastenings into the framing (Clancy 1999). Therefore tensile forces developed within the board from shrinkage are relieved by localised shrinkage or crazing of the fire exposed surface.

Crazing appears as a random formation of fine cracks across the surface of the lining. At approximately 400°C shrinkage becomes more significant, due to crazing of the lining allowing the ingress of radiant heat, which is now becoming the dominant form of heat transfer. Fredlund (1988) reports that radiant heat transfer through pores of the lining becomes significant at temperatures of around 400°C. At higher temperatures, 700-900°C the glass-fibre-reinforcing present in the special purpose boards reduces in viscosity and strength, allowing cracks to open further, increasing the ingress of radiant heat. This process, known as sloughing continues until the minimum temperatures within the board exceed 700°C. At which point it is expected that cracks fully penetrate the board, allowing sections of the board to fall away (Carne 1995, Goncalves *et al* 1996).

Sultan (1996) reports similar behaviour of the exposed gypsum plaster lining occurring once the unexposed face reaches temperatures of about 600°C. However, Sultans work was based on the performance of generic Type X gypsum board, while it is obvious that Carne and Goncalves studies are based on denser plasterboard's.

When gypsum board shrinks and bends at high temperatures, the joint gap between the adjacent sheets increases (Takeda 1999). Once reinforcing tape and plaster stopping are lost, accelerated heat transfer will occur into the cavity or onto studs depending on the location of the joint. It is typical New Zealand construction practice to have joints in linings coincide with stud locations or to provide solid blocking behind joints to provide fixity of the adjacent boards (Winstone Wallboards 1992b). Therefore, the opening of joints over studs will accelerate the general degradation of studs.

4.2.3 Free Moisture Content

The free moisture content of the plasterboard has a significant influence on the performance of the system as a whole. Collier 2000 reported that the free moisture content of plasterboards tested at the BRANZ facility is typically 1.0%, established from drying in an oven at 100°C. Studies performed by Thomas (1997) report moisture contents ranging from 4-8%. Other studies performed by Stray and Bates (1997) and Mehaffy *et al* (1994) have found that gypsum board comprises of 0.5% free moisture content. The differences are undoubtedly due to different drying regimes and types of plasterboard used.

Samples from gypsum plasterboard used to construct the assemblies in this study were subjected to oven conditions of 55°C for a period of approximately two weeks. It was found that after about three days the samples had reached equilibrium, where sample mass remained constant for at least another two days of measurement. The percentage of moisture lost from the board at this equilibrium point was between 0.9-1.0% for both standard and fire rated boards, which agrees with the findings of Collier. After the two weeks of drying the moisture loss from the sample had increased to 4-5% and 1.2-1.3% for the standard and fire rated boards, respectively. This indicates that prolonged drying can remove chemically bonded water from the gypsum core.

A sensitivity study conducted by Collier (2000) showed that varying the moisture content of the gypsum between 0 and 10% within the software model, developed by Collier, provided significant variation in the failure prediction of the model. The model used in this study does not allow the user to directly change the moisture content of the gypsum board, it can however, be indirectly accounted for in the specific heat of the gypsum. The gypsum boards used in this study have very similar free moisture contents, therefore, variation of free moisture content has not been considered.

4.2.4 Ablation of Lining

As gypsum is heated it is transformed into calcium anhydrate. This has the appearance of a dry non-cohesive powder, and tends to fall away from the lining because it is not firmly attached to the unaltered material underneath. This process is known as ablation, where consecutive thin layers of material are shed as a material undergoes chemical and physical changes during heating, which reduces the bonding of the material to itself (Thomas 1997). Ablation occurs at temperatures of about 500-700°C and 700-900°C for standard and fibre reinforced boards, respectively (Collier 2000). The effect of ablation is more apparent when comparing the results of boards of different thickness, obviously a thinner board will be affected more by ablation due the greater proportion of board that is lost.

Being able to simulate the effect of ablation requires a model that can remove consecutive layers from the lining as these layers exceed temperatures at which ablation would occur. This approach originated from research conducted by Gammon (1987) and has been adopted by Collier.

4.3 Thermal Properties of Cold Formed Steel at Elevated Temperatures

4.3.1 General

The temperature rise of a steel member, is a function of the thermal conductivity and specific heat of the material. The accuracy in the determination of thermo-physical properties of steel, such as specific heat and thermal conductivity, has little influence on the thermal modelling of LSF walls exposed to fire because steel framing plays a minor role in the overall heat transfer mechanism of the assembly (Alfawakhiri *et al* 1999). Specific heat and conductivity of steel are affected by changes in temperature. The properties of steel within the SAFIR code are derived from those described in the Eurocodes (EC3 1995).

4.3.2 Density

The ambient density of steel is typically taken to be 7850 Kg/m^3 (Buchanan 2000), which remains essentially constant with increasing temperature.

4.3.3 Specific Heat

The specific heat of steel varies according to temperature as shown in Figure 4-6, where the peak results from a metallurgical change at about 730 °C. The following equations define the relationship shown in Figure 4-6 and have been adopted from EC3 (1995).

For $20°C \leq \theta_a < 600°C$:

$$C_a = 425 + 7.73 \times 10^{-1}\theta_a - 1.69 \times 10^{-3}\theta_a^2 + 2.22 \times 10^{-6}\theta_a^3 \quad \text{(J/kg.K)} \qquad \textbf{[4-4]}$$

For $600°C \leq \theta_a < 735°C$:

$$C_a = 666 + 13002 / (738 - \theta_a) \quad \text{(J/kg.K)} \qquad \textbf{[4-5]}$$

For $735°C \leq \theta_a < 900°C$:

$$C_a = 545 + 17820 / (\theta_a - 731) \quad \text{(J/kg.K)} \qquad \textbf{[4-6]}$$

For $900°C \leq \theta_a \leq 1200°C$:

$$C_a = 650 \quad \text{(J/kg.K)} \qquad \textbf{[4-7]}$$

Where C_a and θ_a are the specific heat and temperature of the steel, respectively.

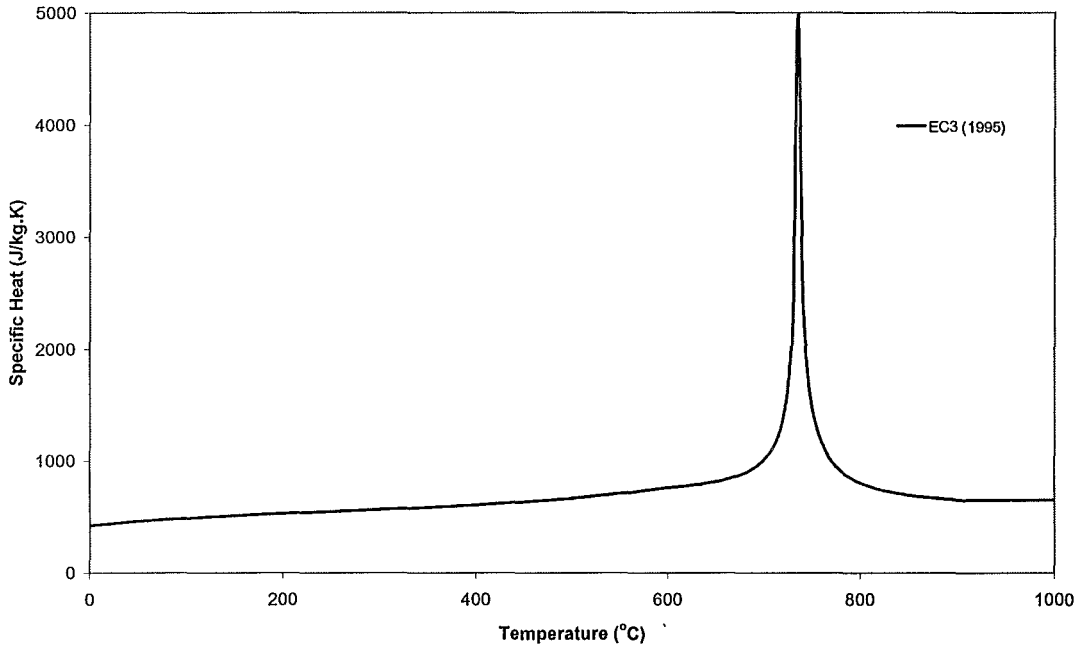

Figure 4-6: Specific heat of steel as a function of temperature.

For simple calculation models the specific heat may be considered to be independent of the steel temperature and can be taken as 600 J/kg.K

4.3.4 Thermal Conductivity

The variation of thermal conductivity with temperature of steel is defined by the following equations, [4-8] and [4-9] (EC3 1995), and illustarted by Figure 4-7.

For $20°C \leq \theta_a < 800°C$:

$$\lambda_a = 54 - 3.33 \times 10^{-2}\theta_a \quad (W/m.K) \qquad \textbf{[4-8]}$$

For $800°C \leq \theta_a \leq 1200°C$:

$$\lambda_a = 27.3 \quad (W/m.K) \qquad \textbf{[4-9]}$$

Where λ_a and θ_a are the thermal conductivity and temperature of steel, respectively.

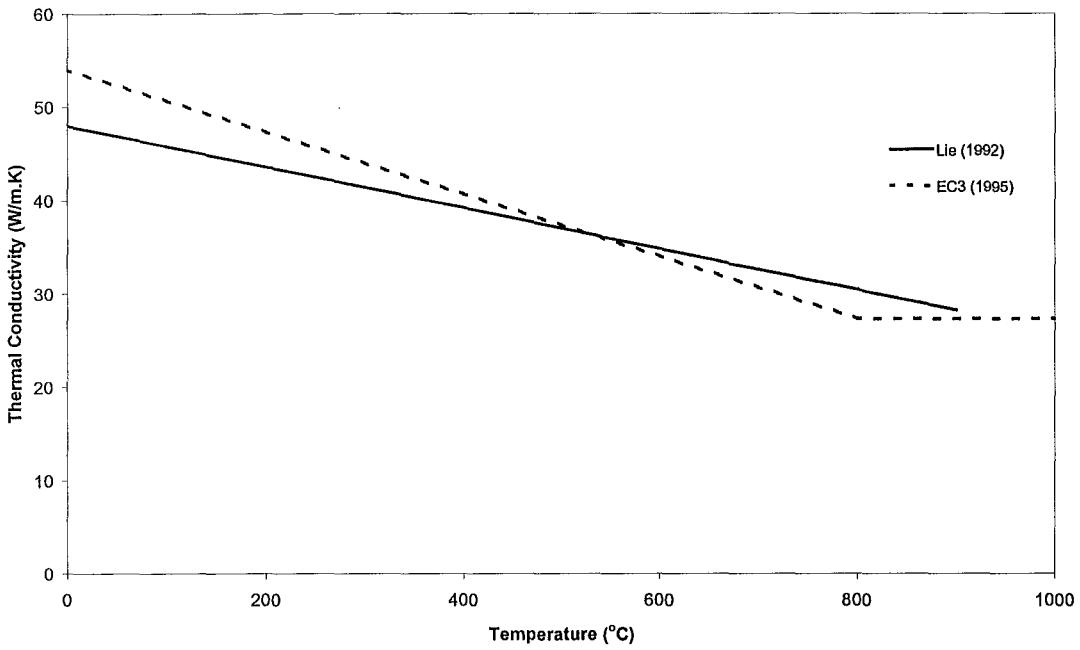

Figure 4-7: Thermal conductivity of steel as a function of temperature.

For simple calculation models the thermal conductivity model may be considered to be independent of the steel temperature and taken as a constant value of 45 W/m.K.

4.3.5 Specific Volumetric Enthalpy

The specific volumetric enthalpy of steel is the product of specific heat and temperature, expressed on a per unit volume basis. The values illustrated by Figure 4-8 are calculated from the constant density and temperature dependent specific heat taken from Eurocode 3, which are default properties within the SAFIR code.

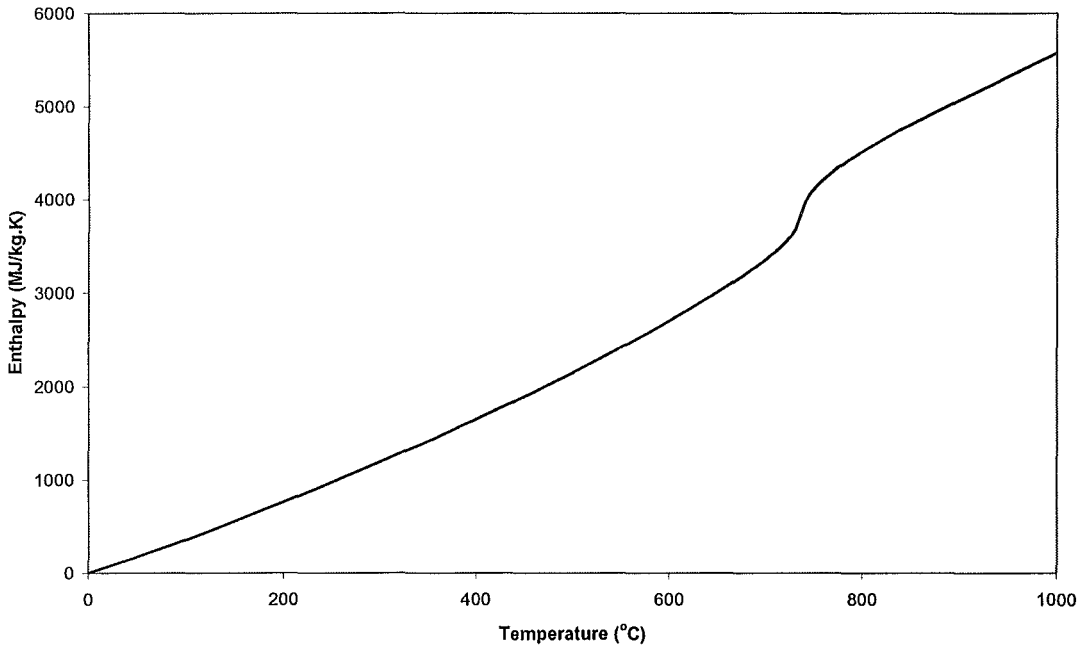

Figure 4-8: Specific volumetric enthalpy of steel.

4.3.6 Relative Emissivity and Convection Coefficient of Cold Formed Steel

Thermal properties of steel are well described in the Eurocodes and it is commonly accepted that they are valid for most types of steel. However, the relative emissivity of galvanised sheets requires additional attention.

Hamerlinck (1991) conducted an experimental study on the relative emissivity of galvanised steel sheets and found that the emissivity remains fairly constant at a value of 0.14 up to a transition domain at 400°C. It is reported that after this temperature the value increases to between 0.8-0.9 due to the melting of the zinc coating. Hamerlinck observed that the temperature domain for the transition is sensitive to the heating rate. Because the heating rate of a fire test would be much higher than that used in his experiments, Hamerlinck proposes that the transition starts at 250°C and lasts until a temperature of 600°C to 800°C.

Franssen (2000) extended Hamerlinck's findings to steel sections within a cavity where the heating rate is lower than on the exposed side. Franssen proposed that the

transition zone would occur between 300 and 500°C, with relative emissivity values of 0.12 up to a temperature of 300°C and 0.5 after 500°C with a linear variation in between. Because the component of heat transfer by radiation is small at low temperatures a constant value of 0.5 for the emissivity of steel has been used for this study.

The convective coefficient for the steel studs within the cavity shall has been as 12 $W/m^2.K$, which is the same value used for the cavity face of the exposed lining.

4.4 Properties of Wood at Elevated Temperatures

4.4.1 General

Unlike heavy timber structures where the char-layer of fire exposed members performs as an effective protection of the remaining unburnt residual cross section, the fire performance of light timber framed members is heavily dependent upon the protection provided by the linings (Konig *et al* 1999). Gypsum board protects the wood studs in a wall assembly for a significant period of time. Eventually, however, the studs become heated.

When the temperature of wood reaches about 100°C, water absorbed into the cellular structure is liberated as water vapour. At temperatures in the range of 200 - 350°C, wood undergoes pyrolysis. A layer of char begins to form on one side of the stud in contact with the fire-exposed gypsum board and on the sides in contact with the air cavity in the wall (Takeda *et al* 1998). The temperature at the interface between the char and wood is generally assumed to be 288°C (White *et al* 1992). However, most studies reviewed use a rounded value of 300°C to define the temperature at which wood chars (Konig *et al* 1999 and Collier 2000).

The two main heat paths into a typical timber stud are:

1. The path from the cavity through the side of the stud and into the core;
2. The path from the fire, through the exposed gypsum board, through the end of the stud and into the core of the stud.

Clancy (1999) reports that the first path of heat transfer would be expected to deliver a fairly uniform distribution of heat flux across the side of the stud. This is due to the size of the cavity compared to that of the stud surface. Clancy also states that the aspect ratio of the cavity dominates the heat flux distribution on the side of the stud irrespective of whether convection or radiation is the main mode of heat transfer across the cavity. Since the wood in the stud has a low thermal diffusivity and thus experiences low heat transfer rates compared with heat transfer rates through the cavity, steep temperature gradients at the edges of the stud are expected. Also considerable curving in the char profiles at the corners near the fire side is assumed to occur, as shown by Figure 4-9, which has been adopted from Collier (2000).

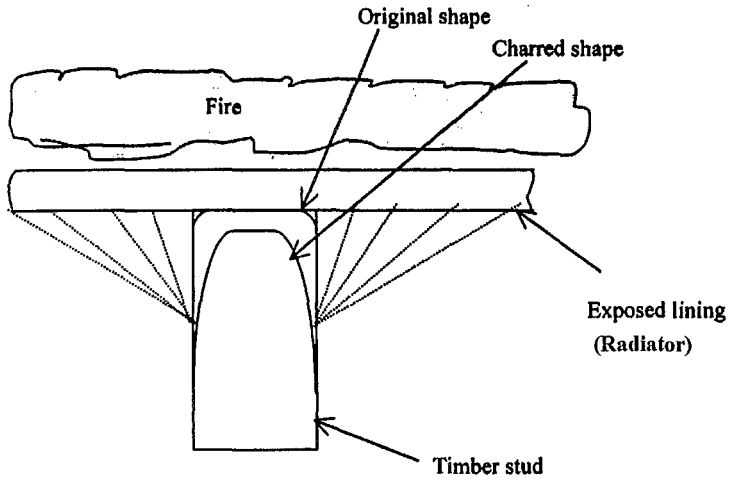

Figure 4-9: Cross-section view of radiation exposure and charring of stud.

As stated by Janssens (1994) the following sections show that there is considerable uncertainty about the thermo-physical properties of wood at elevated temperatures.

4.4.2 Density

The density of wood varies significantly between species. It also varies between trees of the same species and within individual trees. Typically the density of softwoods drops to about 90 percent of its original value when the temperature exceeds 100°C, and to about 20 percent of its original value when the wood is converted to char above 300°C (Buchanan 2000). Mehaffy *et al* (1994) explains that the density loss from 0-200°C is mainly due to vaporisation of moisture, while from 200-350°C it is mainly

caused by loss of volatiles, and thereafter, oxidation of char. This behaviour is illustrated by Figure 4-10.

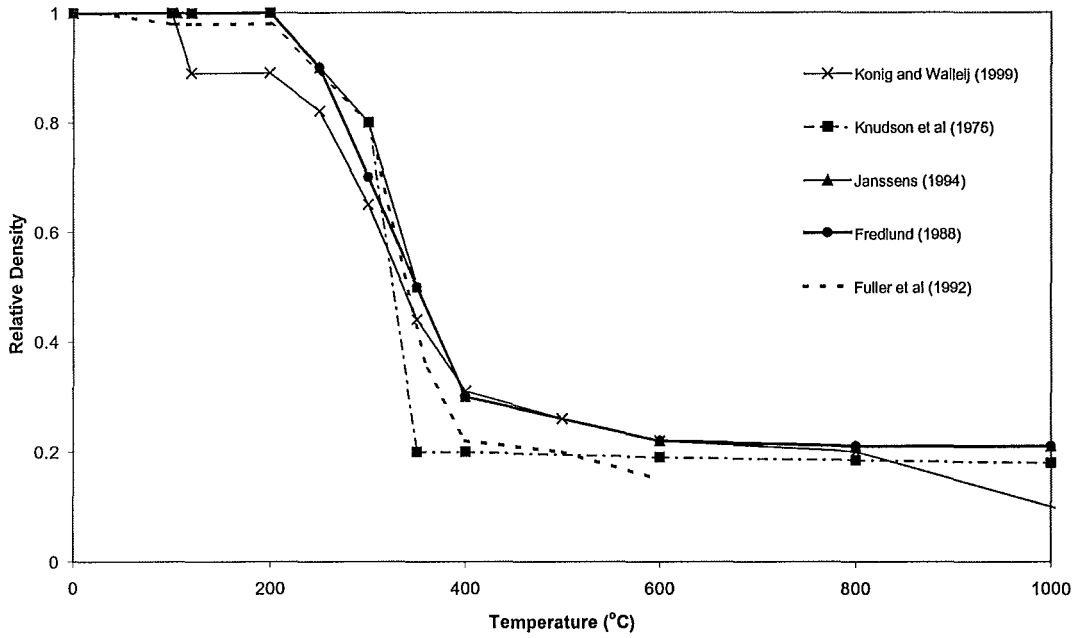

Figure 4-10: Relative oven dried mass of softwoods versus temperature.

Most researchers have based the evolution of softwood densities with temperature from work performed by Tang (1967) on Ponderosa pine sapwood. However, Tang's measurements were only recorded in the range of 200-370°C, which were further extended by Knudson *et al* (1975) up to 1000°C. Other researchers involved in the behaviour of timber framing in fire (Gammon 1987, Lie 1992, Mehaffy *et al* 1994, and Thomas 1997) have adopted this relationship for the relative oven dry mass versus temperature.

Fuller *et al* (1992) reports the evolution of density with temperature of Douglas Fir with an ambient moisture content of 12 percent. Fredlund (1988) reports calibrated density values with a minimum residual relative density of 21 percent. Density values reported by Janssens (1994) are based on results obtained from a mass loss model, which were validated by measurements made by White (1988). Janssens values relate to a softwood with an ambient density and moisture content of 470 kg/m^3 and 12 percent, respectively.

Konig and Walleij (1999) also report calibrated values for the relative oven dry density of timber, which provided good correlation between model and experimental results. Konig and Walleij modified their density curve between 800-1200°C to take account of the consumption of char at approximately 1000°C. However, in standard or non-standard furnace tests of drywall systems it is unlikely that framing members will exceed temperatures of 800°C. Values have been reported up to 1000°C to merely provide a comparison between the various studies.

4.4.2.1 Recorded Density and Moisture Content

Samples were oven dried at a constant temperature of 105°C for at least seven days or until the samples weight remained constant. Measurements of oven dried density and initial moisture content are given in Table 4-3.

Table 4-3: Oven dried density and moisture content of timber used in testing.

Test Specimen	Density (kg/m^3)	Ambient Moisture Content (%)
FP2879	545	13.5
FP2880	539	9.2
FP2881	544	9.5
FP2882	528	9.5
FP2922	446	11.2

Generally the density values given in Table 4-3 are significantly higher than typical values of 450-470 kg/m^3 reported by most studies reviewed, while measured moisture content is generally lower than 12 percent, which is typically an assumed moisture content of timber (Konig *et al* 1999).

4.4.3 Specific Heat

Most research performed on the specific heat of oven dried wood with temperature is consistent with the expression developed by Dunlap (1912), (refer to Clancy 1999), given by Equation [4-10].

$$C_o = 1110 + 4.84T \qquad \textbf{[4-10]}$$

Where C_o is the specific heat (J/kg.K) and T is temperature (°C).

Knudson *et al* (1975) extended the work of Dunlap to account for the latent heat of vaporisation of moisture within the timber by increasing the specific heat to a peak value of 13000 J/kg.K between 100-105°C. Other research in the modelling of heat transfer in timber (Gammon 1987, Mehaffy 1994, Thomas 1997, and Fredlund 1988) have adopted the specific heat values of wood and char reported by Knudson *et al.*

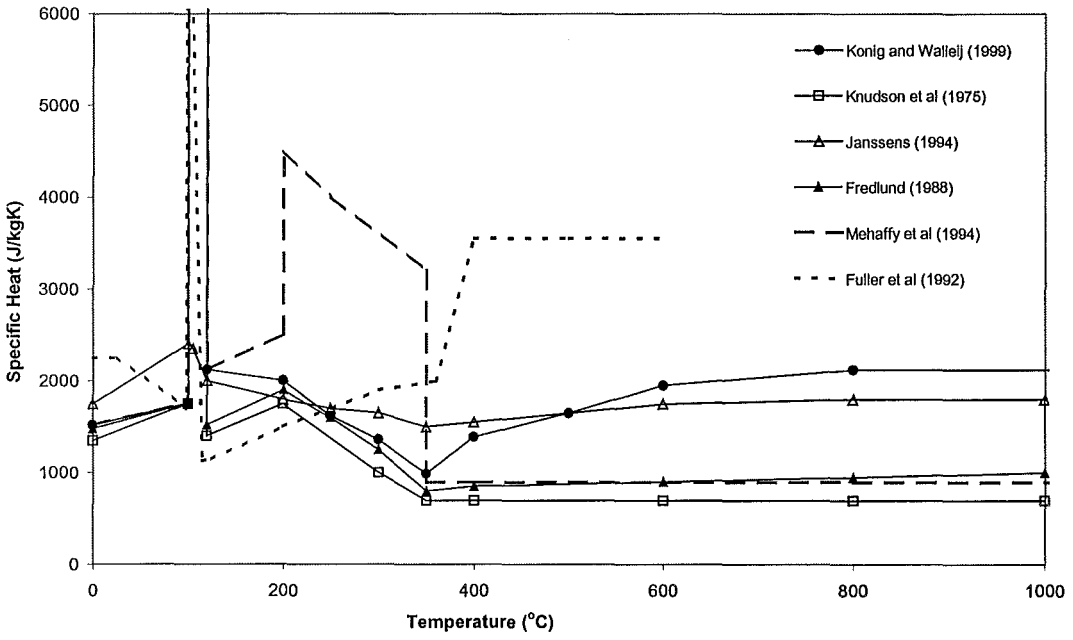

Figure 4-11: Specific heat for timber as a function of Temperature.

Janssens (1994) gives a refined expression for the specific heat of wood with temperature, which takes account of the increase in the specific heat due to water bound in the cell walls of wood. Janssens expression is given by Equation [4-11].

$$C_u = \frac{C_o + 4187U}{1+U} + \Delta C \qquad \textbf{[4-11]}$$

Where $C_o = 1159 + 3.86T$, is the specific heat.

$\Delta C = (23.55T - 1326U + 2417)U$, is the specific heat of water bound in cell walls, above specific heat of free water.

U is the moisture content (%), and T is the temperature (°C).

Fredlund (1988) reports calibrated values for the specific heat of timber with a peak value of 13500 J/kg,K at 100°C, which provided good predictions of experimental results when used in his heat transfer model. Beyond temperatures of 350°C Fredlund's values for the specific heat of char are similar to those reported by Knudson *et al*, as shown in Figure 4-11.

Konig *et al* (1999) report calibrated values with a peak of 13500 J/kg.K at 100°C, with specific heat values above 200°C adopted from Janssens. For temperatures up to 200°C Mehaffy *et al* (1994) report apparent specific heat values adopted from an expression described in Eurocode 5 (1989), with a peak value of 13500 J/kg.K at 100°C. For temperatures above 350°C, Mehaffy *et al* assumed a value of 690 J/kg.K, which is recommended by Lie (1992).

Fuller *et al* (1992) took a similar approach to that of Janssens and added heat of water vaporisation to the apparent specific heat of timber at the temperature of water vaporisation (100°C). However, the values reported by Fuller *et al* seem to be very high, with peak values of 204000 J/kg.K at 100°C and 68900 J/kg.K at 103°C. The author assumes that these values are erroneous and therefore are neglected.

4.4.4 Thermal Conductivity

Values reported by Fredlund (1988), Cuerrier (1993), Atreya (1984), Janssens (1994), Knudson *et al* (1975), and White *et al* (1978) all showed similar relationships for the evolution of thermal conductivity of timber. The relationships provided by Janssens and Knudson *et al* formed the upper and lower values of this group of researchers, and are illustrated by Figure 4-12.

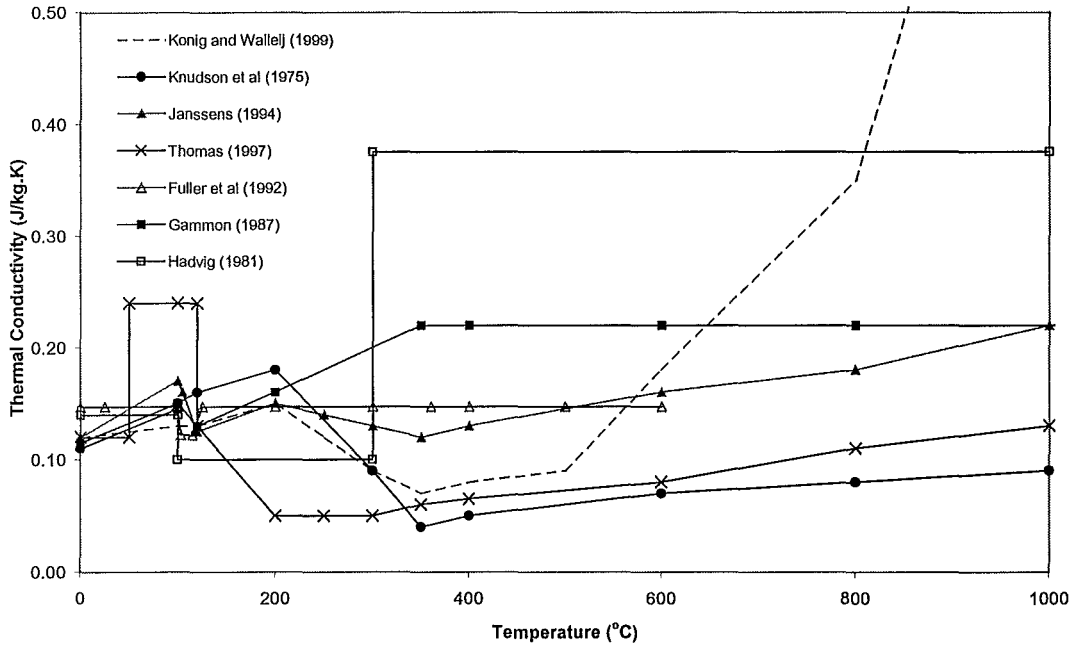

Figure 4-12: Thermal conductivity of wood.

Conductivity values used by Thomas (1997) were based on Fredlund's values below 120°C. But these values were doubled between 60°C and 110°C to allow for the increase in conductivity due to the evaporation of moisture, movement into the wood and subsequent condensation.

Harmanthy (1988) provided values that followed very closely the values reported by Gammon (1987), which are included in Figure 4-12. Fuller *et al* (1992) gives conductivity values up to 600°C recorded from the longitudinal orientation of the grain. It is obvious that the values of Hadvig (1981) and Konig *et al* (1999) are calibrated in order to achieve good correlation between experimental and theoretical results. Clancy (1999) gives a detailed review of the various studies performed on the thermal conductivity of wood at elevated temperatures.

4.4.5 Enthalpy

Figure 4-13 compares the specific volumetric enthalpy of wood, which has been calculated by the same method outlined in Section 4.2.1.5. All relationships have been calculated using an initial oven dried density of 470 kg/m^3.

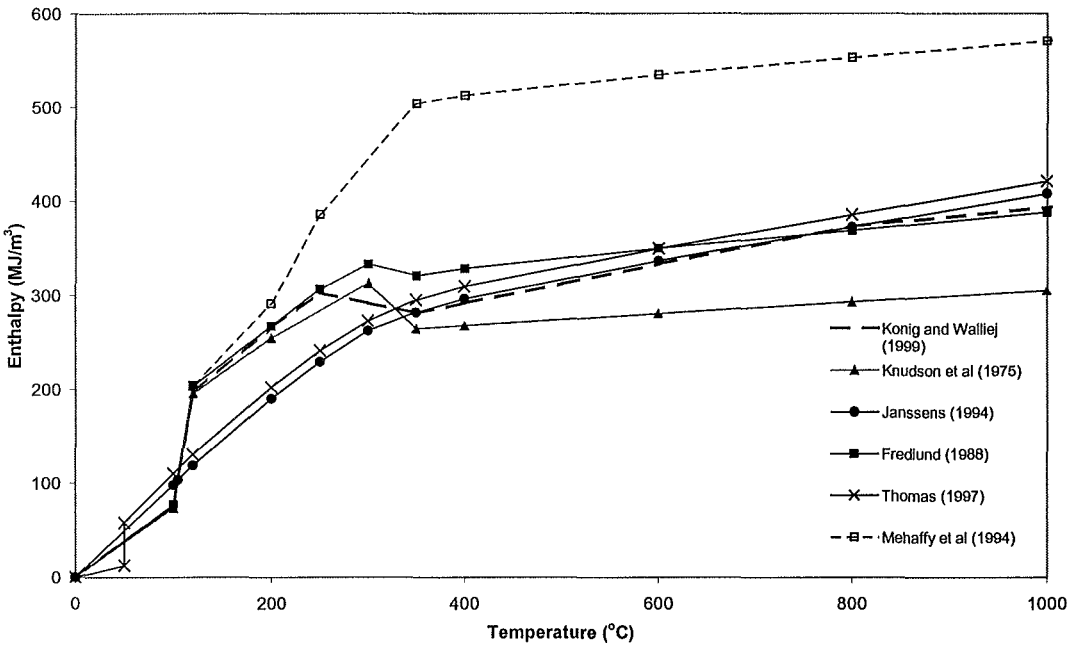

Figure 4-13: Specific volumetric enthalpy of wood.

Relationships from most reported researchers agree reasonably well, except for the much higher values of Mehaffy *et al* after a temperature of 200°C. This arises from the high specific heat values reported by Mehaffy *et al* in the range of 200-350°C.

4.4.6 Relative Emissivity and Convective Coefficient of Wood

At 12 percent moisture content the emissivity of wood is 0.81 and reduces to 0.65 as the moisture is driven off (Gammon 1987). Gammon also gives an emissivity of char of 0.85. Due to the variation of the gas emissivity within the void and for the sake of simplicity, Thomas (1997) assumed an effective emissivity between the wood and the void of 0.6. This was the same value assigned for the emissivity between the gypsum board lining and the cavity. A sensitivity study performed by Thomas found that variations in the value of both relative emissivity and surface convective coefficient, had little influence on the result from modelling.

A similar approach to that of Thomas has been adopted for this study, in which a relative emissivity value of 0.8 and convective coefficient of 12 $W/m^2.K$ are assumed for wood within the cavity. These are the same values used for the gypsum lining.

4.4.7 Charring

For a timber stud wall with no cavity insulation, typical char profiles are shown in Figure 4-14 (Collier 1991b). Charring of wood begins when the temperature reaches about 300°C. Wall linings protect the wood member from direct fire exposure and therefore reducing the rate of charring compared to wood members exposed directly to a fire environment. Charring on the edge of the stud in contact with fire-exposed gypsum board proceeds at about twice the rate as on the wide surfaces exposed to the cavity (Buchanan 2000). This is because the studs exposure to radiative heat from the exposed lining reduces with distance from the fire exposed side of the cavity, as shown by Figure 4-9. The exposed corners of the stud are expected to char at an increased rate due to arris rounding, which is effectively subjected to a double exposure (BSI 1978).

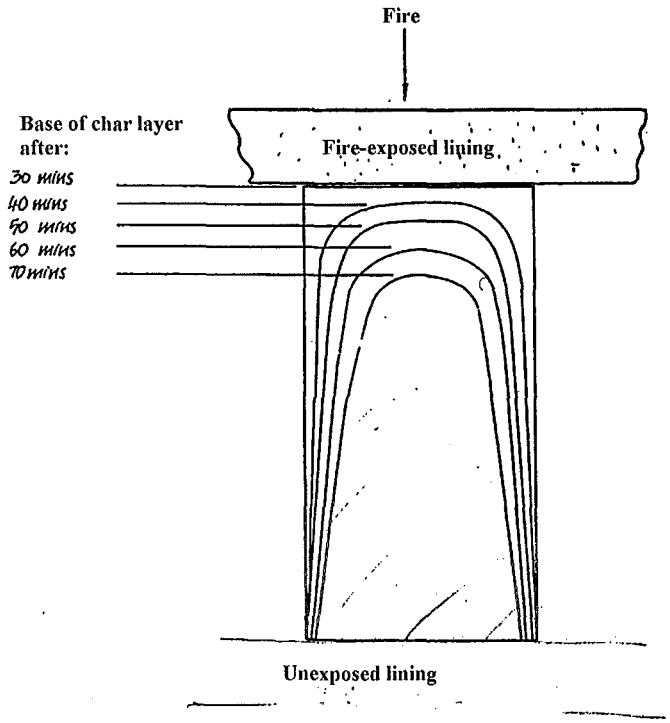

Figure 4-14: Char profiles of timber stud with no cavity insulation.

Some approval organisations permit protected assemblies to be assigned a fire resistance rating if it can be shown that the protected wood will not begin to char during the time of exposure. This is explicitly permitted in New Zealand (SNZ 1991). The listings published by UL (1996) include a "finish rating" for sheet materials fixed

to timber studs, defined as the time at which the wood surface closest to the fire-exposed lining reaches an average temperature rise of 121°C or an individual temperature rise of 163°C. These temperatures are lower than the usually accepted charring temperature of 250-300°C, so the "finish ratings" would be very conservative estimates of initiation of damage to protected wood members (Buchanan 2000). Most Type X gypsum boards have finish ratings of 15 and 20 minutes for 12.7 and 15.9 mm board, respectively (UL 1996).

Butler (1971) developed a radiation induced char model on the basis of incident radiation from the lining impinging on the stud surfaces causing char and surface recession. In agreement with Butler's findings, Mikkola (1990) found that further adjustments to the charring rate can be based on density, moisture content, and oxygen consumption. Mikkola's expressions for the reliance of the rate of char on the density and moisture content of wood are given by Equations [4-12] and [4-13], respectively.

$$\beta \approx \frac{1}{(\rho + 120)} \qquad \textbf{[4-12]}$$

$$\beta \approx \frac{1}{(1 + 2.5U)} \qquad \textbf{[4-13]}$$

Where β is the rate of charring (mm/minute), ρ is the oven dried density of wood (kg/m^3), and U is the moisture content of wood (%).

Reducing oxygen concentration, as a fire progresses, also has the effect of retarding the charring rate. Oxygen concentration varies within testing environments. Typical oxygen content in a cone calorimeter test would be 21 percent, as in ambient air. However, oxygen concentrations of 8-10 percent can be encountered in fire resistance testing, which will reduce the charring rate by approximately 20 percent. In a fully developed fire the oxygen content may drop to zero in which case the charring rate could reduce by 35-50 percent (Collier 2000). Therefore, prediction of charring rates of timber members within a cavity is severely hampered by its dependence on parameters that can very significantly within a fire resistance test specimen.

4.5 Summary of Thermal Properties Used

The temperature dependent thermal properties of the gypsum board used in the modelling of this study are given in the following tables. These apparent thermal properties have been calibrated from modelling the plasterboard systems exposed to the standard ISO834 fire curve. The heat transfer coefficients have also been summarised. Results from the computer model are given in Section 6.

Table 4-4: Density

Temp (°C)	ρ(GIB® Fyreline) (kg/m^3)	Temp (°C)	ρ(Standard) (kg/m^3)
0	747	0	648
100	747	100	648
105	747	105	648
125	725	130	620
140	710	150	620
150	702	160	620
200	702	200	620
205	702	205	580
215	702	210	580
220	680	350	580
400	680	500	580
640	680	660	100
700	680	700	100
1000	680	1000	100
1200	680	1200	100

Table 4-5: Specific Heat

Temp (°C)	c_p(GIB® Fyreline) (kg/m^3)	Temp (°C)	c_p (Standard) (kg/m^3)
0	900	0	800
100	900	100	800
105	38000	105	3000
125	38000	130	5000
140	2000	150	7000
150	2000	160	7000
200	1000	200	9000
205	9000	205	11000
215	9000	210	12000
220	1000	350	15000
400	900	500	5000
640	900	660	100
700	800	700	100
1000	800	1000	100
1200	800	1200	100

Table 4-6: Conductivity

Temp (°C)	k(GIB® Fyreline) (kg/m^3)	Temp (°C)	k (Standard) (kg/m^3)
0	0.3	0	0.4
100	0.3	100	0.4
105	0.12	105	0.4
125	0.12	130	0.12
140	0.12	150	0.12
150	0.12	160	0.12
200	0.12	200	0.12
205	0.12	205	0.12
215	0.12	210	0.12
220	0.12	350	0.12
400	0.12	500	0.12
640	0.12	660	5
700	0.5	700	5
1000	0.7	1000	5
1200	1.0	1200	5

Table 4-7: Thermal Coefficients

Material	Relative Emissivity	Convective Coeff Exp (W/m^2.K)	Convective Coeff UnExp (W/m^2.K)
Gypsum	0.8	5	12
Steel	0.5	12	12

5 PILOT-SCALE FURNACE TESTING

5.1 General

The experimental program was conducted at the testing facilities of the Building Research Association of New Zealand (BRANZ), Wellington. The testing program comprised of one standard and four non-standard non-loadbearing pilot scale furnace tests. The furnace relies on the combustion of diesel fuel to provide heat, which is monitored and controlled by four furnace type sheathed thermocouples. The pilot scale furnace is approximately 2.22 m high by 1.02 m wide, constructed from a steel frame lined with clay bricks. Figure 5-1 and Figure 5-2 show the pilot-scale furnace at the BRANZ testing facility.

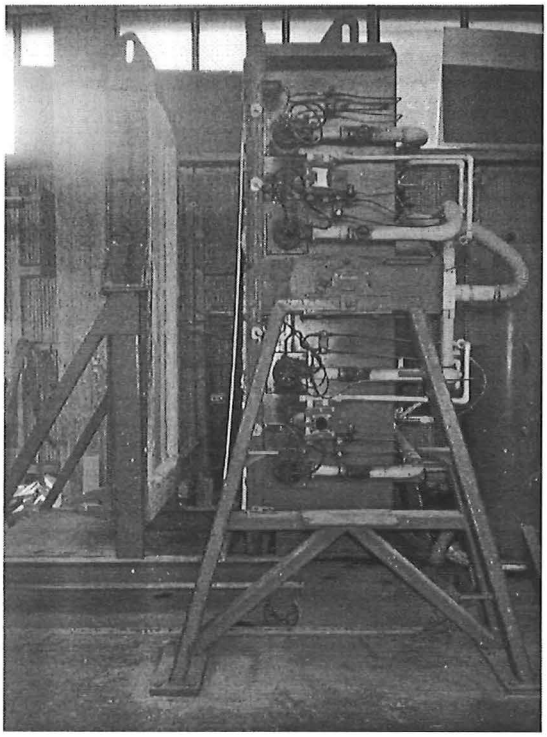

Figure 5-1: Side view of pilot-scale furnace.

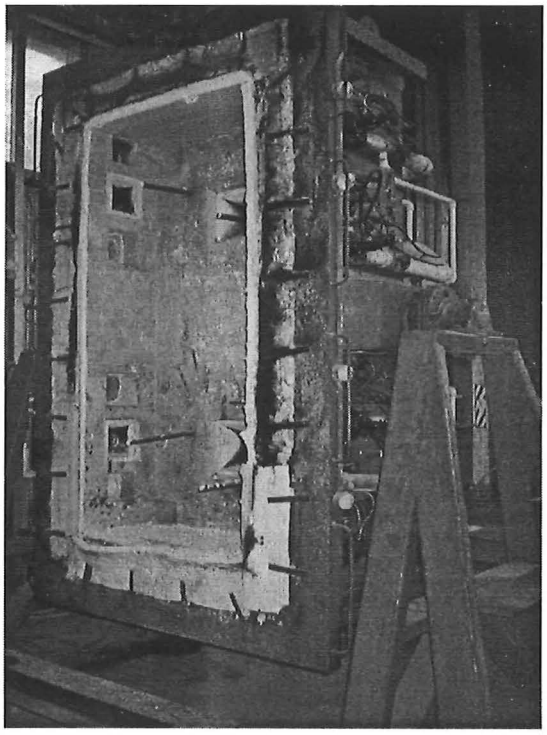

Figure 5-2: Front view of furnace.

The fire resistance rating of a loadbearing test specimen is defined by AS1530: Part 4 (SAA 1990) as the time to failure, expressed in minutes, under one or more of the following failure criteria:

- *Structural failure* is deemed to have occurred once collapse, excessive deflection or significantly reduced loadbearing capacity occurs;
- *Integrity failure* is deemed to have occurred upon collapse or the development of cracks, fissures, or other openings that permit the passage of hot gasses and flames from the unexposed face;
- *Insulation failure* is deemed to have occurred when either the average temperature of relevant thermocouples on the unexposed face of the specimen rises by more than 140°C, or when any one of these relevant thermocouples rises by more than 180°C above the initial temperature.

The first failure criterion does not apply since only non-loadbearing testing was performed. It must also be noted that the performance of a system in a pilot-scale test does not necessarily simulate the same systems performance in a full-scale furnace test due to size effects and boundary conditions.

5.2 Test Specimen Description

Specimens were constructed in steel specimen frames lined with concrete with the same nominal dimensions as specified for the furnace. All five test specimens were identical except for the type of lining. Test specimens had a wall height of 2220 mm and a stud spacing of 600 mm centres. The studs were constructed from 300 MPa cold formed galvanised steel "lipped" C-sections of dimensions 64 x 34 x 0.55 mm thick. All internal studs were constructed in a floating stud configuration. Table 5-1 provides an overview of the test specimens utilised in this study

Table 5-1: Pilot scale fire test specimens.

Furnace Tests No.	Exposed lining	Unexposed Lining	Fire Curve
FP2879	12.5 (Standard)	12.5 (Standard)	Non-standard
FP2880	12.5 (Standard)	12.5 (Standard)	Non-standard
FP2922	12.5 (Standard)	12.5 (Standard)	Standard (ISO834)
FP2881	12.5 (GIB® Fyreline)	12.5 (GIB® Fyreline)	Non-standard
FP2882	12.5 (GIB® Fyreline)	12.5 (GIB® Fyreline)	Non-standard

5.2.1 Steel Framing

Framing members consisted of RONDO® 0.55 BMT lipped steel studs and 0.55 BMT 'C' steel channel in a 'floating stud' construction.

Figure 5-3 gives the dimensions of both the channel and stud sections.

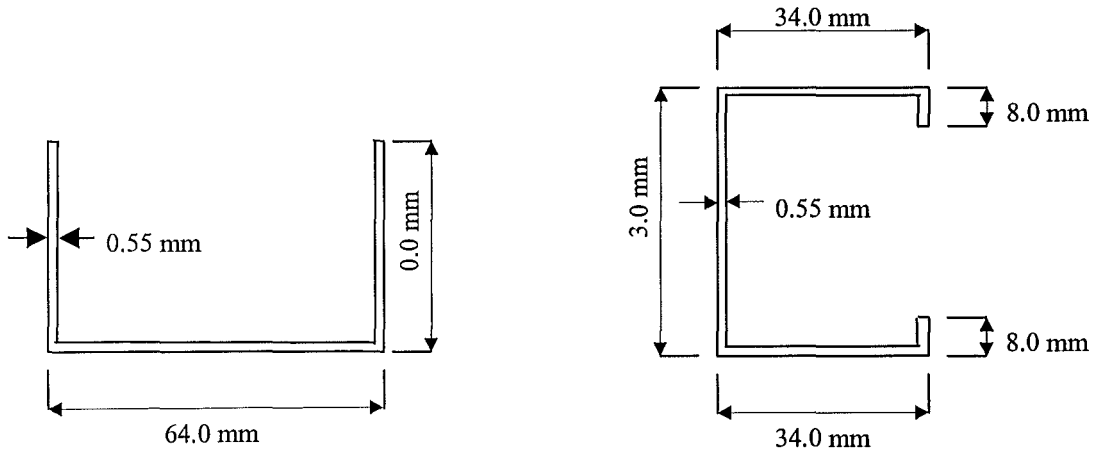

Figure 5-3: 0.55 BMT steel channel and 0.55 BMT steel stud sections.

The steel channel sections were placed at the top and bottom of the specimen frame to hold the studs in place. The studs were cut slightly shorter than the height of the frame to prevent premature failure of the system from buckling of the vertical studs, due to end restraint. Construction of the specimens followed typical industry construction practice, so that behaviour of the specimen during testing would be representable of a wall assembly constructed in a building.

Figure 5-4 displays the configuration and thermocouple layout for each specimen. The cold-formed steel members are identified as the dotted lines in Figure 5-4. No horizontal members (nogs/dwangs) are required because the specimen is non-loadbearing, therefore lateral support to prevent buckling under nominal loading is not necessary. Also, the height of the specimen allows the use of a full sheet of gypsum plasterboard. Had a horizontal joint been required then a horizontal framing member may have been needed to provide fixity and continuity of the lining.

The 1.02 m width allowed two studs at a spacing of 600 mm centres which is typical for non-loadbearing plasterboard wall assemblies.

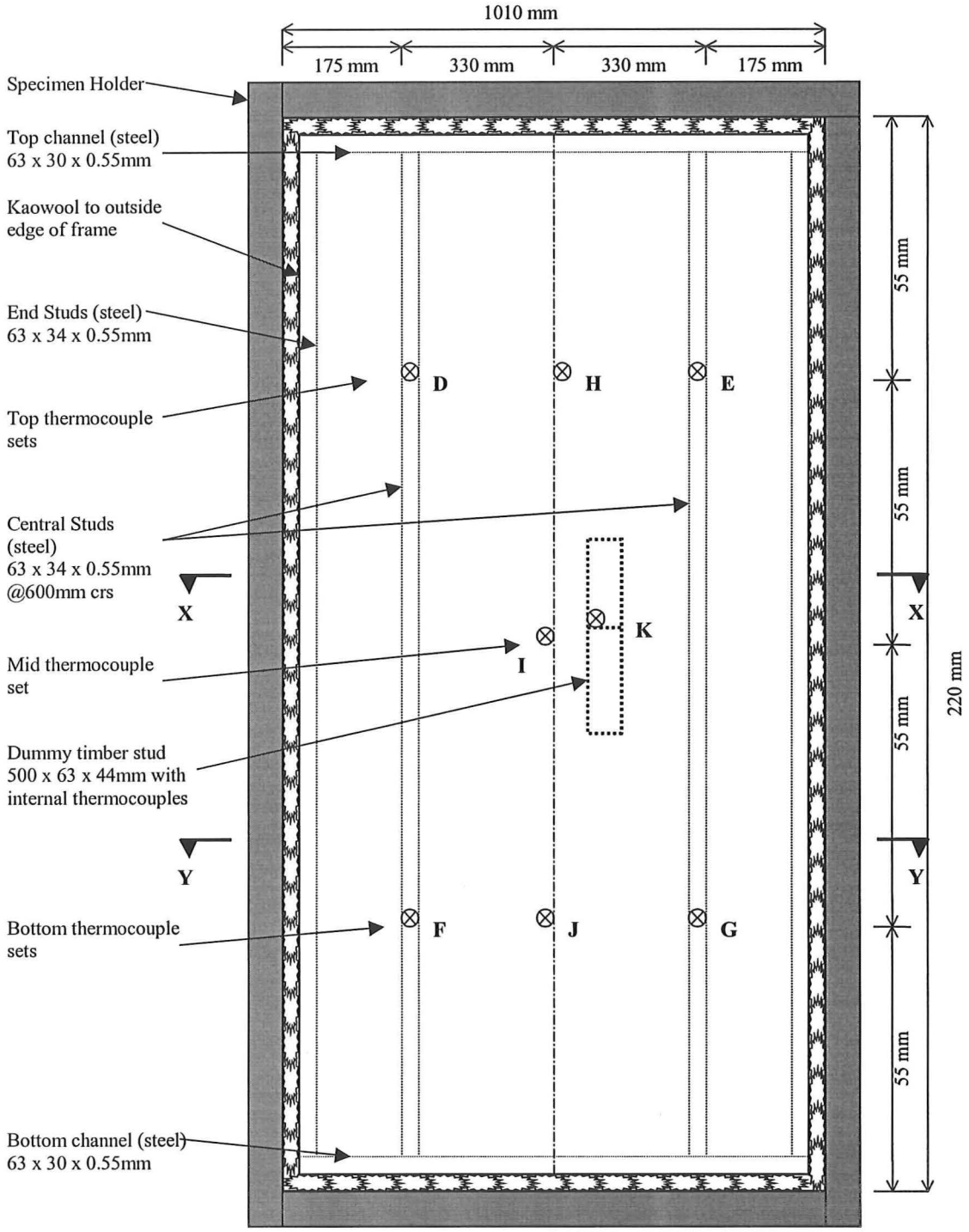

Figure 5-4: Specimen configuration and thermocouple layout.

5.2.2 Gypsum Plasterboard Linings

The steel frames were lined on both the exposed and unexposed face with a single layer of standard or fire rated gypsum plasterboard. The sheets were fixed vertically to all studs with 6-gauge 32 mm long self-drilling drywall screws spaced at 300 mm centres. The vertical sheet joints were formed over studs, tape reinforced and plaster stopped in accordance with recommended trade practice (Winstone Wallboards 1992b) using paper tape and two coats of bedding compound.

Mineral fibre wool (Kaowool) was used to insulate the specimen from the frame to avoid heat loss to the frame and to reduce the leakage between the frame and specimen. Figure 5-5 and Figure 5-6 detail typical cross sections of the test specimens. No penetrations were made in the fire exposed lining other than the single vertical lining joint and the vertical fixing screws into the steel studs. All penetrations in the unexposed lining were either stopped with plaster or filled with heat resistant compound. As can be seen from both Figure 5-5 and Figure 5-6 the vertical joints in the lining on the exposed and unexposed faces are staggered, which is typical commercial practice.

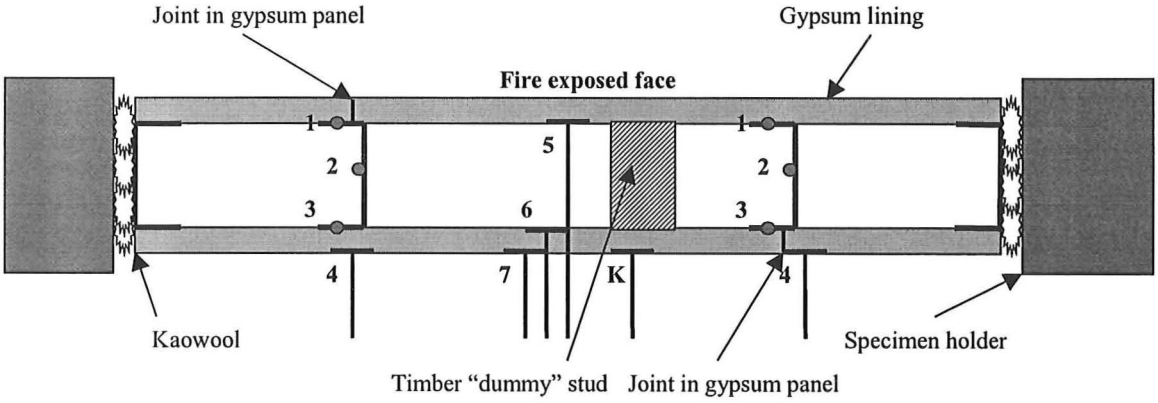

Cross Section XX

Figure 5-5: Cross section through cavity and dummy stud.

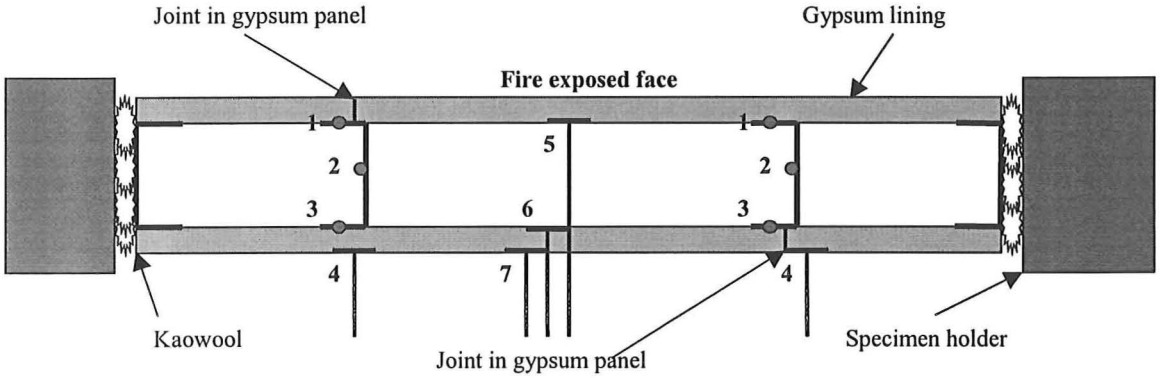

Figure 5-6: Cross section through cavity and studs.

5.2.3 Timber 'Dummy' Stud

The 500 x 63 x 44 mm dummy stud was placed midheight within the cavity of the specimen, instrumented internally with sheathed thermocouples to record temperature evolution through the timber member.

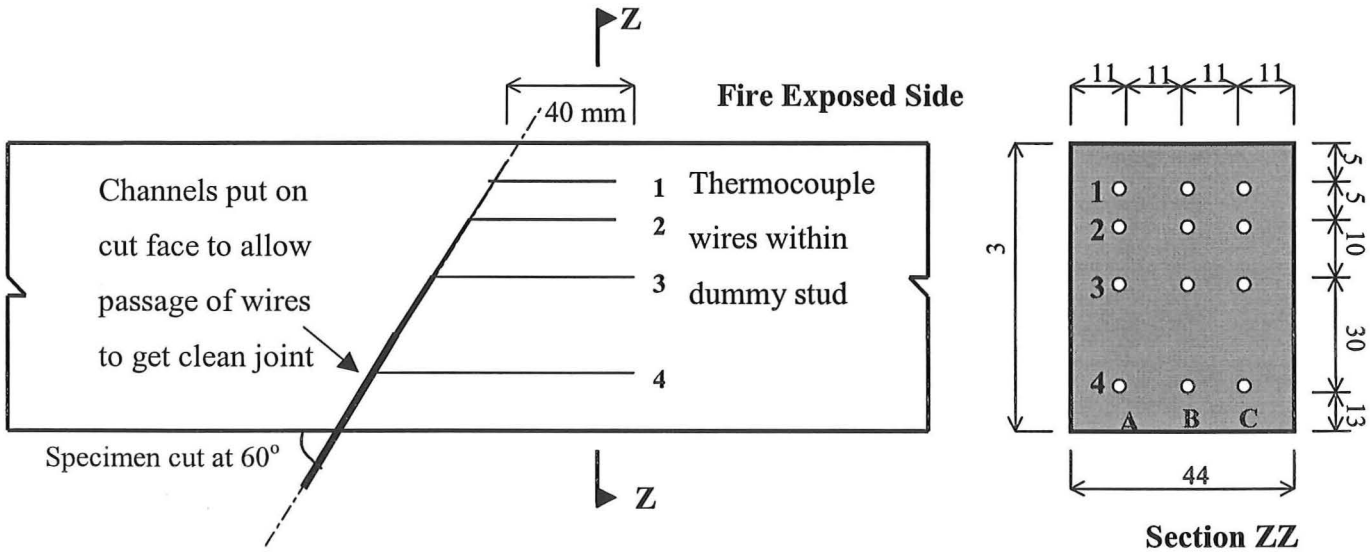

Figure 5-7: Detail and thermocouple configuration of dummy stud.

The most important feature in the design of these dummy studs was that temperature loss by conduction of heat away from the thermocouple tips was prevented by running sheaths parallel with isotherms for at least 25 mm (same direction as the wood grain in this case). Limiting bending to 60 degrees prevented damage to the thermocouple sheaths. To achieve this, the dummy studs were cut in the centre at 60 degrees to the grain and longitudinal holes drilled. The thermocouples were inserted into the holes and the stud sections were glued back together with resorcinol glue.

The reason for using the dummy stud is due to the difference in behaviour of wood and steel under elevated temperature conditions. Steel members tend to bow in towards the furnace due to thermal expansion and thermal gradients. However, wood on the other hand tends to deflect outwards from the furnace due to moisture loss and shrinkage. Emphasis was made on the behaviour of plasterboard systems incorporating the cold formed steel studs. There has been less research performed on the steel stud systems compared to timber framed systems, especially with regard to non-standard fires.

5.2.4 Instrumentation

In total, twelve wire thermocouples were welded to the flanges and web of the steel studs, fourteen copper disc thermocouples were employed to measure cavity and lining temperatures as detailed by Figure 5-4, Figure 5-5, and Figure 5-6. Twelve sheathed thermocouples were embedded into a timber dummy stud as detailed by Figure 5-7. Four furnace grade sheathed thermocouples were employed to monitor furnace performance and record temperatures on exposed lining. All thermocouples were calibrated and checked prior to testing. A typical thermocouple set up is shown by Figure 5-8.

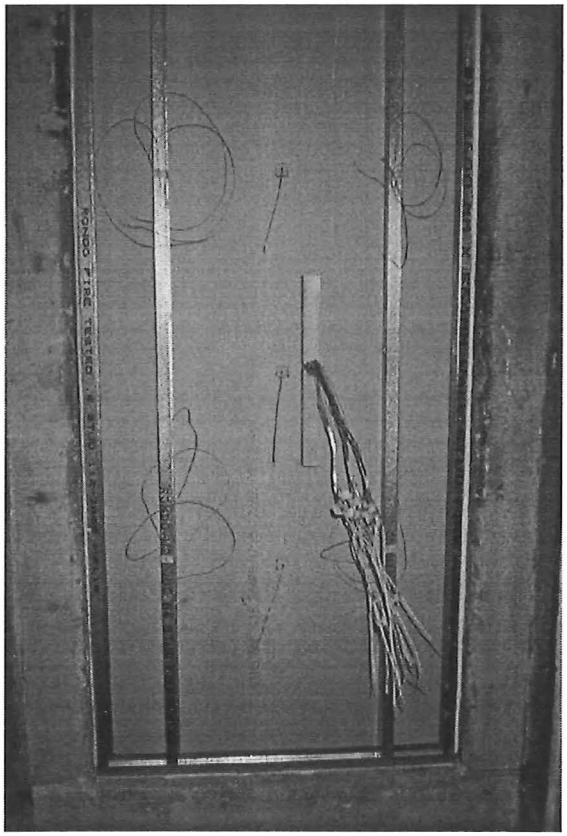

Figure 5-8: Typical thermocouple layout in specimen.

5.3 Furnace Time-Temperature Input

5.3.1 Standard Fire Curve

The furnace time-temperature input for test FP2922 was in accordance with the standard ISO834 fire curve (ISO834 1975) as defined by Equation [5-1].

$$T - T_0 = 345 \log_{10}(8t + 1) \qquad \textbf{[5-1]}$$

Modelling the behaviour of gypsum plasterboard systems exposed to the ISO834 furnace curve will provide calibration for the thermal properties and parameters used within computer software thus providing a baseline from which to extend the software capabilities to model non-standard fires.

5.3.2 Non-Standard Fire Curves

Non-standard time-temperature input curves for furnace tests FP2879, FP2880, FP2881, and FP2882 are extrapolated upon work performed by Collier (1996b). The non-standard time-temperature curves are intended to simulate fires that are both more and less severe than the standard ISO834 fire curve, as shown by Figure 5-9.

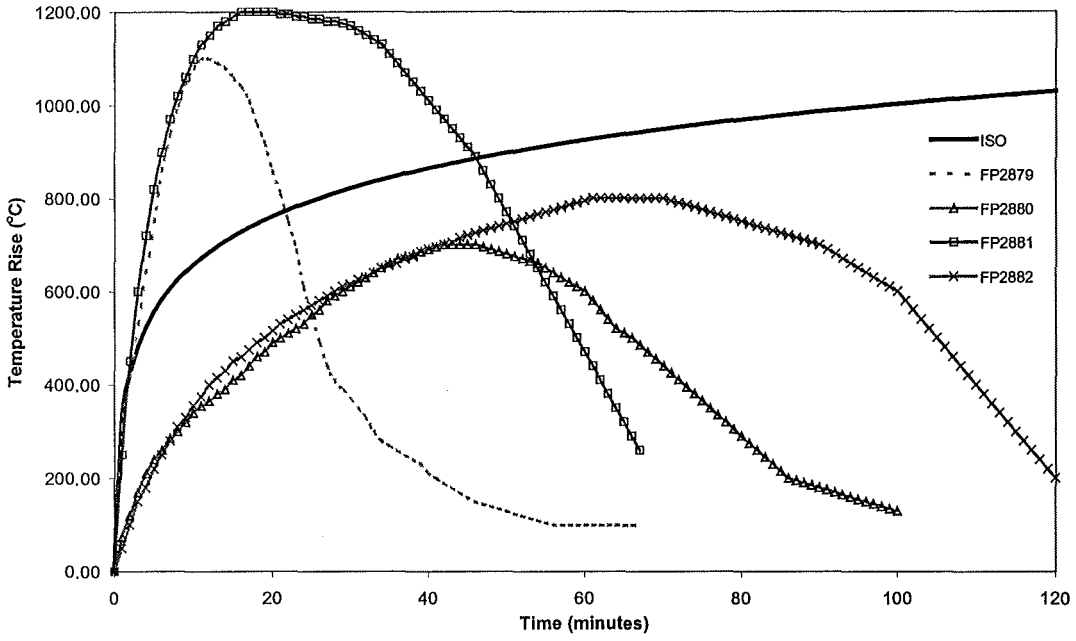

Figure 5-9: Comparison of proposed input time-temperature curves with ISO834 curve.

Proposed furnace curves FP2879 and FP2881 represent rapid growth fires reaching high temperatures early on in the test with relatively rapid decay phases. FP2880 and FP2882 represent slower burning fires with slow growth to near steady state conditions at moderate temperatures and slow decay phase. Testing a significant deviation from the standard ISO834 curve was intended to determine the ability of the theoretical model to predict the performance of light frame drywall systems exposed to realistic non-standard fire conditions.

The fire curves have been formulated to achieve failure within each of the systems. Both time-temperature curves FP2879 and FP2880 are to be applied to a system with

a 30 minute fire rating to the standard curve, whereas FP2881 and FP2882 are to be applied a 60 minute system.

By assigning a Eurocode parametric curve to the non-standard curves, an opening factor for a standard sized compartment may be calculated and provide a comparative value between the curve and other research performed on compartment fires. The Eurocode parametric fire curves are given by Equation [5-2].

$$T=1325(1-0.324e^{-0.2\zeta}-0.204e^{-1.7\zeta}-0.472e^{-19\zeta}) \quad \textbf{[5-2]}$$

Where ζ is a fictitious time (minutes) given by

$$\zeta=\Gamma t \quad \textbf{[5-3]}$$

Where t is the time (minutes) and

$$\Gamma=\frac{(F_v/F_{ref})^2}{\left(\sqrt{(k\rho c_p)/I_{ref}}\right)^2} \quad \textbf{[5-4]}$$

Where F_v is the opening factor ($\sqrt{m}$) given by

$F_v = A_v\sqrt{H_v}/A_t$

F_{ref} is the reference value of the opening, typically taken to be a value of 0.04 ($\sqrt{m}$)

$K\rho c_p$ is the thermal inertia of the compartment walls (W^2s/m^4K^2)

I_{ref} is the reference value of $\sqrt{(k\rho c_p)}$ ($Ws^{1/2}/m^2K$)

A_v is the area of the vertical opening

H_v is the height of the vertical opening

A_t is the total surface area of the compartment

In order to concentrate on the equivalent opening factor related to the furnace curves, the ratio of the thermal inertia to the reference value will be taken as unity and the reference opening factor F_{ref}, will be taken as 0.04 ($\sqrt{m}$), as recommended by the Eurocode. The furnace curves were approximated by the parametric curves by altering the value of the factor Γ. Rearranging Equations [5-3] and [5-4] to solve for the opening factor gives values for the opening factor for each furnace curve in Table 5-2.

Table 5-2: Equaivalent opening factors for non-standard furnace temperature curves.

Non-Standard Furnace Curve	Opening Factor, F_v ($\sqrt{m}$)
FP2879	0.017
FP2880	0.0026
FP2881	0.02
FP2882	0.0027

Typical opening factors for compartment fires are in the range of 0.02 – 0.12 ($\sqrt{m}$) as reported by both Thomas (1997) and Buchanan (2000). Calculated opening factors for the more severe furnace tests FP2879 and FP2881 given in Table 5-2 are approximately equivalent to a parametric curve with a relatively slow growth. The opening factor for the slower furnace test are much lower than typical values. The Eurocode parametric temperature curves relate to compartment fires of varying severity. The equivalent opening factors in Table 5-2 indicate that the time-temperature curves used in the non-standard furnace tests are very mild in terms of their comparison with typical compartment conditions.

5.3.3 Furnace Pressure

The specimen holder containing the wall assembly was sealed against the furnace and the furnace pressure was maintained at least 2 Pa greater than the laboratory pressure over the top two thirds of the specimen as outlined in AS1530: Part 4.

5.4 Behavioural Observations from Furnace Testing

Observations of tests performed at the Building Research Association of New Zealand (BRANZ) have shown variation in the behaviour of gypsum plasterboard exposed to non-standard fire curves. Recorded observations from each test are given in Appendix 2.

5.4.1 Rapid Fire Growth and High Temperatures

When standard gypsum plasterboard (no vermiculite or glass-fibre reinforcing) is subjected to rapid fire growth, small crazing of the exposed face initially occurs.

Much larger concentrated cracking then occurs, due to the shrinkage of the exposed lining. Differential temperatures of the steel studs cause the studs to deflect towards the furnace, which causes the cracking in the exposed face to increase. The large cracks (3 – 5 mm) allow the passage of hot gases into the cavity. Once this occurs the exposed panel degrades quickly and sections of the panel detach from the studs and fall into the furnace. Inspection of the remains of the fallen panel show that the lining has broken down into fragments (10 - 15 cm in diameter) with an appearance similar to that of chalk.

When fibre-reinforced plasterboard with vermiculite (GIB® Fyreline) was subjected to a rapid fire growth, changes in the physiology of the board were quite abrupt. It was noticed that the fire rated board lost the exposed paper face much earlier than the standard board. Simple ignition tests showed that the coloured dye used in the paper facing of the board caused it to become more combustible than it otherwise was. As with the standard board, the exposed face of the fibre-reinforced board began to craze, with small cracking developing as temperatures increased. However, due to the presence of the glass-fibre reinforcing, shrinkage and thermal deformations did not increase the crack openings during the early stages of the fire exposure.

As the vermiculite expanded and the glass-fibres within the lining began to melt, the exposed face began to flake and fall into the furnace. The reduced cross sectional thickness of the exposed lining combined with the tensile forces induced by the deflection of the steel studs caused localised cracking in the lining near the fasteners. The exposed panel then broke into sections and fell into the furnace exposing the light frame. Inspection of the fallen panel after the test revealed that the exposed panel had broken down into sections of similar size to that of the standard board, but with a "flaky" appearance.

5.4.2 Slow Fire Growth Moderate Temperatures

As expected the degradation of the standard board is much slower when exposed to a moderate severity fire curve. The paper facing remained on the exposed lining for almost 10 minutes before burning compared to approximately 5 minutes for the more severe furnace exposure. Once the face paper had burnt off, exposing the gypsum

plaster, small crazing of the lining was observed, which is typical behaviour. Continued exposure leads to the formation of small horizontal cracks, which are more prominent than the effects of shrinkage in the vertical direction. Further shrinkage of the board and bowing of the steel studs towards the furnace increases horizontal crack widths with fine vertical cracking linking the horizontal cracking. Crack widths continue to increase until sections of panel begin to fall into the furnace exposing the internal cavity. The fallen remains of the exposed gypsum panel had broken down into much finer particles (1 – 2 cm) than that of the severe fire test, indicating a more uniform heating of the plasterboard.

Initially the fire rated gypsum plasterboard exposed to the moderate severity fire curve exhibited similar behaviour to that of the fast fire test. The paper facing burned off, exposing the plasterboard with fine crazing and light ablation of the surface. However, the duration in which these processes occurred was much greater for the slow fire exposure. Once the furnace test was out of the growth phase the rate of rise in temperature of the lining reduced and the exposed board remained unchanged for the remainder of the test. Investigation of the exposed lining after the test revealed that although the board was completely dehydrated, the fibreglass reinforcing was still present maintaining the linings integrity. Although the dehydrated lining provided very little thermal barrier, it did prevent the cavity and unexposed lining from being exposed directly to furnace conditions.

5.5 Furnace Temperatures

Figure 5-10 to Figure 5-14 show the actual time-temperature curves produced within the furnace. Considering the difficulties involved with controlling the furnace, the operators achieved a reasonable approximation of the desired curves. Comparing the area under both the proposed and actual furnace curves gives reassurance that the desired severity was achieved.

5.5.1 Standard Plasterboard Exposed to Severe Fire (FP2879)

The furnace conditions obtained are clearly more severe than that of the standard ISO834 curve, at least for the first 20 to 25 minutes. The intention of this fire curve was to impose a greater thermal shock on the drywall system. The accounts of the observations given in Section 5.4.1 indicated that crazing and cracking of the exposed surface occurred much earlier than observed in standard furnace tests performed at BRANZ. However, this was the first test performed in the series of furnace tests and the system did not show signs of failure until well into the decay phase. This is why an insulation failure was not reached and integrity failure did not occur until 34 minutes after ignition.

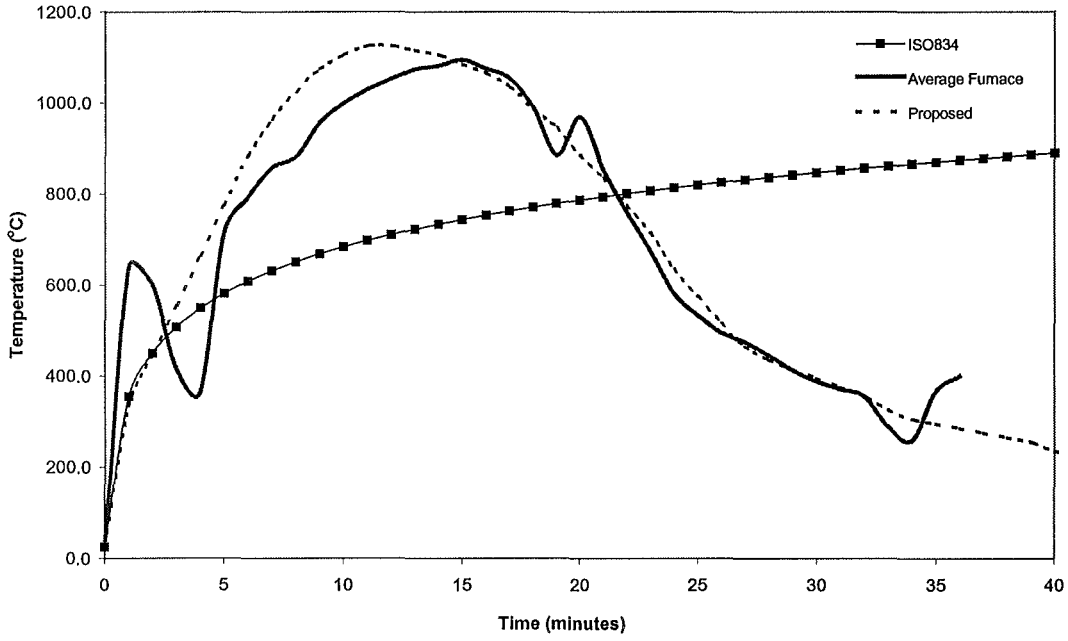

Figure 5-10: Actual and proposed furnace temperatures for FP2879.

The system has a fire rating of 30 minutes (exposure to the standard ISO834 curve). It was expected that the system exposed to the more severe fire would reach failure well before 30 minutes, but the long decay phase of the time-temperature curve used in furnace test FP2879 prolonged the performance of the assembly.

5.5.2 Standard Plasterboard Exposed to Moderate Severity Fire (FP2880)

In comparison to the fast fire used in furnace test FP2879, furnace conditions within FP2880 are much less severe. The oscillation of the actual furnace curve about the proposed curve, as shown in Figure 5-11, was due to difficulties in maintaining ignition of the fuel within the furnace in order to follow the slow growth curve. For the initial fifteen minutes of the test the fuel feed into the furnace was too low to maintain burning, so the fuel feed had to be increased periodically to enable ignition of the fuel. This pattern persisted until desired temperatures within the furnace were high enough to maintain burning within the furnace.

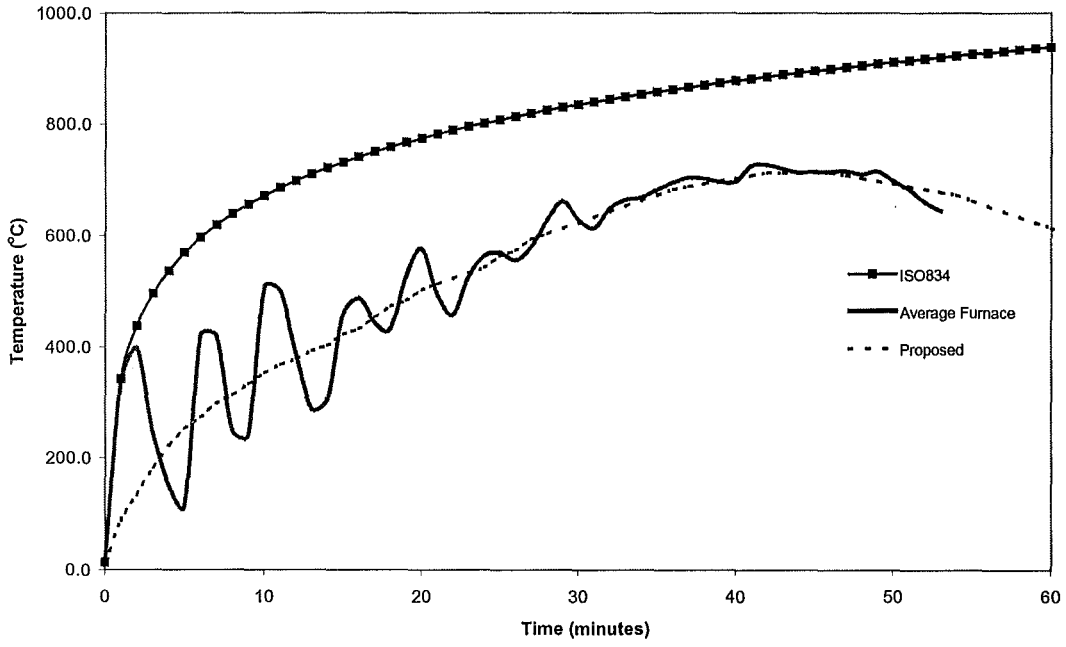

Figure 5-11: Actual and proposed furnace temperatures for FP2880.

This gentler fire curve was used to evaluate the effect of slower heating rates on the system and to determine how long the assembly would provide fire resistance beyond its proprietary rating of 30 minutes.

The severity of the actual furnace curve was very close to that proposed, and it is assumed that the temperature fluctuations at the beginning of the test had little influence on the overall performance of the system.

5.5.3 Standard Plasterboard Exposed to ISO834 Furnace Curve (FP2922)

The furnace drive system is designed for following the standard curve so provides better control over the furnace temperatures. This is why the actual furnace temperatures closely follow the desired curve shown in Figure 5-12.

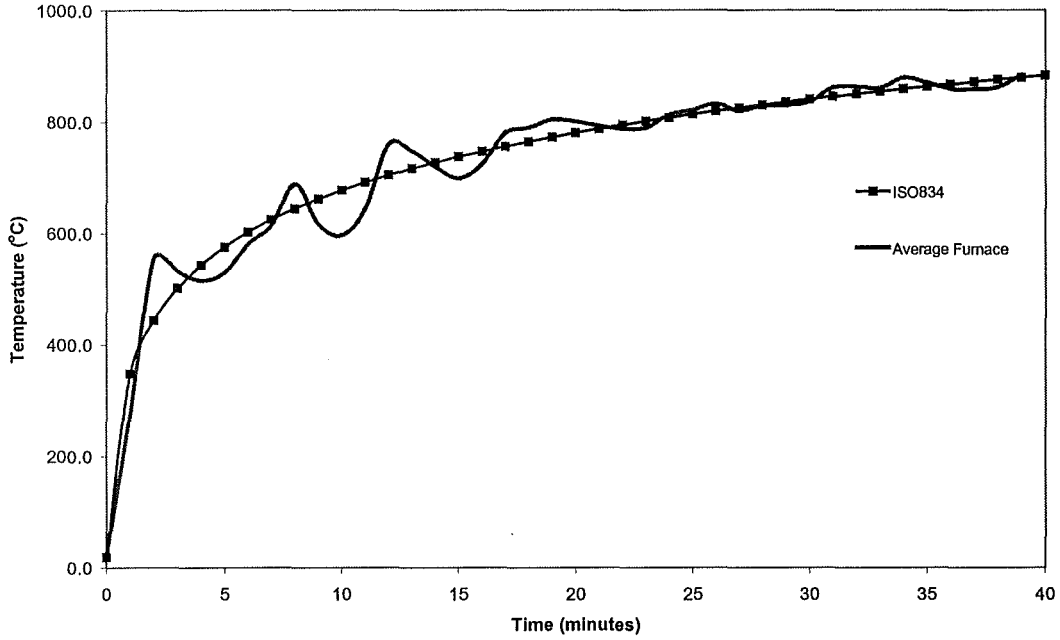

Figure 5-12: Actual and proposed furnace temperatures for FP2922.

Previous proprietary testing of this system to the ISO834 standard curve achieved a fire resistance rating of 30 minutes (Winstone Wallboards 1997). An integrity failure occurred in test specimen FP2922 at approximately 38 minutes, which provides good agreement with the proprietary rating. It must be noted that full-scale furnace testing which is used to assign fire resistant ratings to products, tends to be slightly more severe than an equivalent pilot-scale furnace test.

5.5.4 Fire Rated Plasterboard Exposed to Severe Fire (FP2881)

Although the actual furnace curve depicted in Figure 5-13 varies from the proposed curve, the objective of obtaining furnace conditions that are more severe than the standard ISO834 curve for the same duration was achieved.

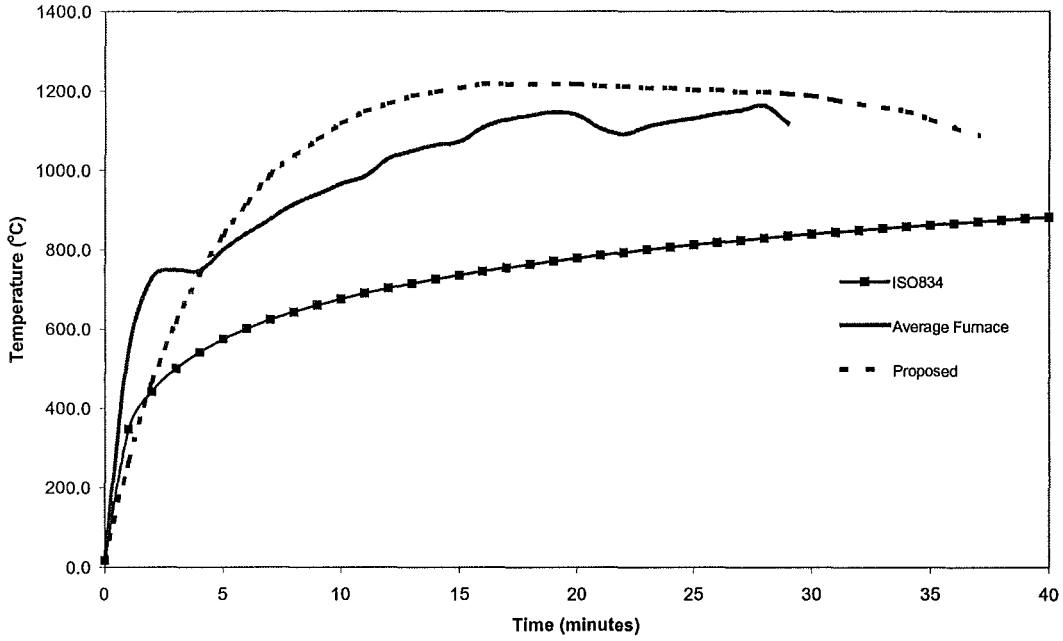

Figure 5-13: Actual and proposed furnace temperatures for FP2881.

The lag in temperatures after approximately five minutes is mainly due to the inability of the furnace system to provide sufficient atomising air to maintain complete combustion. Smoke within the furnace not only played havoc with visibility but may have also affected heat transfer from the furnace to the exposed panel due to its effect on the furnace emissivity. However, Thomas (1997) performed a sensitivity study to evaluate the effect of varying the furnace emissivity, and found that it had little influence on the exposed wall surface temperatures.

Previous proprietary testing of this system to the ISO834 standard curve achieved a fire resistance rating of 60 minutes (Winstone Wallboards 1997). In this test an integrity failure occurred in furnace test FP2881 at 28 minutes, therefore reducing the fire resisting performance of the system by over 50%.

5.5.5 Fire Rated Plasterboard Exposed to Moderate Fire (FP2882)

Similar problems with driving the furnace to low temperatures in furnace test FP2880 also occurred in FP2882. However, the previous experience allowed the operators to follow the curve more closely as indicated by the early stages of the furnace curve shown by Figure 5-14. Cooling the furnace in the decay phase of the fire curve proved difficult, which explains the deviation of the actual furnace curve from the proposed curve.

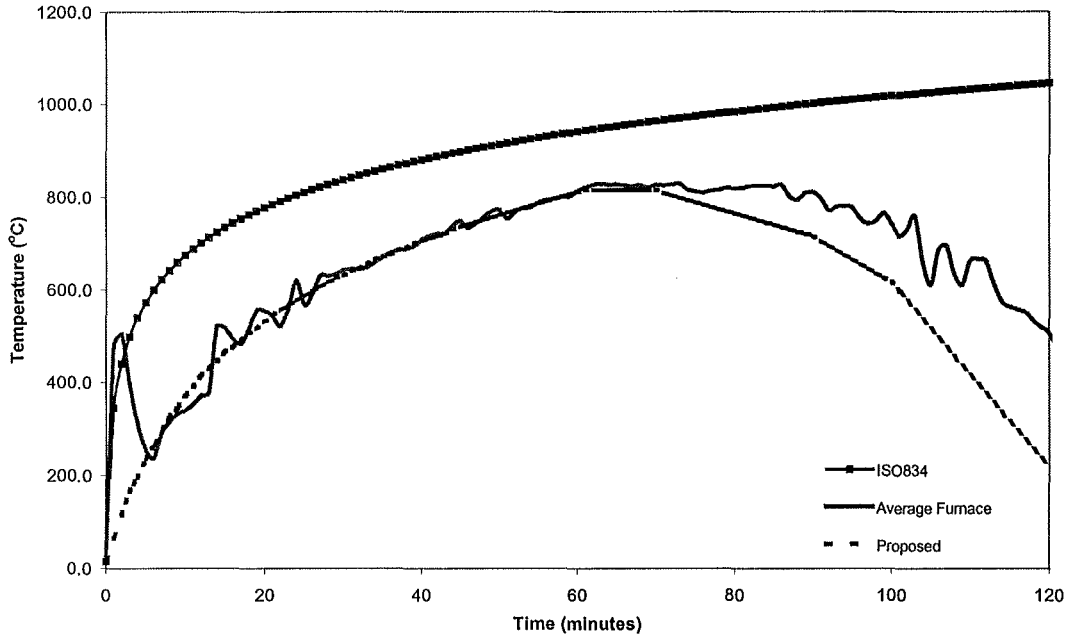

Figure 5-14: Actual and proposed furnace temperatures for FP2882.

The system with a fire rating of 60 minutes sustained the furnace fire for 82 minutes at which point an insulation failure occurred. Allowing the test to proceed into the decay phase produced an integrity failure at 122 minutes. The gentle curve of furnace test FP2882 allowed more uniform heating of elements within the assembly, which is why the unexposed lining was still intact and the steel studs had undergone very little deformation.

5.6 Observations and Temperatures in Steel Studs and Cavity

The averaged evolution of temperature through the steel studs and the cavity between the gypsum plasterboard linings is shown by Figure 5-16 through to Figure 5-20. The temperatures of the steel studs were recorded at four locations on the specimen and the cavity temperatures were measured at three positions on the assembly as indicated by Figure 5-4. Individual temperature readings from each location were plotted for consistency before averaging and spurious results were eliminated if required.

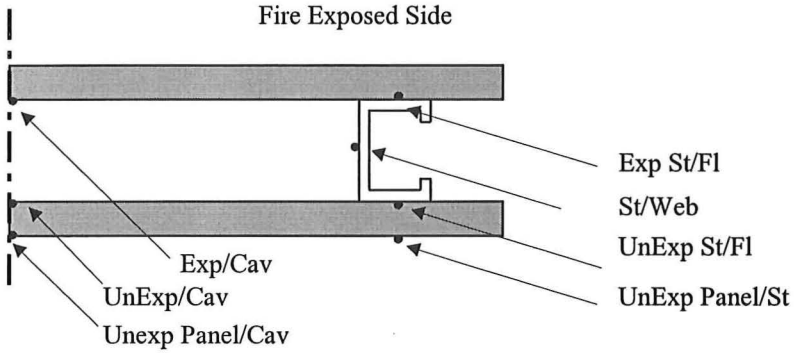

Figure 5-15: Key to temperature measurement in steel stud and cavity.

The locations at which temperature readings were taken from the cross section and their relation to the following plots is given by Figure 5-15. Faulty temperature readings tended to arise from detachment of the thermocouple from the surface being measured. This typically occurred to the welded thermocouples, which were either pulled from the steel stud by the falling panel or popped off the stud due to a poor weld and differential thermal expansion. Several disc thermocouples measuring the temperature of the cavity side of the exposed lining also provided erroneous results once the exposed lining began to fall from the assembly.

5.6.1 Standard Plasterboard Exposed to Severe Fire (FP2879)

The thermal lag created by the gypsum plasterboard lining is clearly portrayed by Figure 5-16. Dehydration of plasterboard maintains the steel stud and cavity temperatures at approximately 100°C, while temperatures within the furnace are exceeding 1000°C. After about 15 minutes the fire exposed board is almost

completely dehydrated and the effect of shrinkage has cracked the board allowing the passage of hot furnace gases into the cavity. This causes a rapid rise in the temperatures of the steel studs and cavity, which relates to observations of the fire exposed lining falling into the furnace at approximately 16 minutes.

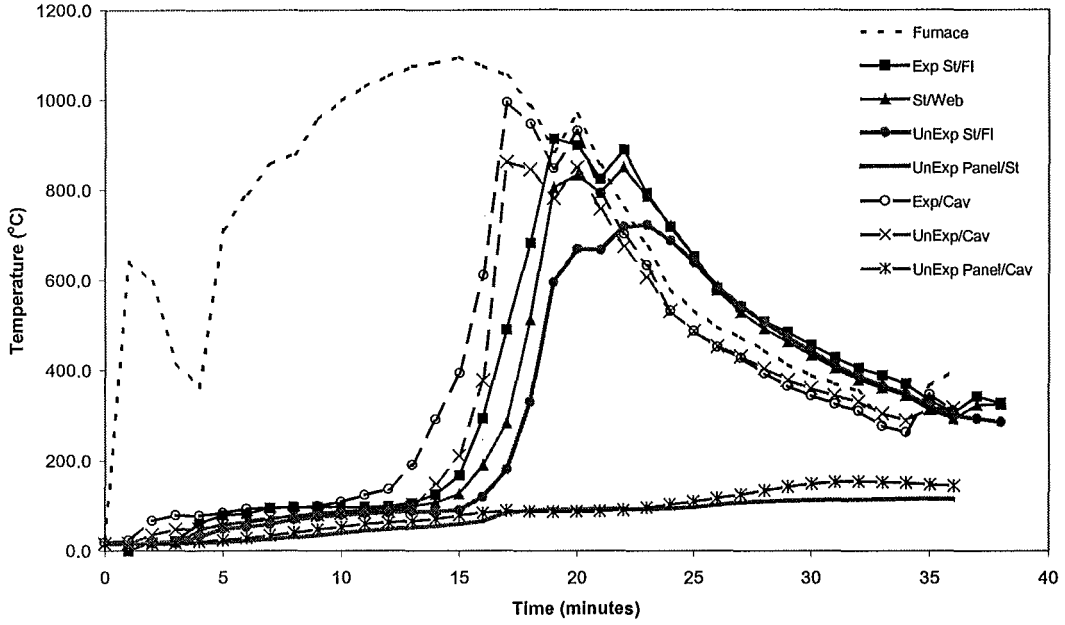

Figure 5-16: Evolution of temperature through steel studs and cavity (FP2879).

Once the fire exposed lining is lost, temperatures of the steel stud and cavity increase rapidly to converge with furnace temperatures. The quick response of the thermocouples to fluctuations in furnace temperature at approximately 20 minutes clearly indicates that the internal components of the assembly are being directly subjected to furnace conditions. Both the exposed flange and web of the steel stud follow similar temperature profiles. The unexposed flange temperatures lag slightly due to the steel stud shielding the thermocouple from furnace conditions and cooling from the unexposed panel.

Once cracking of the exposed lining occurs the temperature profiles of the steel stud begin to lag behind the cavity temperatures due to the passage of hot gases into the cavity and the thermal inertia of the steel studs. The temperature profiles of both the steel studs and the cavity converge once the exposed lining has fallen.

5.6.2 Standard Plasterboard Exposed to Moderate Severity Fire (FP2880)

As would be expected the duration of the temperature plateau arising from dehydration of the gypsum plasterboard is much greater than that obtained in the more severe furnace test FP2879. Figure 5-17 indicates that steel stud and cavity temperatures do not start rapidly increasing until approximately 30 minutes after ignition.

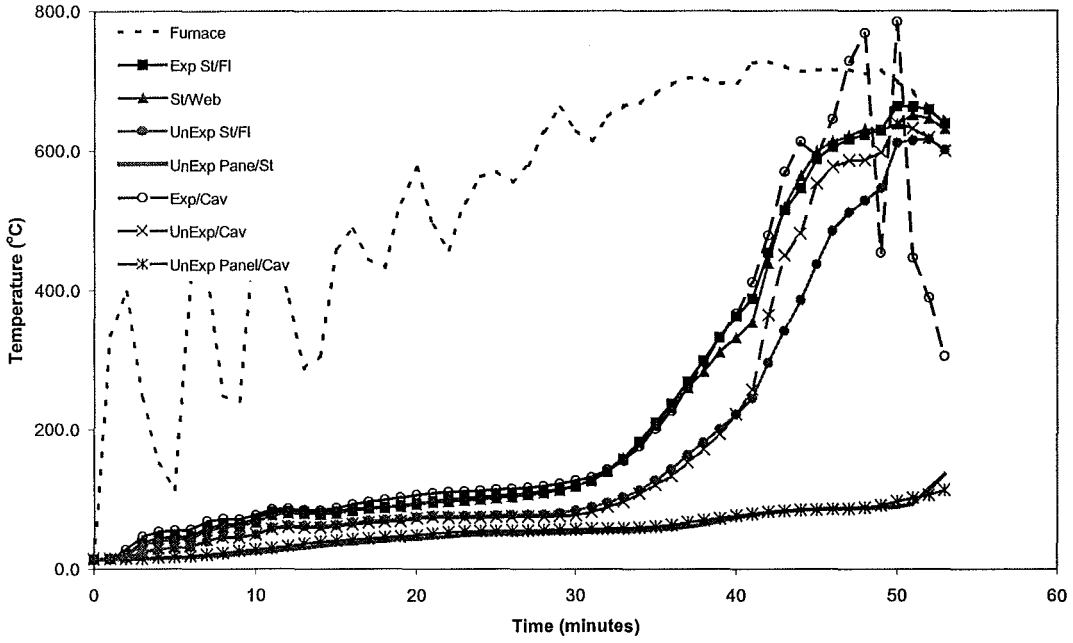

Figure 5-17: Evolution of temperature through steel studs and cavity (FP2880).

The exposed flange and web of the stud follow very much the same temperature profile, which is indicative of the low rates of temperature rise in furnace test FP2880, providing a more uniform heating environment. The unexposed flange temperatures deviate from the temperatures of the rest of the section due to cooling from the unexposed panel. The low heating rate of this furnace test reducing the thermal gradient across the assembly is also portrayed by the closeness of the cavity and steel stud temperatures. In the more severe furnace test of FP2879 the stud temperatures tended to lag those of the cavity until the exposed lining had fallen. At around 45 minutes the temperature profile of the exposed cavity begins to fluctuate due to the exposed panel detaching from the frame and hanging off the thermocouple wire.

It can be seen from Figure 5-17 that the cavity temperatures of the unexposed panel follow the unexposed flange temperatures of the steel stud for the first 40 minutes. At which point the exposed panel begins to degrade. This increases the rate of temperature rise of the unexposed panel within the cavity, while the thermocouples on the unexposed flange of the steel stud were sandwiched between the stud and the unexposed panel, shielding them from the furnace gases. The deviation of the unexposed flange and unexposed cavity temperatures at approximately 41 minutes, is a result of this.

5.6.3 Standard Plasterboard Exposed to ISO834 Furnace Curve (FP2922)

The relatively constant rate of temperature rise after the initial growth phase of the standard ISO834 curve produces a reasonably wide range of temperatures across the steel stud once calcination of the gypsum lining has occurred. Sultan 1996 reports that at temperatures of around 600°C the exposed gypsum plasterboard tended to lose its integrity and either cracked or partially fell into the furnace. Both the results shown in Figure 5-18 and observations from furnace test FP2922 reinforce this concept.

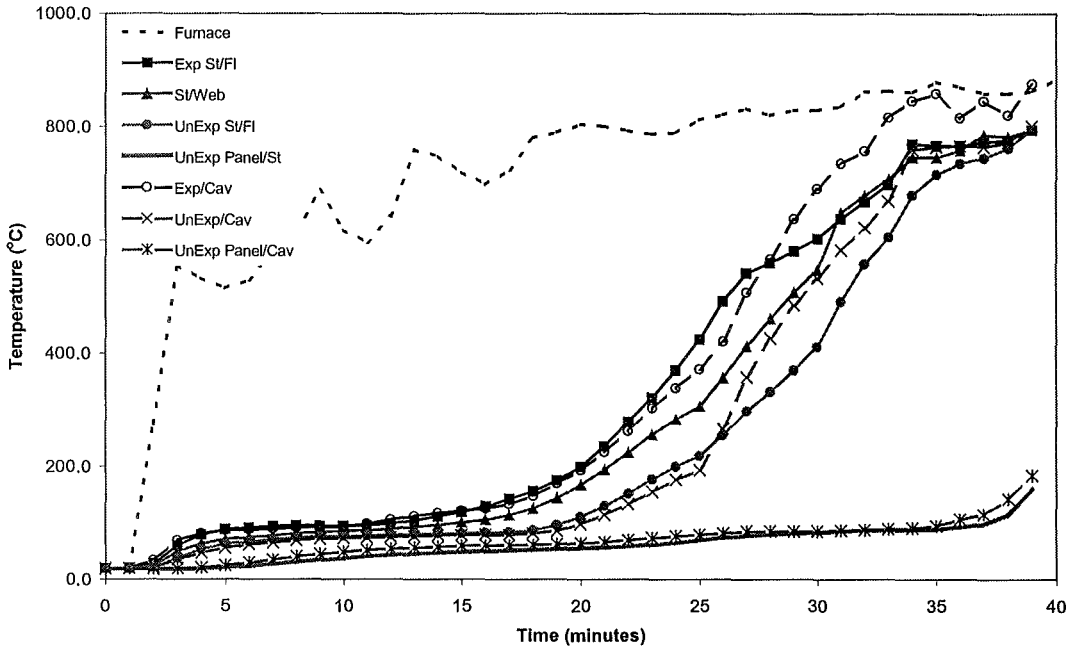

Figure 5-18: Evolution of temperature through steel studs and cavity (FP2922).

The fire exposed gypsum plasterboard lining was observed to begin falling from the assembly at approximately 28 minutes after ignition. This relates to a lining temperature of around 600°C on Figure 5-19, at the same point the steel stud and cavity temperatures converge indicating that the exposed lining no longer exists, as both components are being subjected to the same furnace conditions. Similar to furnace test FP2879, the low rate of temperature rise creates a relatively uniform heating environment. Therefore cavity and steel stud temperatures were not lagging as in furnace test FP2879.

5.6.4 Fire Rated Plasterboard Exposed to Severe Fire (FP2881)

Figure 5-19 clearly depicts the transition between the typical behavioural phases exhibited by an assembly when subjected to elevated temperatures. The rapid rate of temperature rise used in furnace test FP2881 has caused abrupt changes in the heating regime of the steel studs and cavity compared to the more flowing curves obtained in the less severe furnace tests.

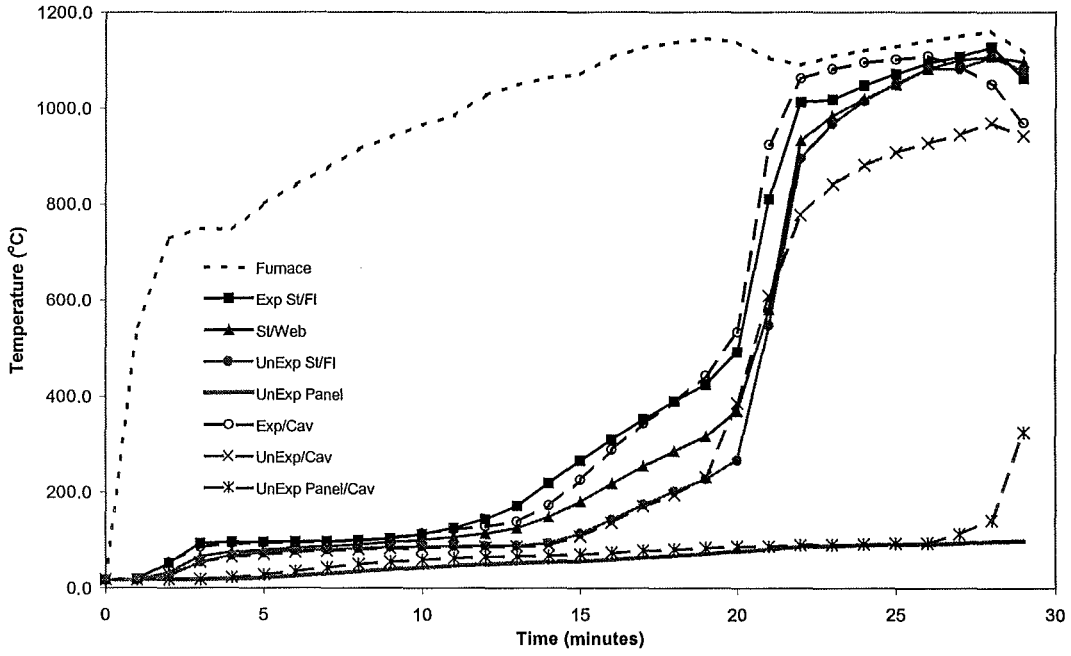

Figure 5-19: Evolution of temperature through steel studs and cavity (FP2881).

Dehydration of the exposed gypsum lining keeps the steel stud and cavity temperatures at around 100°C for the first 12 minutes. At which point the exposed lining is completely dehydrated increasing the thermal conductivity of the plasterboard. This combined with the presence of small cracking allowing the passage of hot gases into the cavity increasing the rate of temperature rise of the studs and cavity. Between 20 to 23 minutes after ignition the exposed lining is falling away exposing the steel studs to full furnace temperatures, which also accounts for the convergence in steel temperature profiles. Direct exposure to the furnace increases the rate of temperature rise until the steel stud and furnace temperatures converge at about 25 minutes after ignition.

Although the presence of smoke in the furnace impeded vision of the exposed panel, it is believed to have remained in place until about 20 minutes after ignition. At which point sounds of material hitting the furnace floor were heard, which agrees with the rapid rise of temperatures in Figure 5-19. The reason why the assembly used in furnace test FP2881 does not exhibit similar behaviour to that of FP2879 with the steel stud temperatures lagging the cavity temperatures once cracking commences is likely to be due to the presence of a fire rated plasterboard. Instead of large cracking occurring once the exposed standard plasterboard had dehydrated allowing hot gases into the cavity (as occurred in furnace test FP2879), the presence of glass fibre reinforcing and vermiculite in the fire rated board restricted crack openings. This reduced the flow of furnace gases into the cavity. Therefore the cavity and steel studs continued to heat at a similar rate until large deflections of the steel studs towards the furnace caused the weakened exposed lining to crack and fall to the bottom of the furnace.

5.6.5 Fire Rated Plasterboard Exposed to Moderate Severity Fire (FP2882)

As can be seen from Figure 5-20 the low severity of furnace test FP2882 has imposed a moderate thermal loading on the exposed assembly with maximum temperatures within the cavity only just exceeding 600°C. This explains the behaviour of the exposed lining as it remained attached to the frame throughout the duration of the test.

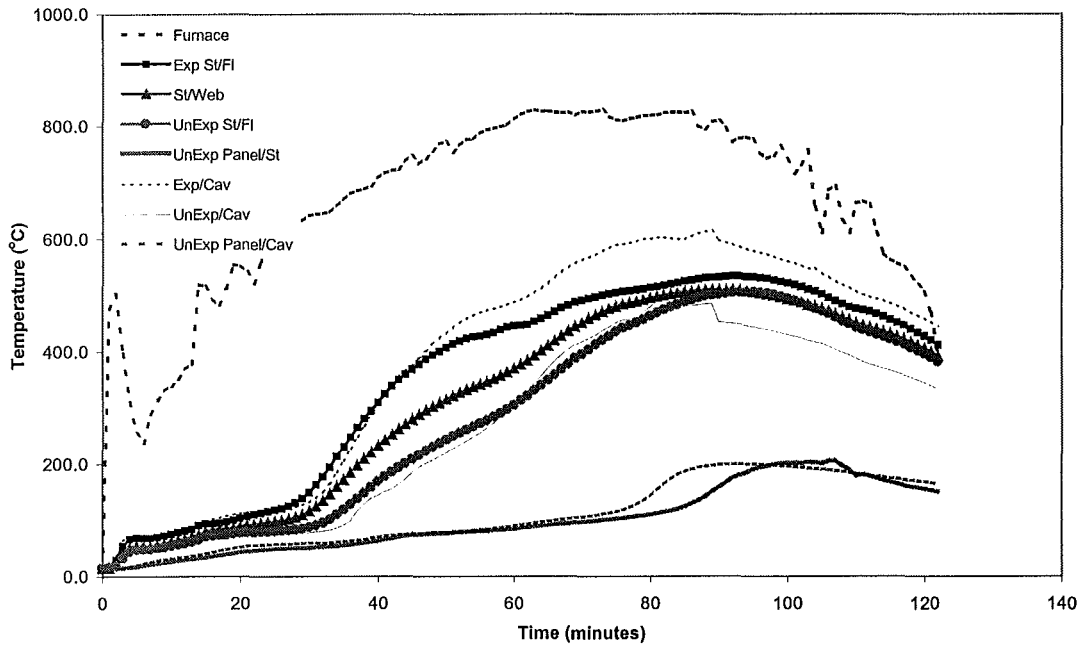

Figure 5-20: Evolution of temperature through steel studs (FP2882).

The low rates of temperature rise allowed the steel studs to heat more uniformly thus reducing the thermal gradient across the section. This reduced the deflection of the studs towards the furnace and minimised the tensile forces imposed on the exposed lining, therefore reducing cracking.

This furnace test clearly indicates the influence that the exposed lining has on the performance of the rest of the assembly. By remaining in place, the exposed lining maintained a thermal lag between the furnace and the cavity/steel studs until well into the decay phase of the time-temperature curve. The assembly failed to maintain a sufficient insulating barrier at approximately 82 minutes. Failure occurred in the cavity region of the unexposed face as shown by Figure 5-20, where temperatures of the unexposed face in the cavity region increase before those of the steel studs. This indicates that radiation across the cavity, rather than conduction through the steel studs, is the governing means of heat transfer through the assembly. The integrity of the exposed lining would have reduced the interference of furnace gases into the cavity.

5.7 Observations and Temperatures in Timber Studs

The evolution of temperature through the timber dummy stud between the gypsum plasterboard linings is shown by Figure 5-22 through to Figure 5-34. The temperatures of the timber stud were recorded internally at twelve locations on the assembly as indicated by Figure 5-7 and Figure 5-21. Individual temperature readings from each location were plotted for consistency before averaging and spurious results were eliminated if required.

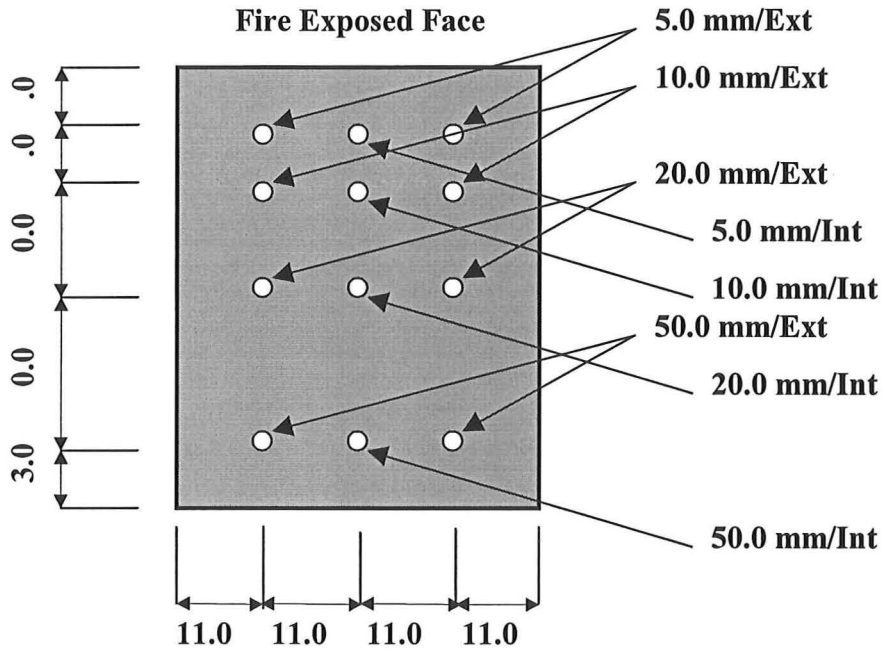

Figure 5-21: Thermocouple key for plots.

The position of the thermocouples and their relation to the following plots is given by Figure 5-21. Measured temperatures from both rows of external thermocouples were averaged to give a temperature profile across the timber stud. Since heat is distributed two dimensionally through the cross section of timber framing members, temperature-time plots give a limited indication of heat flow and likely influential phenomena occurring within the timber member. In order to characterise the two dimensional heat transfer, isothermal plots are used to display the temperature distribution within the timber stud at various times throughout the exposure.

The isothermal plots produced are a crude representation of the temperature distribution within the timber member. Their formulation is based on similar principals mentioned by Clancy (1999), where temperatures along the cavity face of the stud are an average of the measured temperatures from the cavity surface of the exposed and unexposed linings. Temperatures along the stud face attached to the exposed lining are those measured from the cavity surface of the exposed lining, and temperatures measured in the stud at 50 mm from the exposed face are used for the temperatures of the stud face attached to the ambient lining. Temperatures within the stud are based on those measured by the thermocouples described in Figure 5-21. Isothermal plots have been chosen at a time of 10 minutes to provide a comparison between furnace tests while temperatures remain within the dehydration plateau. The second isothermal plot for each test is selected at a time when significant charring of the stud has occurred and the thermal gradient across the section is large.

5.7.1 Standard Plasterboard Exposed to Severe Fire (FP2879)

Figure 5-22 shows that dehydration of moisture from both the exposed gypsum lining and the timber stud maintain temperatures within the timber member below 100°C up to a time of 16 minutes. At which point the gypsum lining begins to detach from the frame and fall into the furnace exposing the timber stud and cavity to furnace conditions, resulting in a rapid rise of temperatures within the timber stud. Figure 5-22 also shows that the temperatures within the stud remain higher than furnace temperatures after approximately 23 minutes due to secondary burning of the studs.

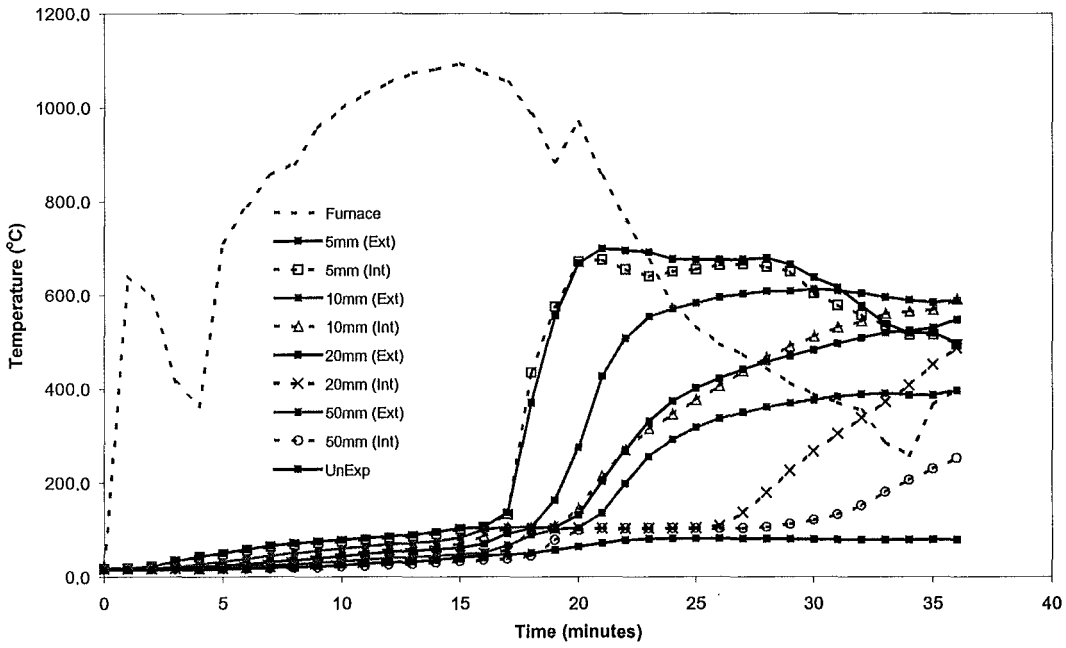

Figure 5-22: Evolution of temperature through timber stud (FP2879).

The influx of atomising air to cool the furnace in order to follow the decay phase of the input time-temperature curve promotes burning within the timber member, this phenomena was also observed by Collier (2000) in his study of timber framed walls. Temperatures within the stud at approximately 35 minutes indicate that the timber section is almost completely burnt. Inspection of the dummy stud after testing revealed that only char material remained with most of the thermocouples directly exposed to furnace conditions.

The energy required to dehydrate moisture within the timber stud and the insulating properties of char reduce the heat transfer through the stud. A two dimensional thermal gradient exists within the stud due to the effects of both moisture movement, which typically occurs at approximately 100°C, and the onset of charring at 300°C (Hadvig 1981). Typical temperature profiles of a timber stud heated from both the exposed lining and cavity are displayed by Figure 5-23 and Figure 5-24. From which it can be seen higher temperatures have penetrated further into the depth of the stud from the fire exposed side compared to that of the cavity side. The semi-elliptical shape of the temperature profiles is also a typical characteristic of two dimensional heat transfer through wood.

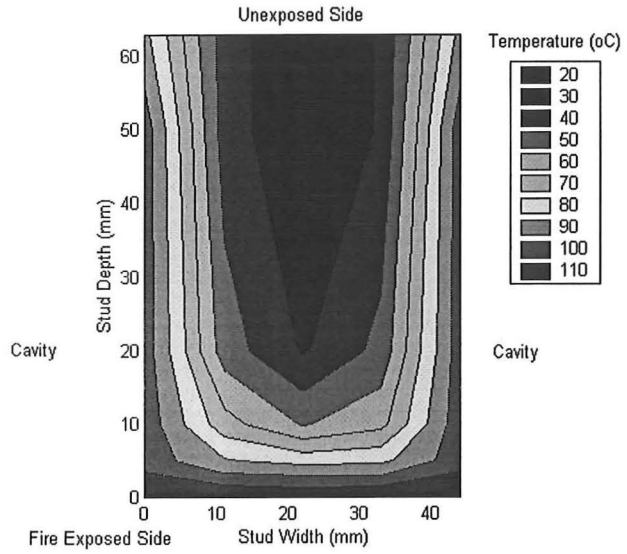

Figure 5-23: Isotherms at 10 minutes.

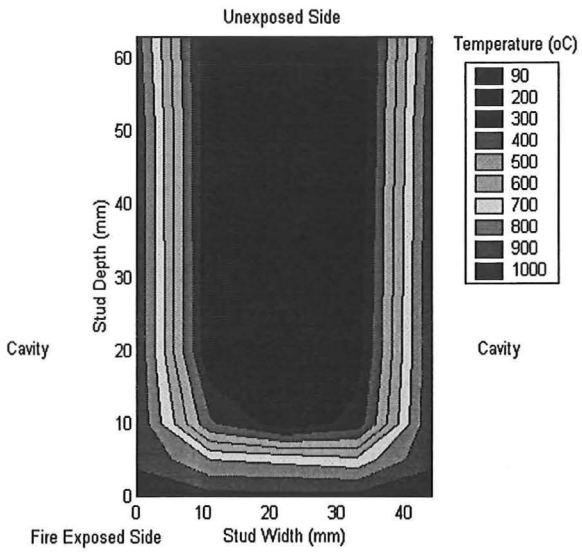

Figure 5-24: Isotherms at 20 minutes.

After 10 minutes of exposure there is a relatively small thermal gradient of approximately 90°C across the depth of the stud with the core maintaining ambient temperatures. Temperatures at the edges of the stud are below 120°C so charring has not commenced, and therefore the stud face remains in full contact with the exposed lining. Once the exposed lining has detached from the frame, exposing the framing directly to furnace conditions, degradation of the timber stud occurs rapidly. At a time of 20 minutes the thermal gradient within the stud is approximately 800°C, indicating that the set of thermocouples located at 5 mm from the exposed lining are no longer embedded in the stud, but are exposed directly to furnace temperatures.

5.7.2 Standard Plasterboard Exposed to Moderate Severity Fire (FP2880)

The slow fire growth and low furnace temperatures keep stud temperatures below 100°C for approximately 40 minutes of exposure. After which degradation of the lining allows the ingress of radiation and furnace gases onto the face of the stud and into the cavity. At approximately 48 minutes Figure 5-25 shows an increase in the slope of the temperatures measured at 5 mm from the exposed lining. This corresponds to a temperature of 300°C at this point, which indicates that charring of

the stud has reduced the timber section and exposed the thermocouples to furnace temperatures.

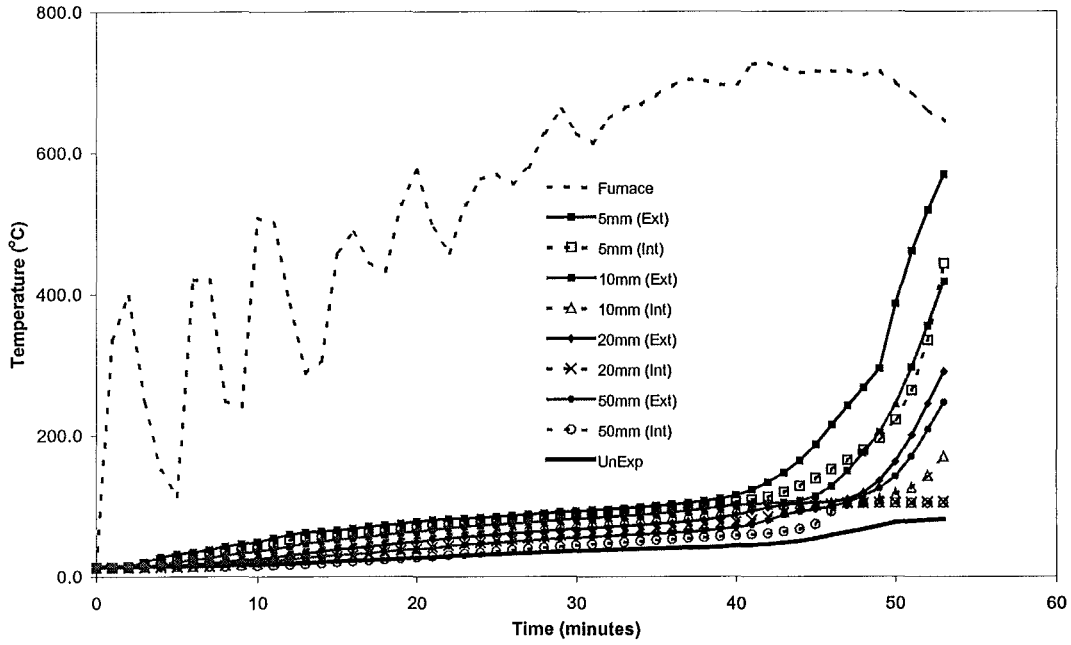

Figure 5-25: Evolution of temperature through timber stud (FP2880).

Comparing stud temperatures from Figure 5-25 with those of the more severe furnace test FP2879 reveals that, temperatures measured with the thermocouples 5 mm in from the face of the stud vary in temperature for FP2880. These are approximately the same for FP2879. This indicates that a thermal gradient exists across the width of the stud at 5 mm from the exposed panel for the less severe test, but does not exist at the same position for the more severe test. This phenomena is also depicted by comparison of the isothermal plots. Temperature contours at 5 mm from the exposed lining for FP2879 are parallel to the exposed face while those of FP2880 are curved.

As indicated by the low stud temperatures at approximately 53 minutes, there was a significant section of wood remaining at termination of the test. The original 64 x 44 mm rectangular section had reduced to a 54 x 30 mm semi-elliptical cross section. This relates to Figure 5-27, where an approximate 300°C contour gives an elliptical cross section of 56 x 29 mm.

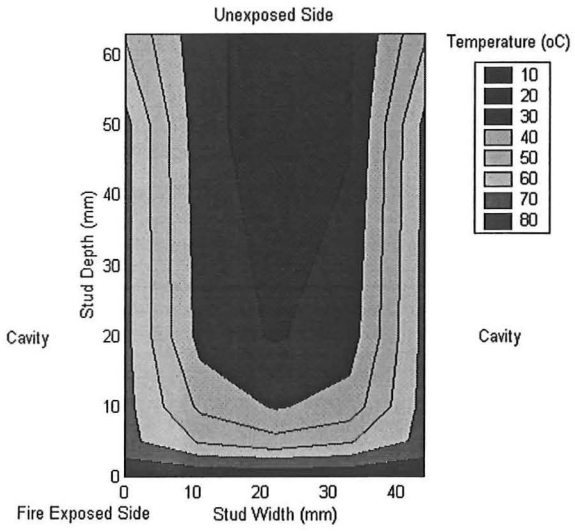

Figure 5-26: Isotherms at 10 minutes.

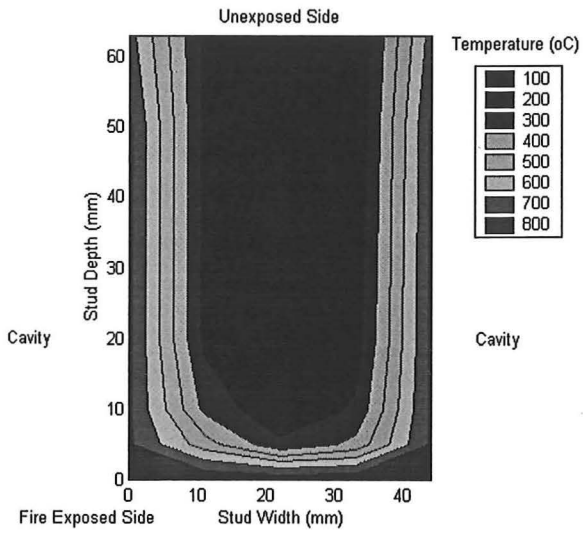

Figure 5-27: Isotherms at 50 minutes.

Figure 5-26 shows that after 10 minutes of exposure, the maximum temperatures in the stud are just over 75°C, and the temperature gradient across the timber section is approximately 60°C. As would be expected, the rate of heat transfer through the stud exposed to the slower fire is much less than that of furnace test FP2879. Also, lower temperatures in the cavity result in less thermal attack on the sides of the stud as shown by the wider temperature contours of Figure 5-26 compared to that of Figure 5-23.

5.7.3 Standard Plasterboard Exposed to ISO834 Furnace Curve (FP2922)

Figure 5-28 displays similar behaviour to that shown by Figure 5-25 for furnace test FP2880, where temperatures within the stud do not begin to rapidly rise until the exposed lining becomes dehydrated after approximately 25 minutes of exposure. As with Figure 5-25, the onset of charring is indicated in Figure 5-28 by the change in slope of the temperatures measured at 5 mm from the exposed lining. Measurements were not recorded internally at 50 mm from the exposed face due to failure of the thermocouple.

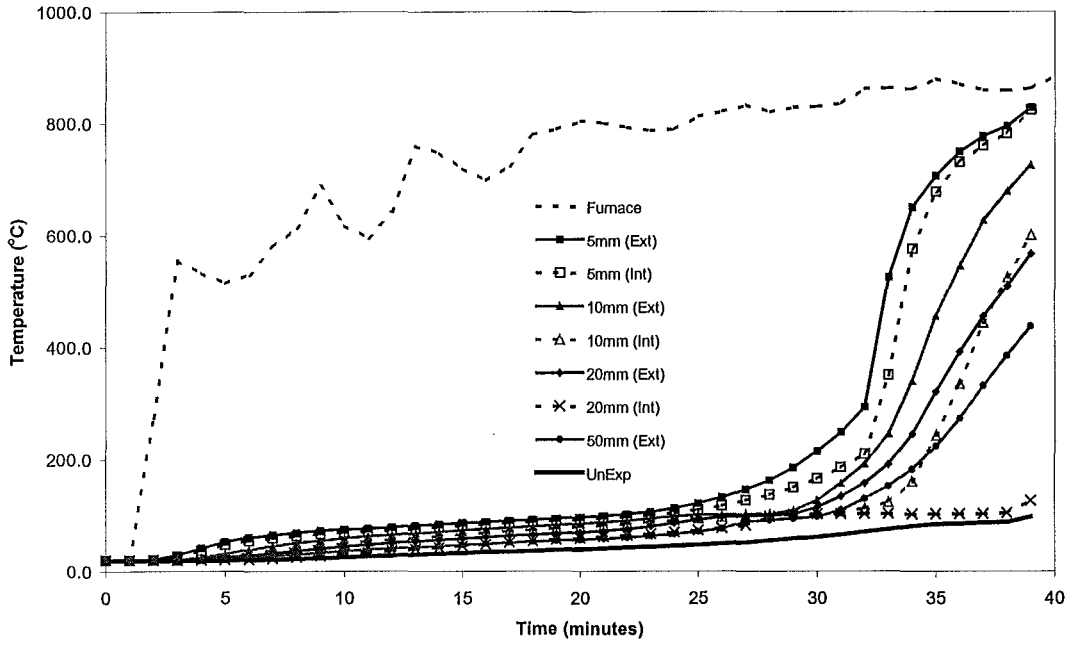

Figure 5-28: Evolution of temperature through timber stud (FP2922).

The temperature lag between the external and internal thermocouples at 5 mm from the exposed lining is intermediate of that from furnace tests FP2879 and FP2880. This agrees with the aforementioned trend that as the fire severity increases the temperature contours across the width of the stud flatten out. Another characteristic that segregates Figure 5-22 from Figure 5-25 and Figure 5-28 is that the temperatures measured at 5 mm from the exposed lining for FP2880 and FP2922 gradually increase up to a temperature of 250-300°C. At which point the rate of temperature rise increases due to exposure of the thermocouples to furnace conditions. This behaviour is not indicated by Figure 5-22, where temperatures measured at 5 mm from the exposed lining for FP2879 increase rapidly at a near constant rate with no gradual rise in temperature or change in slope at the onset of charring.

After 10 minutes of exposure the maximum temperatures in the stud are approximately 90°C with a thermal gradient of 60°C across the depth of the stud. The temperature of the core and ambient side just exceeds 30°C, as shown by Figure 5-29.

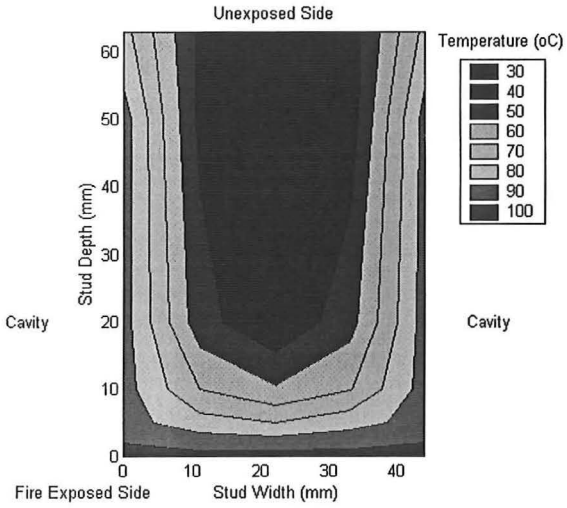

Figure 5-29: Isotherms at 10 minutes.

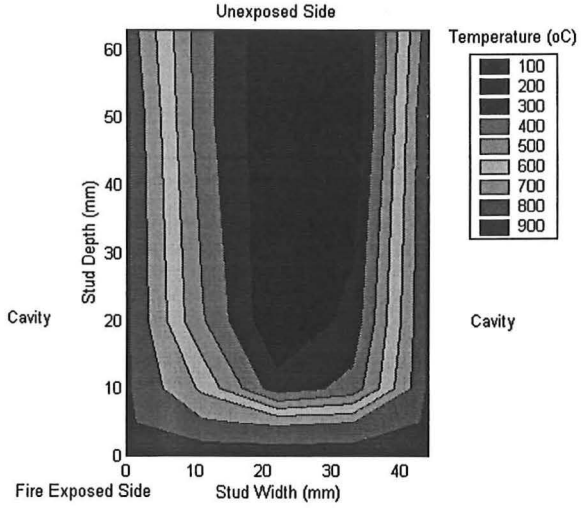

Figure 5-30: Isotherms at 35 minutes.

Failure of the assembly occurred at 39 minutes after ignition, and as shown by Figure 5-30 temperatures near the ambient side of the stud are below 200°C upon failure. The reduced cross section of the stud was rectangular in shape with rounded corners on the exposed face and measured 46 mm deep by 20 mm wide. The 300°C contour from Figure 5-30 indicates a reduced stud cross section of 48 mm by 19 mm, therefore producing a reasonable approximation of the dimensions of the reduced timber member.

5.7.4 Fire Rated Plasterboard Exposed to Severe Fire (FP2881)

Once the exposed lining is lost at approximately 22 minutes the rate of temperature rise within the stud is high, as shown by Figure 5-31. As with the results from FP2879, there is no change of slope in the temperatures measured at 5 mm from the exposed lining at the onset of charring, which is assumed to occur once temperatures reach 300°C. No timber section remained after termination of the test as indicated by the high temperatures near the end of the test.

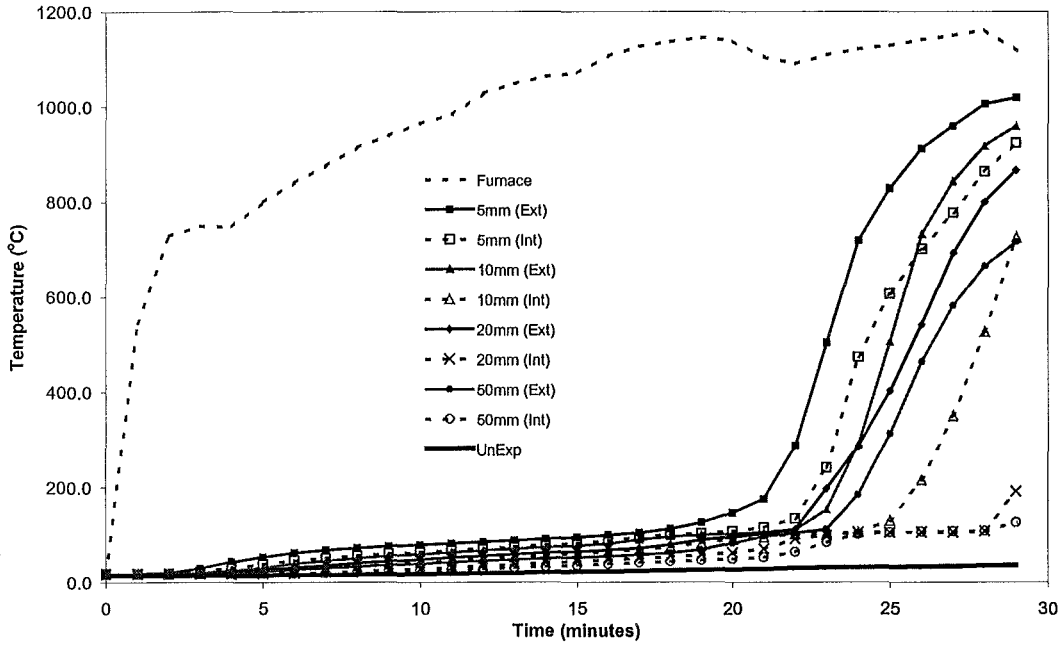

Figure 5-31: Evolution of temperature through timber stud (FP2881).

In contradiction to the trend established from the previous tests, there is a significant lag between the external and internal temperatures measured at 5 mm from the exposed face. It is thought that this lag exists due to persistence of the attached lining. Because the timber stud is both dimensionally small and undergoes similar behaviour to the gypsum lining, where moisture loss causes shrinkage, the stresses between the timber stud and the lining would be small. Therefore reducing local cracking of the lining and maintaining a good hold between the fasteners and lining. When the exposed lining did detach from the steel studs and fell into the furnace, a section remained attached to the timber stud and provided a thermal blanket shielding the face of the stud from direct furnace exposure. However, the cavity sides of the stud did become exposed directly to furnace conditions. The temperature lag across the width of the section is portrayed by the curvature of the isothermal contours of Figure 5-32 and Figure 5-33.

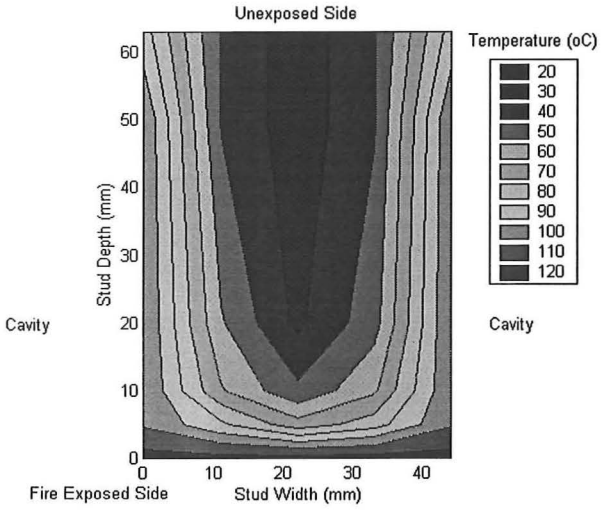

Figure 5-32: Isotherms at 10 minutes.

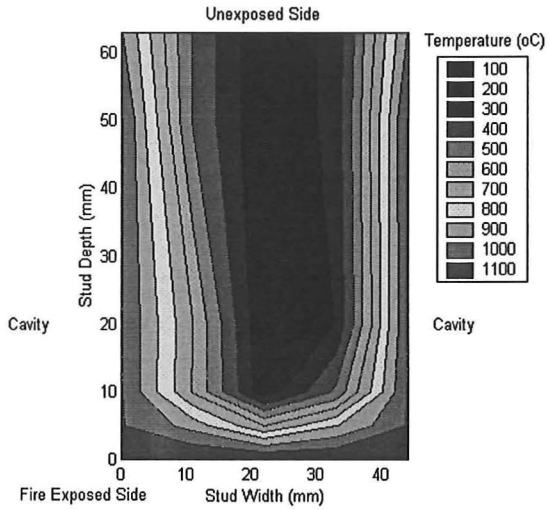

Figure 5-33: Isotherms at 25 minutes.

Maximum temperatures in the stud after 10 minutes of exposure are in the vicinity of 110°C, with a thermal gradient of 90°C across the depth of the section. The long thin profiles of the isotherms at 25 minutes indicate that there has been substantial heat transfer from the cavity sides of the stud. This reinforces the theory of the exposed lining remaining attached to the stud and thus reducing the heat transfer from the exposed side of the stud relative to the cavity sides.

5.7.5 Fire Rated Plasterboard Exposed to Moderate Severity Fire (FP2882)

Figure 5-34 shows that the slow fire growth, low peak temperatures and persistence of the exposed lining results in a fairly uniform temperature distribution in the stud. The near constant rate of temperature rise allowed temperatures within the timber member to gradually rise with time, resulting in much smaller thermal gradients across the stud compared to the more severe furnace test of FP2881. Unlike the other low severity furnace tests of FP2880 and FP2922, there is no change in gradient in the temperatures measured at 5 mm from the exposed lining because the lining remained intact for the duration of the test. Therefore, as charring did not occur, the corresponding thermocouples were not exposed to full furnace conditions.

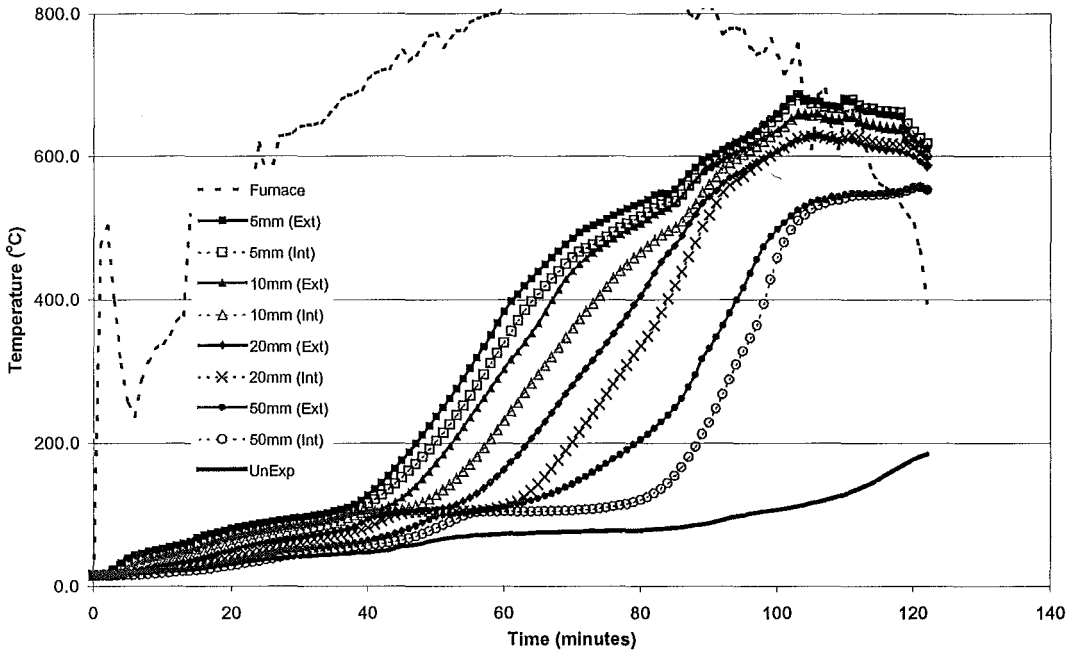

Figure 5-34: Evolution of temperature through timber stud (FP2882).

Beyond 80 minutes the measured temperatures begin to converge and surpass furnace temperatures. This indicates that the thermocouples are exposed to cavity conditions, and that secondary burning of the stud is occurring due to the introduction of cooling air in the decay phase of the furnace test. Although insulation failure of the specimen occurred at 82 minutes the test duration was extended to allow an integrity failure to occur. Therefore the dummy stud was completely consumed before the termination of the test, as shown by Figure 5-34, which indicates that at 85-90 minutes very little cross section of the stud remains since temperatures measured at 50 mm from the exposed face are nearing 300°C.

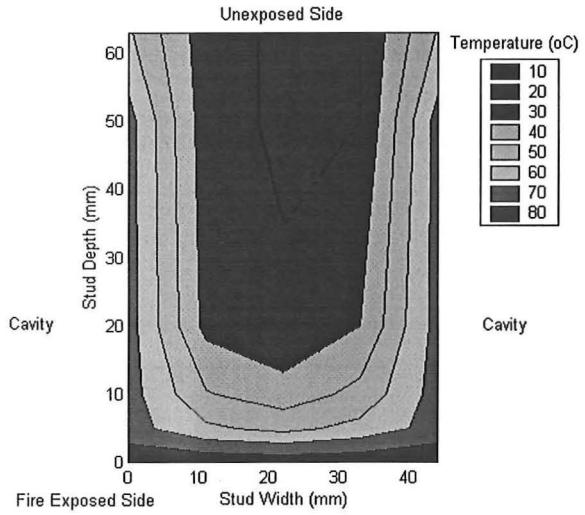

Figure 5-35: Isotherms at 10 minutes.

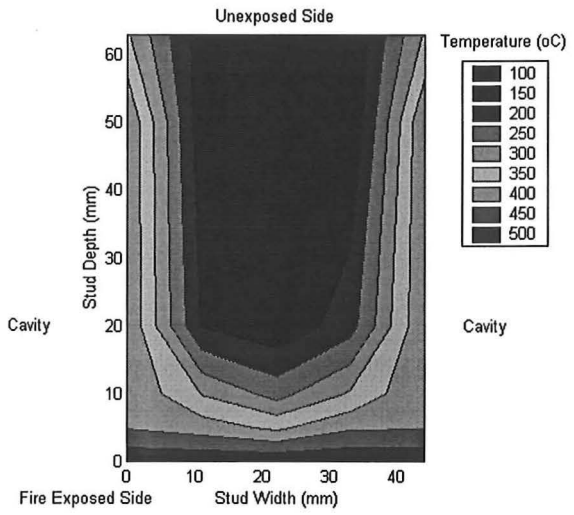

Figure 5-36: Isotherms at 60 minutes.

After 10 minutes of exposure the thermal gradient across the depth of the section is approximately 45 °C, with maximum temperatures reaching 70°C at the stud face attached to the exposed lining. At 60 minutes which is the proprietary rating for this system, the isothermal contours are still relatively wide. This implies that the rate of heat transfer is fairly uniform around the three sides of the stud, unlike the narrow profiles of Figure 5-33 indicating high heat transfer from the cavity.

6 COMPUTER MODELLING RESULTS

This section compares the predictions from the model with experimental results obtained from both full and pilot-scale furnace testing conducted at BRANZ, Wellington. Table 6-1 summarises the furnace tests employed to validate results from modelling. The thermal properties of materials are calibrated against results from the standard test. Once good predictions of temperatures in the assembly exposed to the ISO834 fire are achieved, then these same thermal properties are used in the modelling of non-standard fire exposure.

Table 6-1: Summary of furnace tests used to validate modelling.

Furnace Test	Fire/Specimen Description
FR1579	63 x 34 x 0.55 mm Steel stud/12.5 mm GIB® Fyreline board exposed to ISO834 (NLB)
FP2882	63 x 34 x 0.55 mm Steel stud/12.5 mm GIB® Fyreline board exposed to moderate furnace fire (NLB)
FP2881	63 x 34 x 0.55 mm Steel stud/12.5 mm GIB® Fyreline board exposed to severe furnace fire (NLB)
FP2922	63 x 34 x 0.55 mm Steel stud/12.5 mm standard board system exposed to ISO834 (NLB)
FP2880	63 x 34 x 0.55 mm Steel stud/12.5 mm standard board system exposed to moderate furnace fire NLB)
FP2879	63 x 34 x 0.55 mm Steel stud/12.5 mm standard board system exposed to severe furnace fire (NLB)

NLB = Non loadbearing

6.1 SAFIR Parameters

6.1.1 Geometry

The geometry of the proprietary systems used in testing are described in Section 3.2. Descriptions of the sections and finite element mesh used to approximate the assemblies in the modelling are given in Section 3.3. Locations of temperature measurement used to validate model predictions are given in Section 5.2.

6.1.2 Thermal Properties of Materials

The density, specific heat, conductivity, enthalpy and thermal coefficients of materials used in the computer model are summarised in Section 4.5.

6.2 Comparison with Test Results

Due to time and computing constraints, calibration of the timber thermal properties (in order to gain reportable predictions) was not achieved. Therefore, this section reports model predictions of temperatures within the steel studs and cavity. Predicted temperatures in timber studs have been neglected. It is recommended that modelling the evolution of temperature through the timber section be undertaken in further research.

6.2.1 60 Minute Steel Stud System Exposed to ISO834

Model predictions are compared against temperatures from full-scale furnace test FR1579. Figure 6-1 shows that modelled values provide a reasonable prediction of the actual temperatures across the width of the steel stud. The model under predicts temperatures of the fire-exposed side of the stud up to approximately 450°C, after which predicted values are slightly conservative until failure of the system at 63 minutes, relating to a temperature of 600°C.

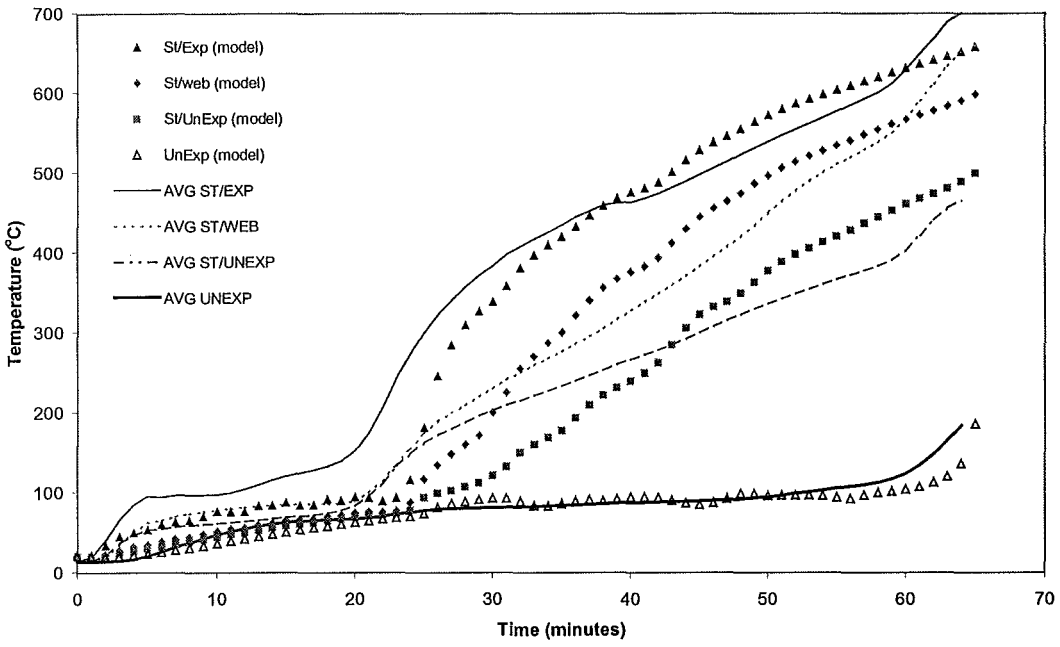

Figure 6-1: Predicted temperatures of steel stud and cavity in 60 minute system exposed to ISO834.

Temperatures on the cavity face of both the exposed and unexposed linings do not differ much from that of the steel stud flanges, and therefore are not included in Figure 6-1. Temperatures of both the web and unexposed flange of the steel section were initially under predicted and then over predicted by the model. However, temperature predictions of the ambient face of the unexposed lining provide good agreement with experimental results.

Although further calibration of the thermal properties, of the materials used in the model, will provide better predictions of temperatures within the system. The current model accurately predicts an insulation failure of the unexposed panel.

6.2.2 60 Minute Steel Stud System Exposed to Moderate Fire

Model predictions are compared against temperatures from pilot-scale furnace test FP2882. Figure 6-2 shows that the model slightly under predicts the temperature evolution through the assembly. The model over predicts the duration of the

temperature plateau at 100°C, due to dehydration of the exposed lining. This results from the peak values of the apparent specific heat at 100°C being too high.

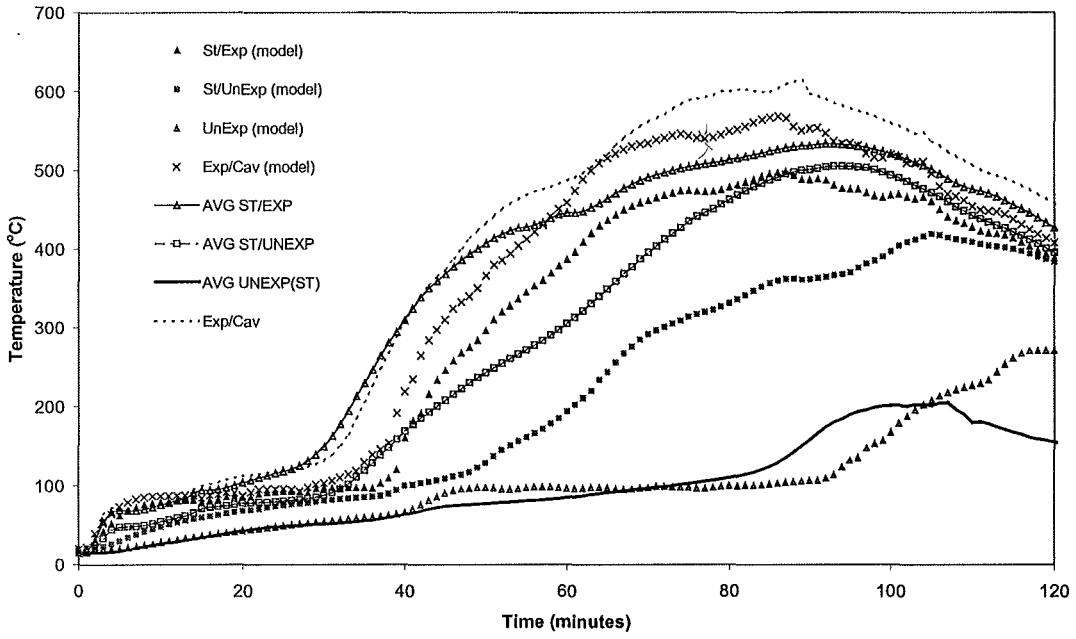

Figure 6-2: Predicted Temperatures for steel stud and cavity in 60 minutes system exposed to moderate fire.

Beyond 60 minutes of exposure, modelled temperatures of the cavity face of the exposed lining and the exposed steel flange tend to lag the actual temperatures by approximately 50°C. Web temperatures of the steel stud have been neglected from Figure 6-2 to maintain clarity. Predicted temperatures of the unexposed steel flange are much lower than actual temperatures up until failure of the system at approximately 120 minutes, at which point modelled and predicted temperatures, converge. Thermal failure of the system is under predicted, since an insulation failure of the unexposed panel occurred at 82 minutes, whereas the model predicts equivalent temperatures of the unexposed panel at approximately 95 minutes.

6.2.3 60 Minute Steel Stud System Exposed to Severe Fire

Model predictions are compared against temperatures from pilot-scale furnace test FP2881. Figure 6-3 clearly shows that the model poorly predicts the temperatures of the steel studs and cavity exposed to the severe fire.

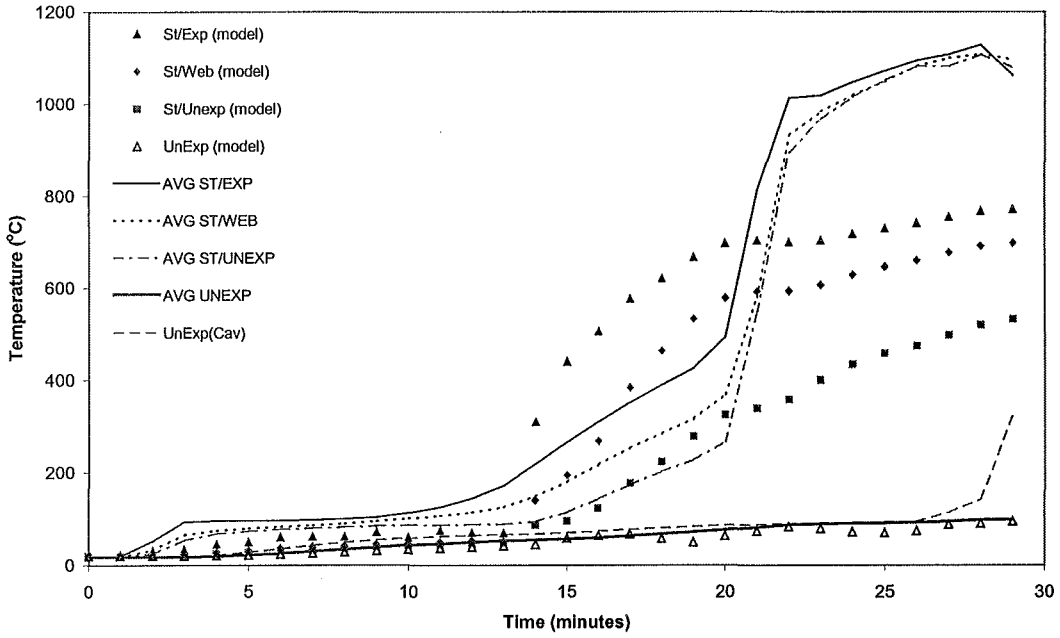

Figure 6-3: Temperature predictions for steel stud and cavity in 60 minute assembly exposed to severe fire.

The model over predicts the effects of cracking, resulting in the rapid rise of temperatures at approximately 14 minutes. However, at 20 minutes the exposed lining falls off resulting in a rapid increase of temperatures, the model is unable to accurately predict when this occurs. Further development of the model so that the exposed lining can take on the properties of air once its temperature reaches 600°C may be one way of accounting for the loss of the exposed lining in modelling.

Temperatures of the ambient face of the unexposed board in the cavity region are also given in Figure 6-3. Predicted temperatures of the unexposed panel agree well with experimental results up until failure, as indicated by the rapid increase in temperatures of the ambient face. However, the model fails to predict the insulation failure at approximately 28 minutes.

6.2.4 30 Minute Steel Stud System Exposed to ISO834

Predicted temperatures are compared against those obtained experimentally by pilot-scale furnace test FP2922.

The review of the gypsum plasterboards thermal properties in Section 4.2.1 are based upon high density fibre reinforced boards. It was initially thought that the thermal properties of standard plasterboard would be similar to those of the fibre reinforced boards, except with lower density values. However, the thermal behaviour of the standard plasterboard differs significantly from that of the fibre reinforced board, resulting in the apparent thermal properties summarised in Section 4.5.

As can be seen from Figure 6-4, further calibration of the apparent thermal properties of gypsum board is required to attain a better approximation of the thermal behaviour of the 30 minute system exposed to standard conditions.

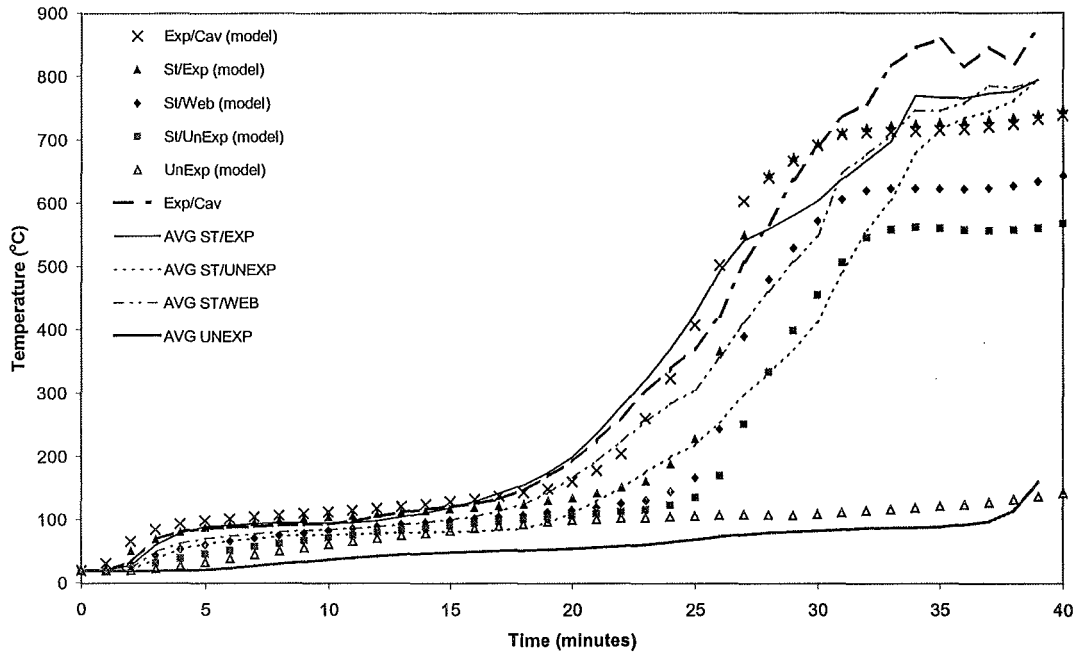

Figure 6-4: Predicted temperatures of steel stud and cavity for 30 minute system exposed to ISO834 fire.

Temperatures on the cavity face of the exposed lining have been included in Figure 6-4, because they differ significantly from those of the exposed flange of the steel

stud beyond 25 minutes. Cavity face temperatures of the exposed lining are well predicted by the model up to temperatures of 700°C. However, model predictions of the exposed side of the steel stud lag experimentally derived temperatures beyond 20 minutes of exposure.

Predicted temperatures on the unexposed side of the steel stud agree well with actual values up to a temperature of 550°C, at which point modelled values level off while actual temperatures continue to rise until failure of the system at approximately 39 minutes. The model slightly over predicts the temperature on the ambient face of the unexposed panel up until failure, at which point actual temperatures of the ambient face rise rapidly due to integrity/insulation failure of the panel. Due to the rough calibration of the thermal properties of standard plasterboard, the onset of thermal failure of the unexposed lining is not predicted.

6.2.5 30 Minute Steel Stud System Exposed to Moderate Fire

Predicted temperatures are compared against actual temperatures from furnace test FP2880. Figure 6-5 clearly shows that there is a poor correlation between experimental and predicted results. Temperatures are over predicted up to 30 minutes, due to high thermal conductivity values for temperatures below 100°C. The rise in experimental temperatures at approximately 30 minutes is not predicted until 45 minutes after ignition. This results from peak values of the specific heat at 100°C being too high. The model does, however, predict a similar rate of rise of temperatures, after the exposed lining has dehydrated and assembly temperatures begin to rise.

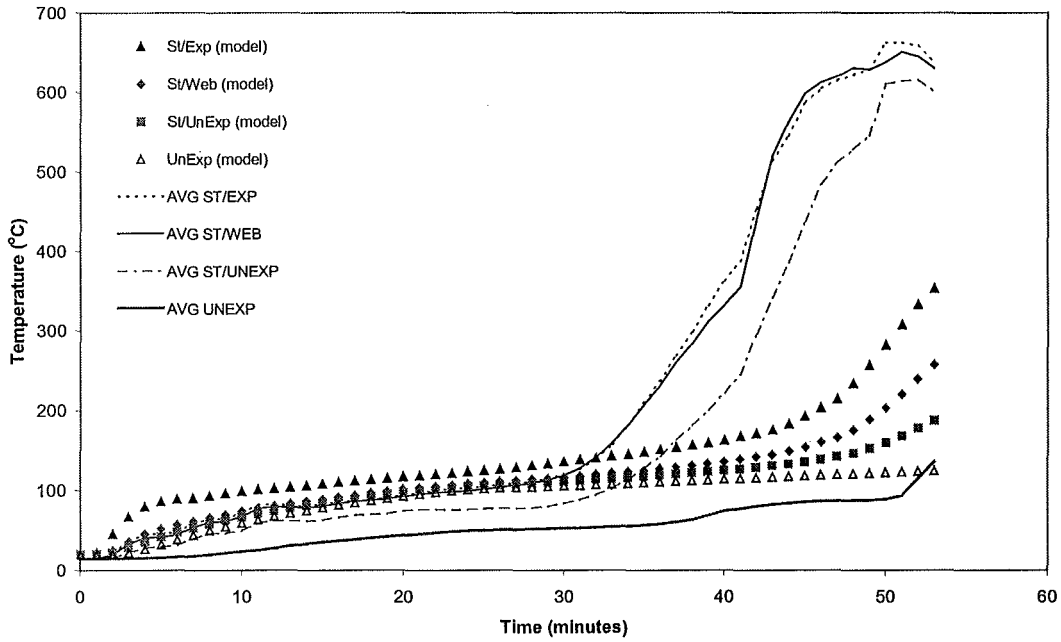

Figure 6-5: Predicted temperatures of steel stud and cavity for 30 minute system exposed to moderate fire.

6.2.6 30 Minute Steel Stud System Exposed to Severe Fire

Model results are compared against temperatures obtained from pilot-scale furnace test FP2879. During the dehydration plateau at 100°C, temperatures are reasonably well predicted by the model, as shown by Figure 6-6. The model predicts a faster rate of temperature rise up to peak temperatures. The model under predicts peak temperatures on the cavity face of the exposed lining. While predicted peak temperatures on the exposed side of the steel stud, show good agreement with experimental values.

The model under predicts the peak temperatures on the unexposed faces of the stud up until the assembly is in the cooling phase. At approximately 25 minutes, predicted temperatures exceed those obtained in furnace testing, as indicated by Figure 6-6. An integrity failure of the unexposed lining occurred at 30 minutes. There is no indication, by the temperature curve of the unexposed lining, that excessive temperatures were reached. Therefore, it is difficult to determine a thermal failure from the modelling. The model does predict a temperature rise on the unexposed

panel at 25 minutes and temperatures of approximately 200°C at 34 minutes. This is due to the temperatures on the exposed side of the assembly being over predicted by the model.

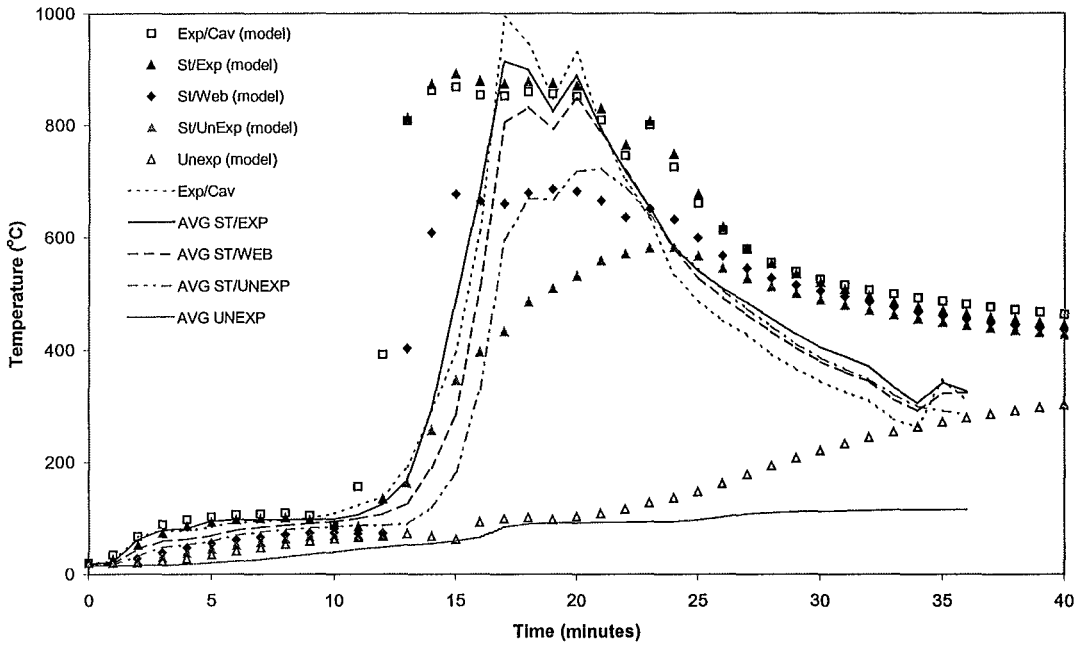

Figure 6-6: Predicted temperatures of steel and cavity for 30 minute system exposed to severe fire.

6.3 Failure Predictions from Modelling

Times for both integrity and insulation failures from furnace testing, compared with predicted times to reach insulation failure, are given in Table 6-2. Predicted insulation failure times are taken as the time at which temperatures on the ambient face of the unexposed lining reach an average of 140°C.

Note that the insulation failure time for a drywall system with steel studs and a single layer of 12.5 mm fire rated gypsum plasterboard on each face exposed to the ISO834 time-temperature curve is approximately 63 minutes (BRANZ 1990). The steel stud/12.5 mm standard board assembly achieved a failure time of approximately 38 minutes, subjected to the ISO834 fire curve in the pilot-scale furnace.

Table 6-2: Comparison of predicted and actual thermal failure times.

Furnace Test	Integrity Failure Time (mins)	Insulation Failure Time (mins)	Predicted Insulation Failure Time (mins)
FR1579	NR	63	62
FP2882	NR	82	91
FP2881	28	29	NR
FP2922	38	39	40
FP2880	50	51	NR
FP2879	34	NR	22

NR = Not Reached

It is expected that the model should provide accurate predictions of the failure time for the 12.5 Standard and GIB® Fyreline, when exposed to the ISO834 fire. Since results from both these furnace tests have been used to calibrate the thermal properties of the gypsum plasterboards. Table 6-2 indicates that the model predicts the insulation failure time of both standard tests (FR1579 and FP2922) with good accuracy. However, insulation failures of the non-standard fire tests are not so well predicted.

7 IMPLICATIONS OF FURNACE TESTING

This section looks at the significance of the results from the furnace testing and the effect of realistic fire exposure on the fire resisting performance of gypsum plasterboard assemblies.

7.1 Equivalent Area Concept

The 'severity' of a fire resistance test is established by comparison of the area under the furnace curve with the area under the standard ISO834 curve for the same period. It was initially thought that this concept would allow prediction of the failure time for systems subjected to non-standard fires.

Figure 7-1 shows the area under the proposed time-temperature curves for the non-standard furnace tests compared with the area under the standard ISO834 curve for the same duration of exposure.

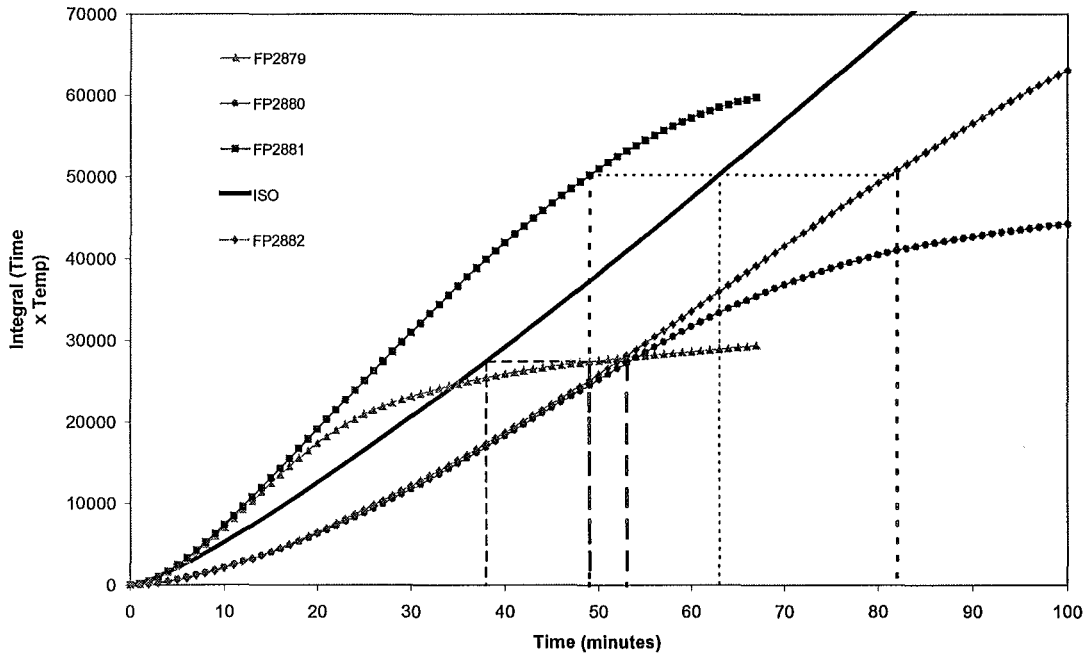

Figure 7-1: Comparison of area under time-temperature curves.

The vertical lines on Figure 7-1 represent the times at which the equivalent fire severity to the ISO834 curve is reached by the integral of the non-standard fire curves.

Therefore, if the 30 minute system exhibited an insulation failure at approximately 38.0 minutes, then the equivalent fire severity for furnace curve FP2879 is 49 minutes.

Comparison of the area under the actual furnace curves with the relative area under the proposed furnace curves indicated that the furnace closely followed the desired severity. Therefore, the area under the proposed curves has been compared with that of the standard ISO834 curve in order to predict the failure time of the specimens subjected to the non-standard time-temperature curves. Table 7-1 summarises the failure times for each test specimen and compares them to the failure times predicted by the equivalent area concept.

Table 7-1: Failure time for each test specimen.

Test Specimen	Time to Reach Integrity Failure (mins)	Time to Reach Insulation Failure (mins)	Predicted Time to Failure (mins)
FP2879	34	NR	49
FP2880	50	51	53
FP2881	28	29	49
FP2882	NR	82	82
FP2922	38	39	N/A

NR = Not Reached

Results from Table 7-1 indicate that the equivalent area concept provides a good prediction of the failure time for assemblies that are subjected to fire curves less severe than the standard curve. These are the moderate growth, low peak temperature, and long duration fires. However, failure time prediction for systems exposed to rapid growth fires with greater severity than the standard curves is poor.

The physical and chemical processes that occur within the drywall system under elevated temperature conditions are occurring much more rapidly in a severe fire exposure compared to a less severe exposure.

7.2 Effect of Fire Severity on the Behaviour of the Assembly

7.2.1 Gypsum Plasterboard Lining

Observations from furnace testing have shown that the ability of the fire exposed lining to remain intact has a major influence on the performance of the overall system. The duration in which the exposed lining remains intact is highly dependent on the severity of the fire exposure. Table 7-2 summarises the integrity of the exposed lining for each test specimen. The fire exposed lining of a steel stud drywall system with one layer of 12.5 mm GIB® Fyreline on each face exposed to the standard ISO834 furnace curve remained intact for the duration of the exposure, being 63 minutes (BRANZ 1990).

Table 7-2: Integrity of exposed gypsum plasterboard lining.

Test Specimen	Lining Type	Time at which Exposed Lining is Lost (mins. secs)
FP2879	Standard	16:30
FP2880	Standard	36:00
FP2881	GIB® Fyreline	20:00
FP2882	GIB® Fyreline	Remained Intact (122:00)
FP2922	Standard	26:00

(All linings are 12.5 mm thick.)

The influence of the fire severity on the integrity of the exposed lining is made clear by Table 7-2. For the drywall system incorporating the standard plasterboard lining there is approximately 20 minutes difference between the time to lose the exposed lining for the two non-standard tests. Over 100 minutes separates the times at which the exposed lining is lost from tests FP2881 and FP2882.

For the systems exposed to the more severe furnace conditions (FP2879 and FP2881), the temperature gradient across the thickness of the exposed lining is greater than that in the standard or low severity furnace tests (refer to Section 5.6). Calcination of the plaster board lining is releasing moisture, in the form of steam, which escapes through the cracking of the heated lining. The severe heating conditions and increased

thermal gradient imposes a thermal shock on the lining, which causes it to degrade faster than standard conditions. Observations from early stages of the testing, approximately 6 minutes after ignition, revealed that small particles (about 5 mm in diameter) were falling from the exposed face of the exposed lining.

It is thought that in the early stages of the fire exposure, as the dehydration front moves from the exposed face to the unexposed face, the escaping moisture is held up by the movement of the dehydration front. This causes greater expansion within the lining forcing small particles to break from the surface. This phenomenon was particularly evident in test FP2881 where ablation of the fibre reinforced board was enhanced by the expansion of vermiculite particles within the board. This behaviour was not observed in the less severe furnace tests, the lining either fell in sections or remained intact throughout the test, due to the more uniform heating of the lining and reduced thermal gradient across the thickness of the lining.

Cracking within the exposed lining was also enhanced by the increased severity of the furnace fire. Rapid temperature rise within the lining caused horizontal cracking to concentrate at certain locations within the lining rather than distributed as smaller cracks over the face as in a fire with a more gradual temperature rise. This concentrated cracking (5 – 10 mm wide) allowed the passage of hot gases into the cavity, which increased the degradation of the exposed lining markedly. Vertical cracking tended to occur at the joint in the exposed lining, particularly in the test with the fibre reinforced board. Once the paper reinforcing was burnt away, exposing the plaster stopping, cracking began to appear along the vertical joint.

7.2.2 Steel Studs

As with the exposed lining, the more severe furnace conditions created a greater thermal gradient across the depth of the cold-formed steel studs due to thermal lag (refer to Section 5.6). This caused increased deflections and deformation of the steel studs. Although deflections were not monitored, observations during the testing can attest to the increased deflections of the assembly, towards the furnace, for the more severe fires. Observations of the steel studs once testing had been completed revealed that significant deformation of the stud exposed to the more severe conditions had

occurred in comparison to the less severe furnace tests with lower rates of temperature rise. Figure 7-2 and Figure 7-3 show the condition of the steel studs after furnace tests FP2881 and FP2882, respectively.

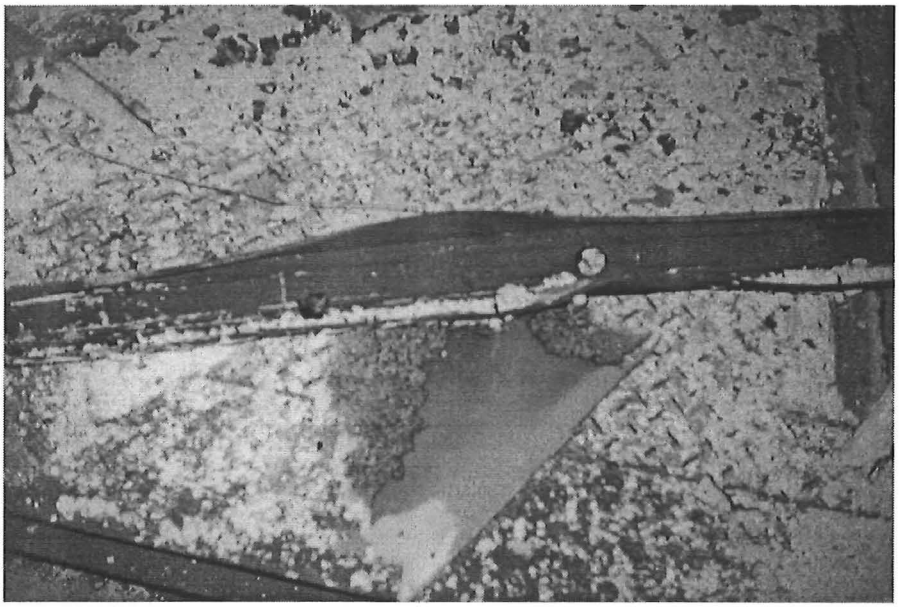

Figure 7-2: Buckling of steel stud from furnace test FP2881.

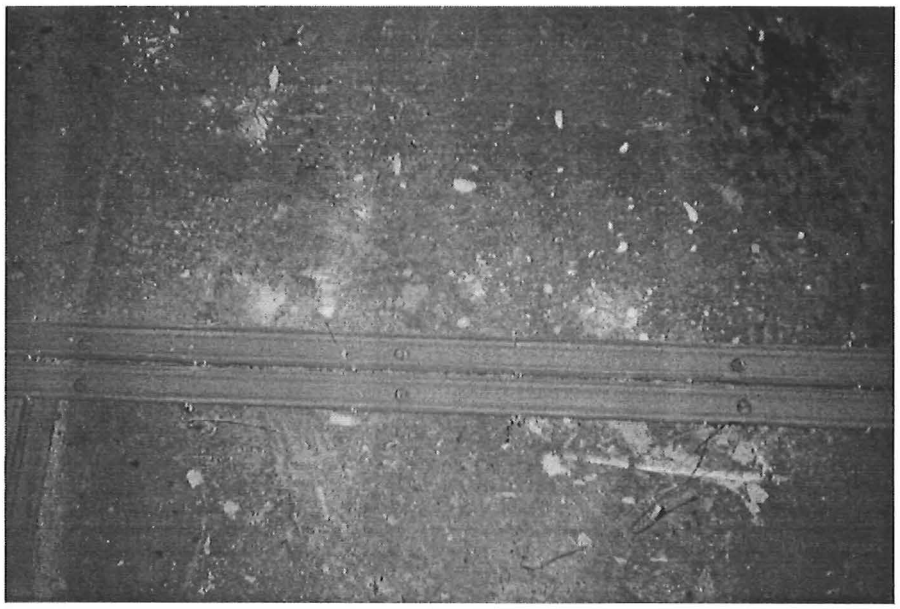

Figure 7-3: Relatively unaltered studs after furnace test FP2882.

The deflection of the steel studs towards the furnace induced tensile forces into the exposed lining increasing the widths of cracks initiated by shrinkage of the panel. For the more severe furnace conditions, deflection of the steel studs was enhanced

therefore opening cracks further and allowing a greater flow of hot gases into the cavity, which in turn increased the rate of degradation of the linings.

An important observation made from furnace tests FP2880 and FP2882 is the effect of restraint conditions on the top and bottom steel channels. Premature failure of the unexposed lining resulted from local buckling of the top channels. Not enough allowance was made for thermal elongation of the channel sections. Axial forces induced by pushing of the heated section against the concrete lined frame, this caused buckling in the channel near the location of the vertical joint in the lining. Conduction of heat through the fasteners degraded the strength of the plaster around the fasteners, so when the flange of the channel buckled, it pushed out the lining and allowed flames to propagate from the opening (shown by Figure 7-4). Therefore, it is important that allowance is made for the thermal behaviour of steel framing within drywall assemblies, otherwise failure to do so can result in premature failure of the system.

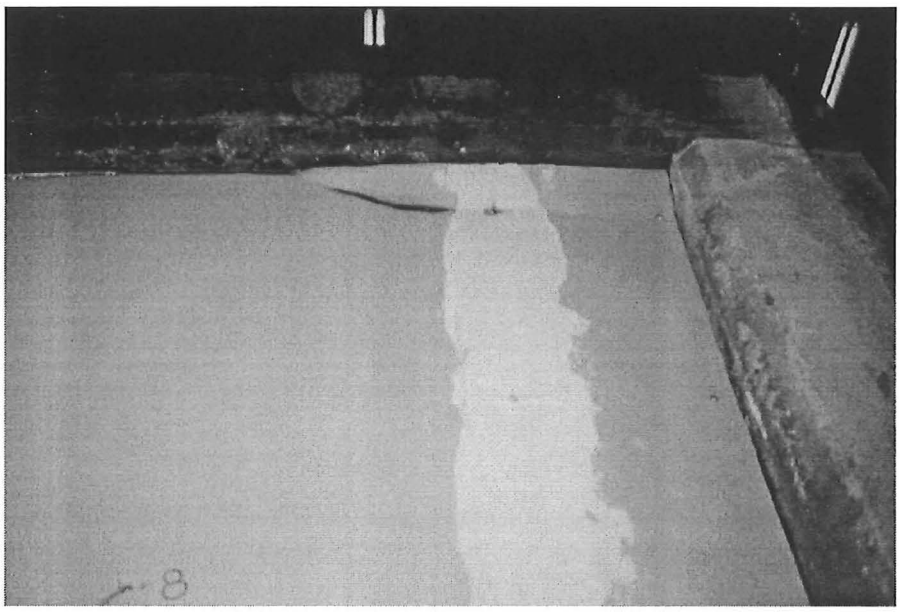

Figure 7-4: "Push-out" of the unexposed gypsum lining.

7.2.3 Timber Dummy Stud

As would be expected, the temperature gradient across the depth of the stud was greater for the more severe fire tests, due to greater heat fluxes and accelerated degradation of the gypsum lining. Temperature contours within the timber stud exposed to the slower fire tended to be wider than those of the faster fires. This was due to higher temperatures and increased radiant heat transfer within the cavity during the hotter fire tests.

Temperature contours near the face of the stud are parallel to the exposed lining for severe tests while they are curved for less severe fire exposure. This indicates that for the faster more severe fire, radiation impingement from the cavity face of the exposed lining is less than the direct heat transfer through the lining/stud interface. This results in reduced corner rounding of the stud. The stud in the less severe furnace test is influenced more by heat from within the cavity as indicated by increased curvature in the isothermal contours near the face of the stud.

Temperature measurements recorded within the timber section, at 5 mm from the exposed lining indicate that for the faster fire tests, temperatures rise rapidly with a constant temperature increase from the point when the gypsum lining becomes dehydrated. Whereas, results from the same position for the slow fire tests give a gradual temperature rise once the lining has dehydrated with a change in slope at the onset of charring. It is thought that the rapid increase in temperature once the lining has dehydrated is due to the preheating of the stud from steam escaping from the gypsum lining. The fast fire growth and high temperatures increase shrinkage of the lining, therefore allowing the ingress of radiation through cracking directly onto the timber member. This combined with the increased rate of water vaporisation within the stud may explain the constant but rapid increase of stud temperatures for the severe fire tests.

7.2.3.1 Charring Rates

The times at which the 300°C isotherm reached the internal thermocouples at 5, 10, and 20 mm from the fire exposed lining along with the corresponding rate of char through the depth of the stud for each furnace test are given in Table 7-3. Char rates have been calculated from the charred distance divided by the time for that section to char. For example, the char rate at 10 mm from the exposed face for FP2879 is given by: (10 mm – 5 mm)/(22 mins – 17 mins) = 1 mm/min.

Char rates through the depth of the stud are based on measurements from the internal thermocouples. The external thermocouples have been neglected as they are heavily influenced by heat from the cavity and therefore will over estimate the charring rates through the depth of the stud.

Table 7-3: Time to char through stud depth at 5, 10, and 20 mm from exposed lining with corresponding char rates.

Test Specimen	T_{CHAR} (5mm) (mins)	T_{CHAR} (10mm) (mins)	T_{CHAR} (20mm) (mins)	Average Char Rate (mm/min)
FP2879	17 (0.3)	22 (1)	30 (1.3)	0.9
FP2880	51 (0.1)	NR	NR	-
FP2922	32 (0.2)	35 (1.7)	NR	1
FP2881	23 (0.2)	26 (1.7)	29 (3.3)	1.7
FP2882	60 (0.1)	68 (0.6)	80 (0.8)	0.5

NR = Not Reached

Values in brackets are char rates (mm/min).

The times at which the 300°C isotherm has reached the thermocouples at 11 and 22 mm from the side exposed parallel to the cavity along with the corresponding char rates through the width of the wood are given in Table 7-4. Time measurements at 10, 20, and 50 mm from the exposed lining have been averaged to give the mean time for the 300°C temperature contour to reach the external and internal rows of thermocouples. Values measured at 5 mm from the exposed face have been neglected

due to the influence of the heat from the exposed lining and the effect of corner rounding. Char rates have been calculated as described previously.

Table 7-4: Average time to reach 300°C isotherm through stud width at 11 and 22 mm from cavity side with corresponding char rates.

Test Specimen	T_{CHAR} at 11mm (mins)	T_{CHAR} at 22mm (mins)	Average Char Rate (mm/min)
FP2879	24 (0.5)	27 (2.8)	1.7
FP2880	51 (0.2)	NR	-
FP2922	32 (0.3)	36 (2.8)	1.6
FP2881	25 (0.4)	29 (2.8)	1.6
FP2882	73 (0.2)	79 (1.8)	1.0

NR = Not Reached

Values in brackets are char rates (mm/min).

Results from Table 7-3 indicate that the charring rate through the depth of the stud can range from 0.1 to 3.3 mm/minute, while the char rate through the width of the section can vary between 0.2-2.8 mm/minute (Table 7-4). Both tables indicate that the charring rate increases with increasing depth into the stud. Many national codes specify a constant charring rate for unprotected softwoods of 0.60 to 0.75 mm/minute (BSI 1978, SAA 1990).

It is typically accepted that charring rates of wood framing protected by linings are less than that of wood members exposed directly to a furnace environment for charring rates measured at 5 mm from the exposed face this was so (Table 7-3). However, as heat penetrated further into the depth of the stud, the rate of char increased. For the faster fires the average charring rate was greater than the standard constant charring rate of 0.6-0.75 mm/min, for fully exposed members. It is thought that the rapid increase in charring rates through the section is the result of large cracking existing within the char layer allowing the ingress of radiation and hot gases.

As would be expected, the charring rates of the more severe fire exposure are greater than the less severe tests. The results from the standard test (FP2922) provided intermediate values.

It is typically accepted that charring on the edge of the stud in contact with the fire-exposed gypsum board proceeds at about twice the rate as on the wide face exposed to the cavity (Buchanan 2000). However, results from Table 7-3 and Table 7-4 indicate that the charring on the cavity exposed face proceeds at approximately 1.5 times the rate exhibited by the face parallel to the exposed lining. This slight inconsistency may result from the combination of the small stud width and from sections of the lining remaining in contact with the face of the stud.

It was observed at the end of the tests that small sections of lining remained fastened to the fire exposed side of the stud even though significant charring had occurred. This persistence of the lining would effectively shield the stud face from direct fire exposure while the cavity sides of the stud are exposed.

The depth of the stud (64 mm) is less than the nominal stud depth of 94 mm, typically used in test specimens constructed from timber framing. Therefore, heat accumulation within the cavity and radiation impingement onto the stud while the exposed lining is in place are increased for the smaller stud due to the decreased volume of the cavity.

7.2.3.2 Onset of Char

As mentioned in Section 4.4.7, a fire resistance rating may be applied to an assembly on the basis of a "finish rating", which is defined as the time at which the wood surface closest to the fire reaches an average temperature rise of 121°C or an individual temperature rise of 163°C. Column two of Table 7-5 gives finish ratings calculated from thermocouple measurements and column three of Table 7-5 gives the time at which temperatures of the stud face reach 300°C. These results are based on an average of the three thermocouples located 5 mm from the exposed gypsum lining.

Table 7-5: Finish ratings and onset of char for each specimen.

Test Specimen	Finish rating (mins)	Time to 300°C (mins)
FP2879	16	17
FP2880	41	51
FP2922	25	32
FP2881	19	22
FP2882	39	55

The finish ratings were generally governed by the time to reach an average temperature of 121°C at 5 mm from the exposed lining. Results from Table 7-5 indicate that the finish ratings provide a good estimate of the time at which damage to protected wood members may occur for the severe fire tests. However, they tend to provide relatively conservative estimates for the slower and standard fires. This implies that finish ratings may be a conservative method for assigning fire resistance ratings to assemblies. They do, provide a good estimate of the performance of the system to protect the timber studs when subjected to a more realistic fire exposure.

8 FULL-SCALE COMPARTMENT TESTING

8.1 Background

Three full-scale compartment burns were completed at the Masterton Fire Service Station in association with the New Zealand Fire Service, Winstone Wallboards Ltd, and the Building Research Association of New Zealand (BRANZ). Initially the compartment burns were proposed as a practical component for the post fire investigation seminar held at the Masterton Station. Further consultation with both Winstone Wallboards Ltd and BRANZ led to the supply of materials and instrumentation of the compartments to record temperature evolution. Figure 8-1 shows the compartments located at the testing site, and gives an indication of their size.

Figure 8-1: Testing site for compartment tests with the three modules in place.

8.2 Description

All three compartments were constructed from timber framing and GIB® plasterboard internal wall/ceiling lining following New Zealand standard building practices. The floor lining consisted of 12 mm plywood. Each compartment was a 2.4 m cube, with a 2 m high by 0.8 m wide opening and 0.4 m by 0.26 m glazed viewing window, as shown by Figure 8-2.

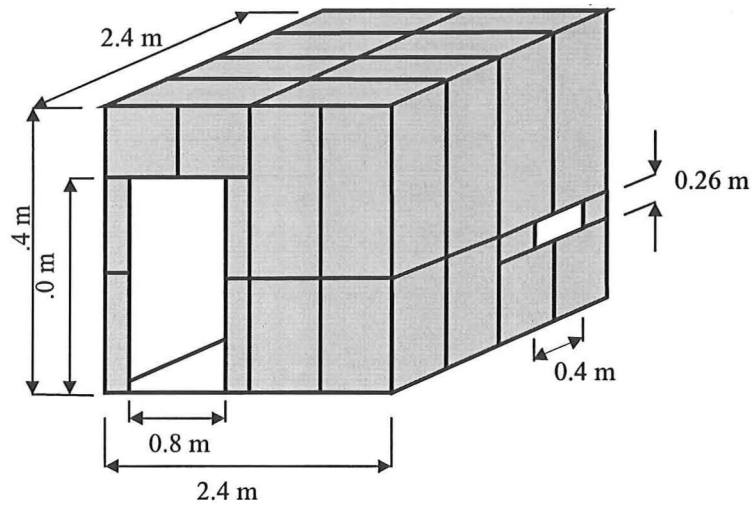

Figure 8-2: Compartment dimensions and configuration.

The frame of each compartment consisted of nominal 100 mm by 50 mm timber framing at 600 centres, with the plasterboard screwed to the framing members. Alternating panels of 9.5 mm standard and Fire Rated plasterboard lined the interior of the compartment to providing a performance comparison between each board. Exterior lining was provided in one location for each compartment in order to record cavity temperatures. The doorway was maintained in an open position for the duration of the tests and the small viewing window remained closed.

8.3 Scenarios

Three scenarios were investigated: the compartment outfitted as a lounge, bedroom and office setting. Each scene consisted of the following fuel items:

8.3.1 Lounge

2 x single seater upholstered armchairs;

1 x small electric bar heater;

Synthetic carpet with underlay;

1 x 14 inch television;

1.2 m x 0.3 m x 0.9 m high timber framed cabinet with sliding glass doors;

1 x small wooden bookshelf filled with an assortment of magazines.

The scene was designed to simulate a fire initiating from the upholstered armchair which was ignited by the electric bar heater.

8.3.2 Bedroom

1 x single bed with timber slat base and inner-sprung mattress, duvet and blankets;
1 x 1.2 m x 0.5 m x 0.9 m high wooden drawer set;
1 x wooden table with small television and game console;
1 x cane basket filled with papers;
Synthetic carpet with underlay;
Wooden framed chair with duvet.

The scene simulated a cigarette being dropped onto loose papers next to the bed, which then ignited the bed and subsequent furniture.

8.3.3 Office

1 x workstation: 1.5 m 0.5 m 0.9 m high wooden desk with drawers;
Computer, printer, monitor, and keyboard;
Stacked books and plastic ornaments;
1 x upholstered steel framed chair;
1 x Wooden framed chair with paper and polystyrene packing material;
1 x 0.5 m 0.4 m x 0.4 m high wooden drawers;
1 x upholstered 2 seater sofa (loveseat);
Synthetic carpet with underlay;
1 x small bar heater;
Synthetic curtains and plastic railing;
1 x plastic Christmas tree approximately 1 m high;
1 x cane waste paper basket filled with paper items.

Initially this scenario was to simulate the sofa being ignited by the small electric heater. However, a reluctant start caused the scenario to be altered to a fire beginning under the christmas tree next to the sofa.

8.4 Instrumentation

A thermocouple tree was located centrally in each compartment to measure the temperature within the room at eight different heights above the floor. A single thermocouple was wrapped in paper and located elsewhere in the room at floor level to indicate when full room involvement is reached. A single thermocouple was employed at the origin of the fire to measure flame temperatures. Cavity temperatures were measured using thermocouples placed on the cavity face of the external lining. Temperatures within the vent plume (doorway) were measured only in the bedroom scenario using a vertical tree with six thermocouples located at various heights.

8.5 Results

8.5.1 Lounge Scenario

Temperatures within the compartment recorded from the eight-thermocouple tree are shown by Figure 8-3.

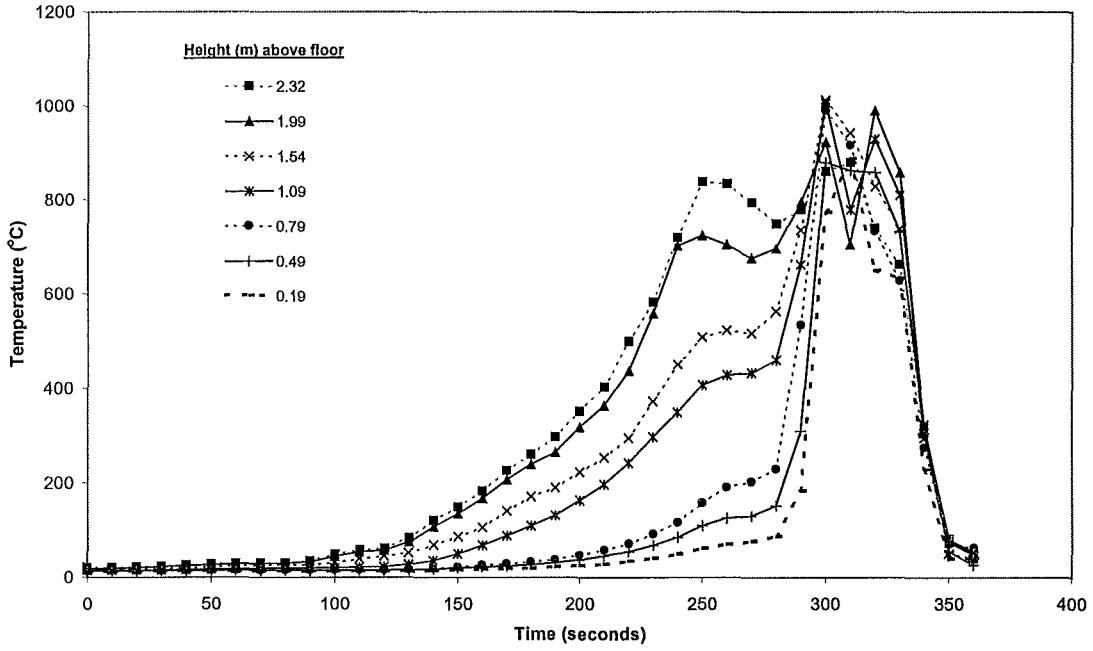

Figure 8-3: Lounge compartment temperatures.

The characteristic behaviour of a typical compartment fire is clearly portrayed by Figure 8-3, with slow growth in the incipient phase of the fire up to 120 seconds (2 mins). At which point temperatures increase rapidly reaching flashover at about 300

seconds (5 mins). The fire was extinguished shortly after flashover was reached as indicated by the rapid decay of the compartment temperatures.

Figure 8-4 displays the flame temperature at the origin of the fire and shows the rapid increase in temperatures of the second curve, indicating full room involvement has occurred.

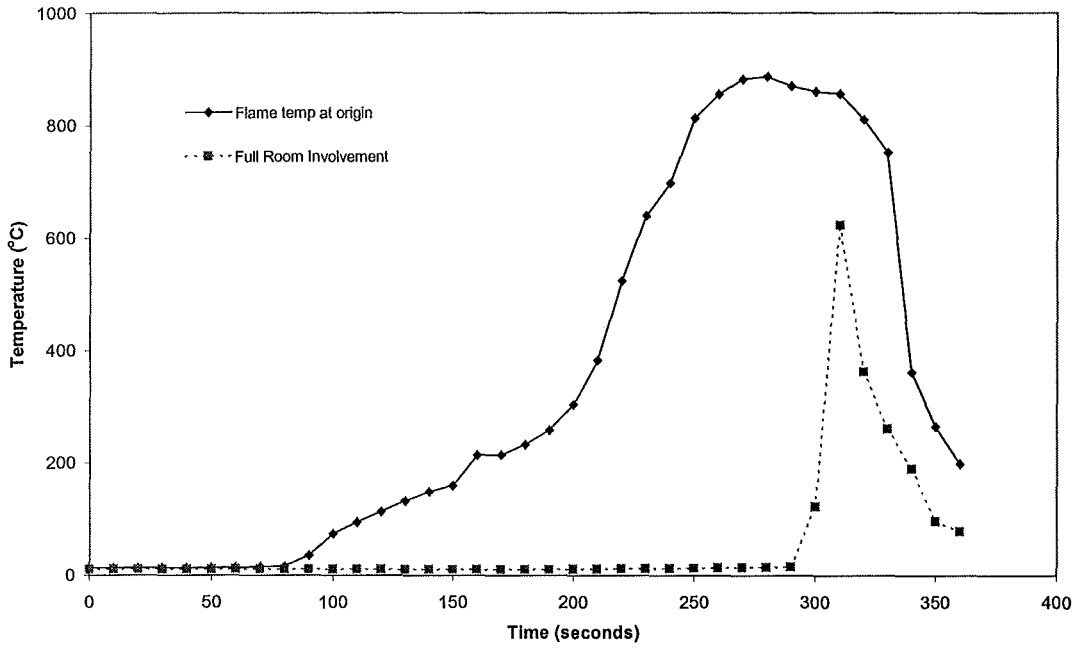

Figure 8-4: Flame temperatures above fire origin and temperatures at floor level.

In agreement with Figure 8-3 all combustibles within the compartment are contributing to the fire at approximately 300 seconds at which point temperatures within the compartment appear to become reasonably uniform.

The wall cavity temperatures in comparison to the compartment temperatures are shown by Figure 8-5. The flame temperature at the origin compares well with the overall temperatures within the compartment. Evolution of temperature through the cavity provides little information for the performance of the wall system due to termination of the fire once the post flashover phase was reached. Figure 8-5 does however indicate the large difference in temperature across the cavity (up to 500°C)

due to the rapid growth rate, short duration of the fire and insulting properties of the air cavity.

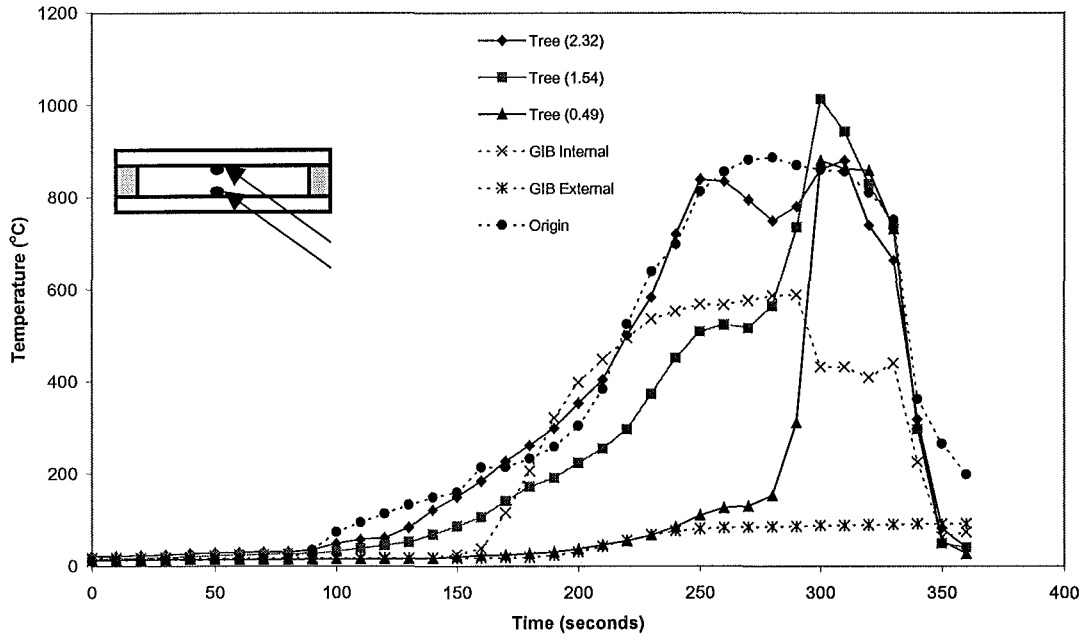

Figure 8-5: Compartment and wall cavity temperatures for lounge scene.

The thermal lag on the unexposed side of the internal lining due to moisture loss from the gypsum plaster is evident up to a time of 180 seconds (3 mins) at which point the lining temperatures follow the compartment temperatures flattening off at 600°C.

8.5.2 Bedroom Scenario

Figure 8-6 displays the distribution of temperature within the compartment. In comparison to the lounge scenario, the incipient phase is shorter and flashover occurs after approximately 240 seconds (4 mins). However, the growth rate is more gradual indicating the combustion of slower burning fuels but with a greater fuel surface area.

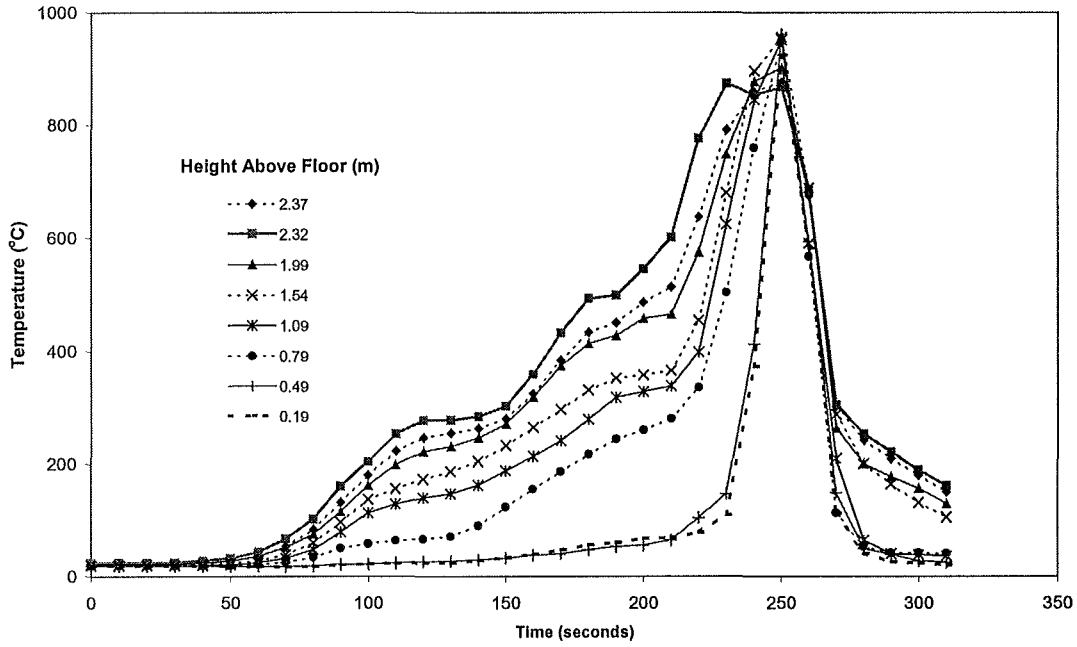

Figure 8-6: Bedroom compartment temperatures.

The point at which flashover is reached within the compartment is clearly indicated by the convergence of the temperatures measured by the thermocouples at different heights within the compartment. Again the fire was extinguished once post-flashover conditions were reached.

Figure 8-7 also shows an approximately constant rate of increase of flame temperature within the bedroom compartment, with the onset of flashover at approximately 240 seconds.

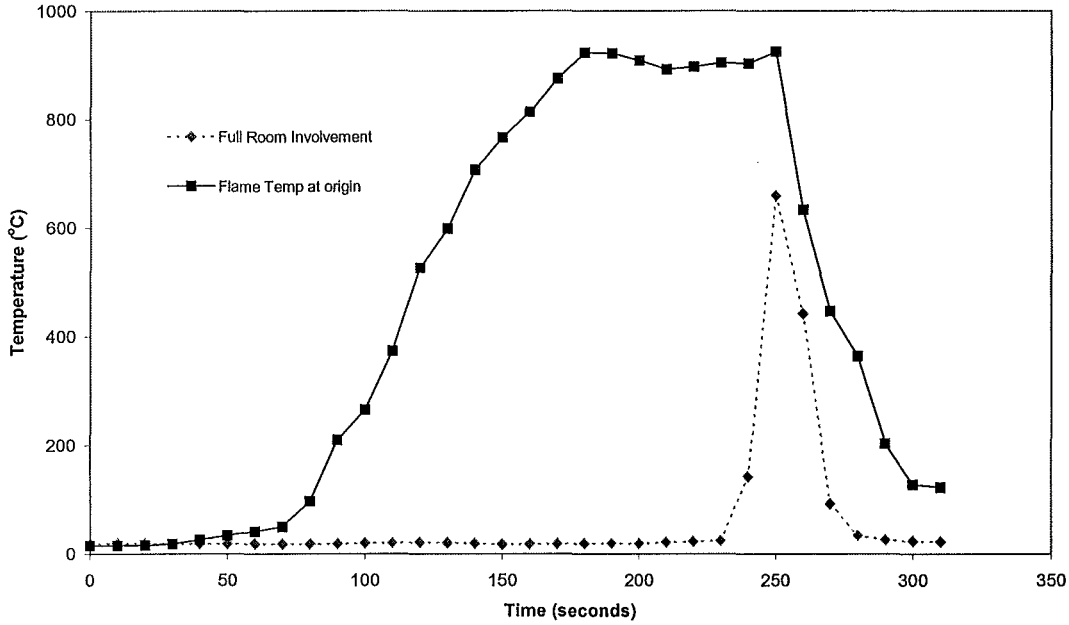

Figure 8-7: Flame temperatures above fire origin and temperatures at floor level.

Although the variation in temperature with height within the doorway of the bedroom scenario was recorded, this has little relevance to the behaviour of the plasterboard system lining the compartment and therefore has been neglected from this report.

Figure 8-8 compares the temperatures reached within the compartment with those of the flame temperature at the origin of burning and temperatures within the wall cavity.

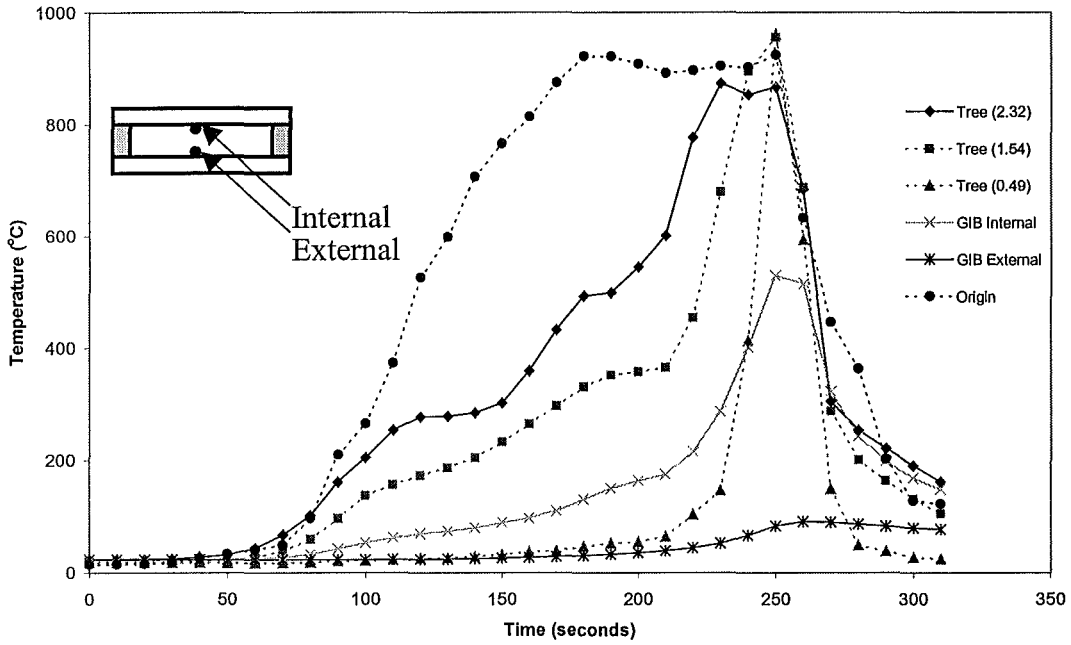

Figure 8-8: Compartment and cavity temperatures in bedroom scenario.

The difference between the flame temperatures at the origin of the fire and the compartment temperatures is greater when compared to that of the lounge scenario. This can be attributed to the nature of the fuel within the compartment and the location of the origin in relation to the centrally positioned thermocouple tree measuring compartment temperatures.

The maximum temperature difference across the cavity is smaller than that recorded in the lounge scenario. This results from the more constant rate of fire growth within the bedroom compartment, shorter exposure duration and therefore lower temperatures on the unexposed face of the internal lining.

8.5.3 Office Scenario

Figure 8-9 shows the very rapid growth of the fire within this compartment. The fire crew organising this scenario experienced a reluctant start initially, but modification of the contents within the room ensured ignition would occur and was maintained.

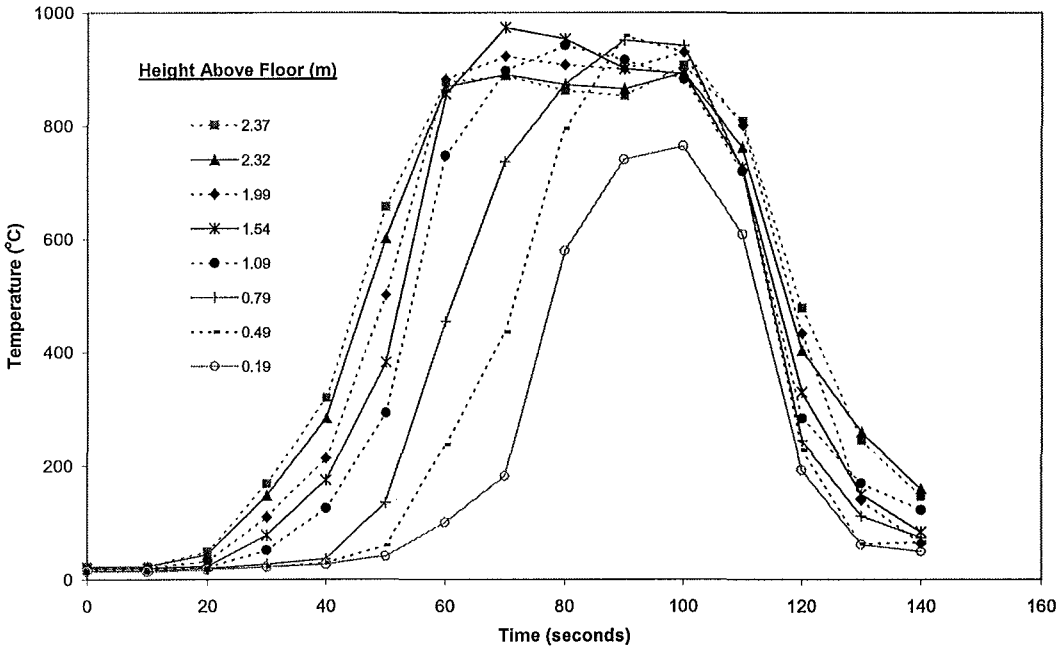

Figure 8-9: Office compartment temperatures at various heights above floor level.

The short incipient phase and rapid fire growth is the result of vertical flame spread up a plastic Christmas tree which then ignited the exposed foam cushioning of the adjacent sofa. Resulting in full room involvement occurring approximately 90 seconds (1 min 30 secs) after ignition. Maximum temperatures within the compartment are in the range of 900°C to 1000°C with rapid decay upon suppression.

The flame temperatures at the origin of the fire, as displayed by Figure 8-10, shows the temperatures reaching the first peak of nearly 600°C as the Christmas tree burns and ignites the sofa leading to flashover within the compartment.

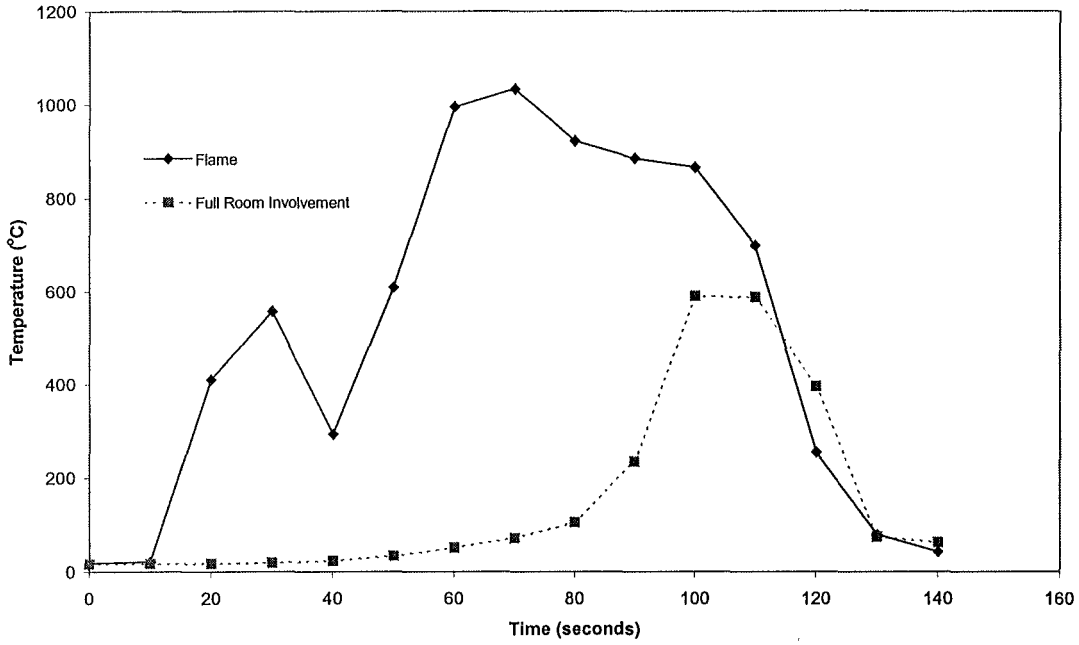

Figure 8-10: Flame temperatures above fire origin and temperatures at floor level.

The dotted curve shows the floor temperatures increasing gradually up until 90 seconds at which point flashover occurred and temperatures within the compartment were reasonably uniform.

The flame temperatures at the origin and the compartment temperatures compare well once the sofa is ignited after the initial peak in the flame temperature curve in Figure 8-11. The Christmas tree was positioned in the corner of the compartment, resulting in the initial flame temperature peak not being recorded by the centrally located thermocouple tree. Once the sofa became involved both flame temperatures at the origin and the room temperatures increased with similar rates.

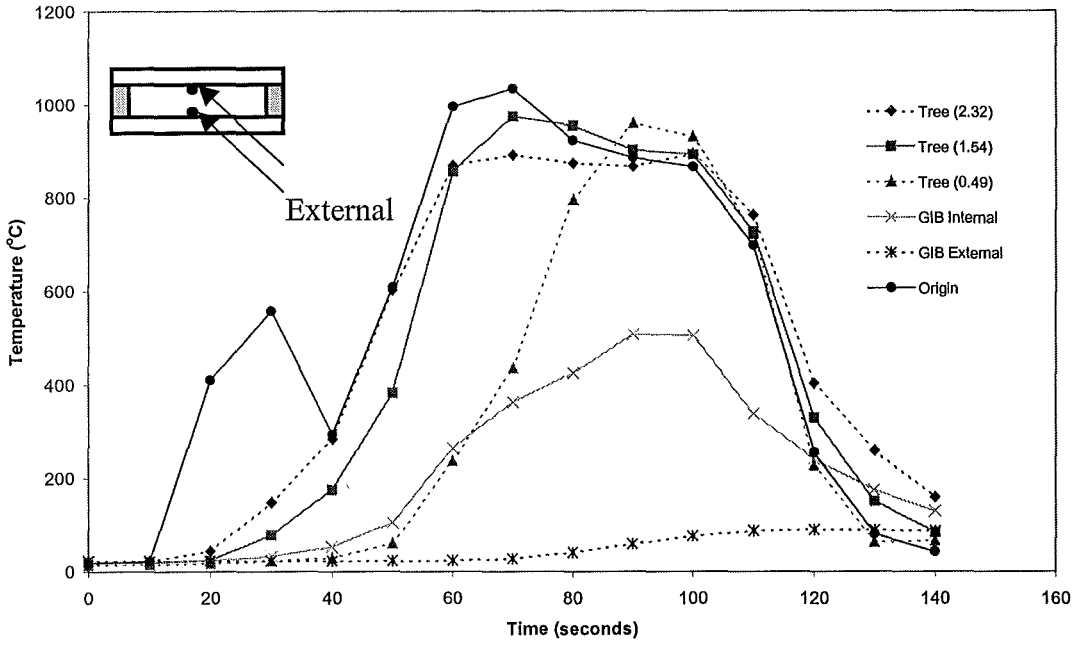

Figure 8-11: Compartment and cavity temperatures in office scenario.

The rapid fire growth is responsible for the large temperature lag experienced by the unexposed face of the internal lining compared to the other compartment scenario's. A temperature difference across the cavity of similar magnitude to that recorded in the bedroom scenario is the result of short fire duration and rapid fire growth.

8.6 Observations from Compartment Tests

Inspection of the gypsum plasterboard lining after the fires were extinguished revealed that although the lining had remained intact, it had become considerably brittle due to the loss of the internal paper lining and from the loss of chemically bound water through calcination of the gypsum plaster. Closer inspection of sections cut from the lining indicated the change in the physical and chemical composition of the board. A frontier was noticeable where moisture was moving through the board from the exposed face leaving dehydrated plaster with very little strength. This could be easy scraped off to reveal the reduced cross section of unaffected gypsum plaster.

In relation to the fire investigation course this may provide an indication of the origin of the fire. The reduced section will indicate where the wall has been exposed to fire

conditions for the longest duration. However, an area in a wall with the greatest reduction in cross section may also indicate a local hotspot where an item of fuel was located next to the wall. Typically in fires requiring Fire Service intervention wall linings are destroyed by both fire and by water streams from hoses, thus limiting the use of such a concept.

Although the inherent properties of both the standard and fire rated 9.5 mm GIB® plasterboards are similar, differences in the integrity of the boards were noticeable after exposure to the same fire. The addition of glass fibre and vermiculite in the fire rated board significantly reduced the cracking and prevented the board from becoming brittle when a force was applied, in contrast to the standard board which was brittle and exhibited cracking on the exposed face.

Another observation made once the tests were completed is the loss of paper lining on the exposed face. The paper on the exposed face of the fire rated board tended to burn off much faster than the standard board, producing a chequered appearance within the compartment (shown by Figure 8-12). Further investigation found that the dye used to distinguish the fire rated board improved the combustibility of the paper compared to the unaltered paper on the standard board. As mentioned in Section 4.2.2 Mehaffy *et al* (1994) indicated that paper burn-off will affect the heat transfer through the lining due to a reduction in the board's thickness. However, this occurs early on in the fire exposure of the board while the gypsum core remains relatively unaltered. The effect that this has on the overall fire performance of a gypsum plasterboard system is negligible and is mentioned only to explain the observations of those attending the fire investigation course.

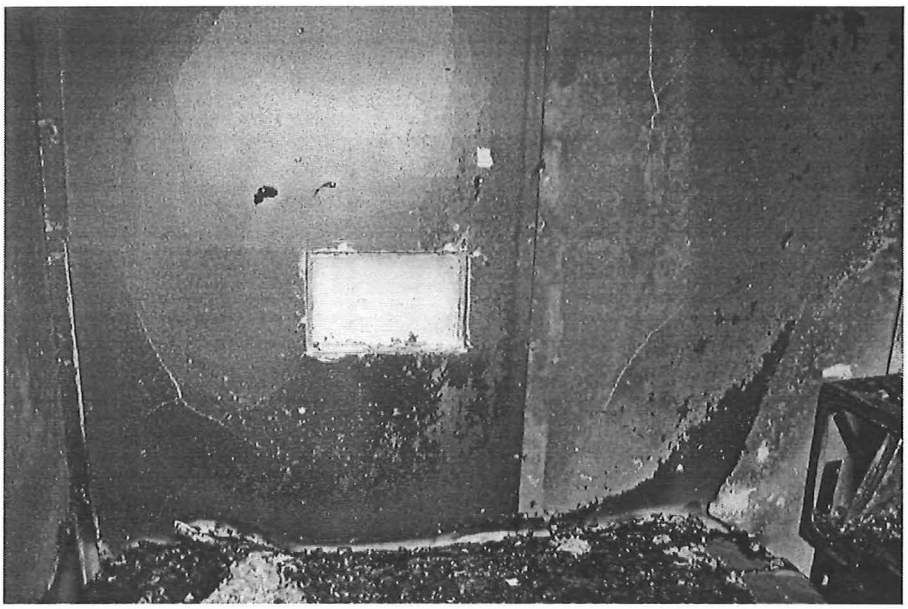

Figure 8-12: Different burn-off behaviour of paper exhibited by standard and fire rated plasterboard. (Note that GIB® Fyreline is on the right of the picture and standard GIB® board is on the left).

8.7 Significance of Compartment Tests

Although the compartments were not quite standard dimensions of 3.6 m by 2.4 m by 2.4 m high, they are however realistically sized compartments with typical fuel loads and realistic fire scenarios. The open door provided a ventilation factor (A_V/A_F) of 0.28 and an opening factor ($A_V\sqrt{h}/A_t$) of 0.069 which is well within the range of opening factors (0.02 – 0.12) used by Magnusson and Thelandersson 1970, in their research on compartment fires.

As mentioned previously the compartment tests performed provide very little information on the performance of gypsum plasterboard systems exposed to realistic fire conditions, they do however question the philosophy behind assigning ratings to systems and their relation to fire performance within buildings. The performance of gypsum plasterboard assemblies is typically evaluated in accordance with standardised test methods such as BS476, AS1530 or ASTM E119. Standard time-temperature curves give good comparison between tested materials. However, they do not have a decay phase, which may be conservative for long duration fires, and generally provide a poor representation of 'real' building fires. It is not common

knowledge that test time-temperature relationships, such as ISO834, have not significantly changed since they were originally formulated in the early 1930's.

Figure 8-13 provides a good comparison between the growth curves from the compartment tests, standard curve and furnace tests conducted at BRANZ. The flame temperature at the origin has been used to represent the compartment fires, since all compartment fires were ignited near a wall and this represents the actual exposure experienced by the wall lining local to the origin.

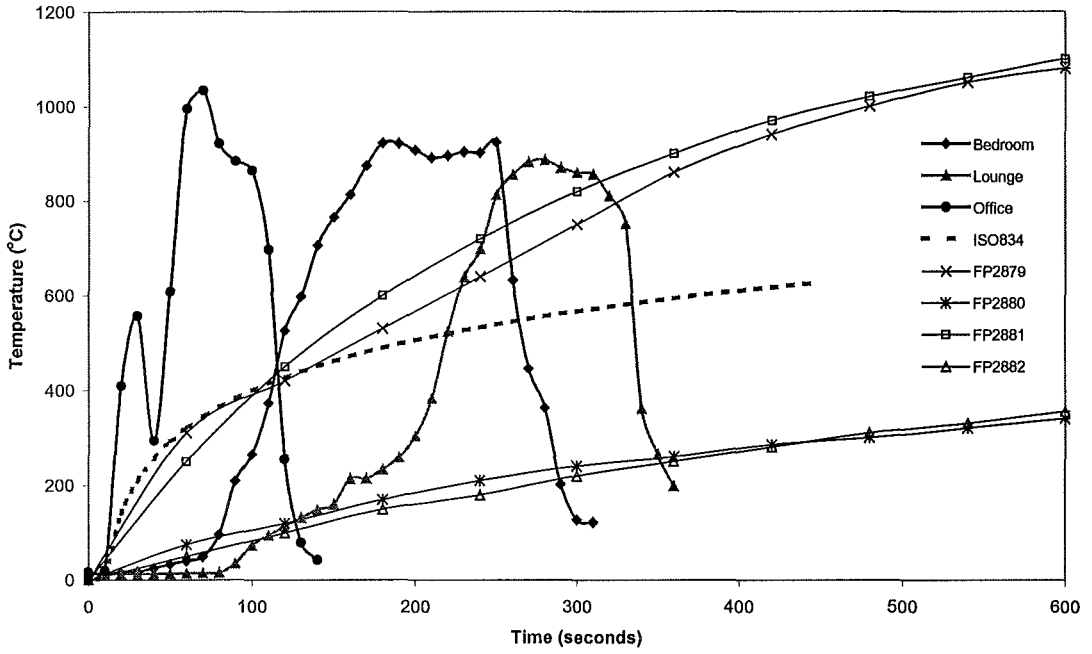

Figure 8-13: Comparison of compartment tests, furnace tests and standard curve (First 10 minutes).

The incipient phase of each compartment fire has been included in order to maintain clarity. Figure 8-13 clearly shows the severity of the compartment fires in comparison to both the standard and non-standard furnace tests. Rapid growth leading to temperatures exceeding 1000°C can occur within a few minutes of ignition. Such exposure will significantly reduce the fire performance of any gypsum plasterboard system. The viability of furnace testing to predict the performance of gypsum plasterboard exposed to realistic fires is also questioned. The growth rates of furnace tests FP2879 and FP2881, which utilised the full potential of the furnace, are

much less severe than those obtained in the compartment tests. The thermal shock and increased physical and chemical phenomena that are occurring within the gypsum plasterboard when exposed to realistic compartment fires are difficult to simulate in test furnace environments. There is an increasing need for further compartment testing combined with realistic computer software.

9 SUMMARY AND CONCLUSIONS

9.1 Summary

This study was carried out to develop an understanding of the behaviour of light framed gypsum plasterboard assemblies exposed to both realistic and standard fire conditions.

A commercially available finite element program (SAFIR), capable of analysing both thermal and structural behaviour of light-framed gypsum plasterboard assemblies has been used. For this study, only the thermal model within this computer package was utilised to predict the thermal behaviour of the assemblies, subjected to both ISO834 and realistic time-temperature curves.

A review of the thermal properties reported by various researchers in this field of study was performed to determine the variability of these parameters, and to provide boundaries for the properties used within the model of this study.

Five pilot scale furnace tests were performed to provide an insight into the behaviour of these systems exposed to non-standard conditions, and also to validate predictions from the model.

Three full-scale compartment tests were carried out to achieve time-temperature histories within the compartments, and to provide observations of the performance of plasterboard systems exposed to such environments.

9.2 Conclusions

- Non-standard furnace testing has showed that the fire resisting performance of gypsum plasterboard assemblies is highly dependent on the severity of fire exposure.

- Compartment testing and approximation to Eurocode parametric curves has indicated that the severe furnace tests approximate only a moderate compartment fire. Rapid growth fires, which are typical of domestic compartment fires, are difficult if not impossible to simulate with current furnace testing facilities.

- Finite element heat transfer modelling by computer (SAFIR) can be used to predict the time-temperature history of LSF assemblies exposed to the standard (ISO834) fire, by manipulating the thermal properties of the gypsum plasterboard.

- The calibrated model can also predict the thermal behaviour of assemblies exposed to conditions cooler than the standard fire with reasonable accuracy. Further refinement of material properties should improve accuracy of the model.

- Computer model predictions for heat transfer through LSF plasterboard systems, exposed to fire conditions that are more severe than the standard (ISO834) fire curve, are relatively poor. Further additions to the model are required to account for the accelerated degradation of the gypsum plasterboard and framing.

- Furnace testing and calibration of the thermal properties within the model have indicated that the thermal behaviour of the standard gypsum plasterboard is more variable than that of the fire rated board.

- The equivalent fire severity concept provides conservative predictions of thermal failure time for systems exposed to conditions equivalent to, or less than the standard curve. Thermal failure of systems exposed to conditions more severe than the ISO834 time-temperature is poorly predicted.

- Further development of the computer modelling package is required in order to obtain accurate results within a realistic time frame. Currently, the time required to set up input files, run the model and interpret output files, would make it impractical to use in a consulting environment.

- Results from this report question the suitability of current standard testing to determine the fire resisting performance of gypsum plasterboard assemblies. With the adoption of performance based design within fire engineering, it is becoming increasingly important to ascertain the difference between product comparison and fire resisting performance.

10 RECOMMENDATIONS

10.1 Recommendations Arising from this Study

Many sophisticated computer programs such as FAST and SIMULEX have been developed to predict fire conditions within a compartment/building, and to simulate occupant evacuation. Fire resistance requirements of passive protection within these buildings are being based on standardised fire resistance testing, and not the fire environment predicted by computer modelling. For some cases fire resistance ratings may provide ample protection for occupants, fire safety personnel, and also possessions. However, severity of a compartment fire modelled on a typical residential scenario generally exceeds that of standard fire curves, at least for the duration when occupants are expected to be evacuating.

From the experimental results of this study it is evident that the thermal behaviour of light framed gypsum plasterboard assemblies is highly dependent on the severity of the fire exposure. Therefore, it is recommended that if compartment fire modelling predicts conditions within a compartment that exceed standard time-temperature conditions, then fire resistance ratings should be increased, or the performance of the passive protection should be evaluated based on the predicted fire exposure.

There are many variations of light frame construction, and although they all exhibit different behaviour when exposed to fire, it is assumed that increased fire severity will reduce their fire resisting performance. The extent to which their fire resisting performance is reduced, by the accelerated conditions, needs to be evaluated by either testing or modelling.

It is unlikely that such recommendations will be met in the near future, due to both costs and prediction accuracy of current modelling.

10.2 Further Research for this Model

To improve the predictions and increase the capabilities of this model the following topics are recommended for further research.

Temperature in Timber Studs

The use of two user defined materials with highly variable thermal properties (wood and gypsum), require very small time steps in order to complete a calculation. This has the adverse effect of significantly increasing the run time of the model. Further research is required to reduce the number of elements defining the assembly while maintaining accurate predictions. A coarser finite element mesh combined with increased computing power will reduce the required run time significantly.

Ablation and Paper Burn-off

To improve the accuracy of the model without having to calibrate the thermal properties to account for ablation and paper burn-off. It may be possible to reduce the thickness of the exposed lining by changing the properties of thin elements of the section, from gypsum to air, once a temperature defining the onset of paper burn-off and ablation is reached. A similar approach may be adopted to model the loss of the fire exposed lining into the furnace once temperatures exceed 600°C.

Variation of Assembly

To increase the range of systems the model is able to predict the behaviour of, further research into the influence of the following factors will be required:

- Non-symmetric assemblies (different lining thickness on either side of assembly);
- Lining thickness and multiple layers of gypsum board;
- Framing size (different stud sizes and steel stud gauge);
- Stud spacing and configuration (use of staggered studs);
- Insulation in cavity
- Sound transmission requirements (presence of resilient rails etc);

Shrinkage of Timber Members

Loss of moisture from timber members causes them to shrink. This creates an air gap between the lining and the stud. A similar approach as mentioned above may be

applied, where the properties of thin layers of the stud are changed to that of air, to approximate the presence of an air gap. This may improve the predictions of heat transfer through the stud.

Structural Analysis/Load-bearing

SAFIR is a very powerful finite element program and is capable of performing both two and three-dimensional structural analysis. Once predictions from the thermal model are of acceptable accuracy, then a mechanical analysis may be performed. Experimental verification will still be required to validate predicted results.

Floors/Ceilings

This model has the flexibility to be extended to predicting the behaviour of floor/ceiling assemblies. The models ability to do so needs to be assessed.

10.3 Further Research in this Field of Study

In terms of modelling the behaviour of gypsum plasterboard assemblies subjected to standard fire conditions, there has been a marked increase in the accuracy of predictions presented by models over the past decade. Complex models such as those developed by Clancy (1999), Collier (2000), Takeda and Mehaffy (1988), and others, provide very good predictions of both thermal and structural behaviour of light framed gypsum board systems. Some of these models have the capability to replace some standard furnace tests. However, the ability of such models to simulate the behaviour of plasterboard systems exposed to realistic time-temperature conditions is either poor, or has not been validated.

Therefore, further study is required into the behaviour of light framed assemblies exposed to realistic fire conditions, and the development of models that have the flexibility to model such scenarios.

11 REFERENCES

Alfawakhiri, F., Sultan, M.A., and MacKinnon, D.H. 1999. *Fire Resistance of Loadbearing Steel-Stud Walls Protected with Gypsum Board: A Review.* Fire Technology, Vol. 35, No. 4, pp 308-335.

Alfawakhiri, F., Sultan, M.A., and Kodur, V.K.R. 2000. *Loadbearing LSF Walls Exposed to Standard Fire.* 3rd Structural Speciality Conference of the Canadian Society for Civil Engineering. London, Ontario, pp114-121.

Andersson, L. and Jansson, B. 1987. *Analytical Fire Design with Gypsum – A Theoretical and Experimental Study.* Institute of Fire Safety Design, Lund, Sweden.

Babrauskas, V. 1979. *COMPF-2, A Program for Calculating Post-Flashover Fire Temperatures.* U.S. Dept. of Commerce/National Bureau of Standards. NBS Technical Note 991. Gaithersburg, United States.

Babrauskas, V. and Williamson, R.B. 1975. *Post-Flashover Compartment Fires.* Fire Research Group, Report No. UCB FRG 75-1. University of California-Berkeley, United States.

Boral 1997. *Boral Plasterboard Installation Reference Manual.* Book 2, October 1997, Boral, Australia.

BRANZ 1990. *FR 1579: Report on the Fire Resistance Properties of a Non-Loadbearing Steel Framed Wall Lined with 12.5 mm GIB® Fyreline Gibraltar Board.* BRANZ Test Report. Building research Association of New Zealand. Wellington, New Zealand.

BRANZ 1991. *FR 1611: Report on the Fire Resistance Properties of a Loadbearing Timber Framed Wall Lined with One Layer of 12.5 mm GIB® Fyreline Gibraltar Board.* BRANZ Test Report. Building research Association of New Zealand. Wellington, New Zealand.

British Gypsum Fireline. *The White Book.* 1996, United Kingdom.

British Gypsum Glasroc. *The Glasroc Fire Book.* January 1995, United Kingdom.

British Standards Institution (BSI) 1978. *Code of Practice for the Structural Use of Timber. Part 4: Fire Resistance of Timber Structures. Section 4.1 Method for Calculating Fire Resistance of Timber Members.* BS 5268: Part 4: Section 4.1:1987. London, United Kingdom.

Buchanan, A.H. 2000. *Structural Design for Fire Safety.* University of Canterbury, Christchurch, New Zealand.

Buchanan, A.H and Gerlich, J.T. 1997. *Fire Performance of Gypsum Plasterboard.* Proceedings, 1997 IPENZ Conference, Wellington.

Butler, C.P. 1971. *Notes on Charring Rates in Wood.* Fire Research Station, Note FR 896. Borehamwood, United Kingdom.

Carne, D. 1995. *Melt Temperatures of Glass Fibre Used in Fyrechek.* CSR Gyprock Bradford Report No. 001292DC.

Collier, P.C.R. 1991b. *Design of Loadbearing Light Timber Frame Walls for Fire Resistance: Part 1.* BRANZ Study Report SR36. Building Research Association of New Zealand.

Collier, P.C.R 1996b. *A Model for Predicting the Fire Resisting Performance of Small-Scale Cavity Walls in Realistic Fires.* Fire Technology, Vol. 32, No. 2, pp. 120 – 136.

Collier, P.C.R. 2000. *Fire Resistance of Lightweight Framed Construction.* Fire Engineering Research Report 00/2. University of Canterbury, Christchurch, New Zealand.

Cooper, L.Y. 1997. *The Thermal Response of Gypsum-Panel/Steel Stud Wall Systems Exposed to Fire Environments – A Simulation for the use in Zone-Type Fire Models.* NIST Report NISTIR 6027. Building and Fire Research Laboratory, National Institute of standards and Technology, Gaithersburg, MD 20899.

Clancy, P. 1999. *Time and Probability of Failure of Timber Framed Walls in Fire.* Doctorate Thesis. Centre of Environmental Safety and Risk Engineering, Faculty of Engineering and Science, Victoria University of Technology, Victoria, Australia.

CSR Gyprock 1997. *CSR Plasterboard Installation Manual.* August 1997, Australia.

Draft Eurocode 5, Part X. 1989. *Structural Fire Design for Timber Structures.* European Committee for Standardisation, Brussels, pp19.

EC3 1995. *Eurocode 3: Design of Steel Structures. ENV 1992-1-2: General Rules – Structural Fire Design.* European Committee for Standardisation, Brussels.

Franssen, J.M. 1999. *Thermal Properties of Gypsum Board Submitted to the Fire Literature Survey.* Universite De Liege – Institut Du Genie Civil, Liege, Belgium.

Franssen, J.M., Kodur, V.K.R., and Mason, J. 2000. *User's Manual for SAFIR98a: A Computer Program for Analysis of Structures Submitted to the Fire.* Universite De Liege – Institut Du Genie Civil, Liege, Belgium.

Fredlund, B. 1988. *A Model for Heat and Mass Transfer in Timber Structures During Fire, A Theoretical, Numerical and Experimental Study.* Lund University, Sweden, Institute of Science and Technology, Department of Fire Engineering, Report LUTVDG/(TVBB-1003), (a-pp178).

Fuller, J.J, Leichti, R.J., and White, R.H. 1992. *Temperature Distribution in a Nailed Gypsum-stud Joint Exposed to Fire.* Fire and Materials, Vol. 16, pp95-99.

Gammon, B.W. 1987. *Reliability Analysis of Wood Frame Wall Assemblies Exposed to Fire.* Berkeley, California: University Microfilms Dissertations Information Service, University of California.

Gerlich, J.T. 1995. *Design of Loadbearing Light Steel Frame Walls for Fire Resistance.* Fire Engineering Research Report 95/3. University of Canterbury, Christchurch, New Zealand.

Gerlich, J.T., Collier, P.C.R., and Buchanan, A.H. 1996. *Design of light Steel-framed Walls for Fire Resistance.* Fire and Materials, Vol. 20, pp 79-96.

Goncalves, T, Jong T, Clancy, P, and Poynter, W. 1996. *Mechanical Properties of Fire Rated Gypsum Board.* Department of Civil and Building Engineering, Victoria University of Technology.

Gypsum Association 1993. *Application and Finishing of Gypsum Board.* GA-216-93, 1993, United States.

Gypsum Association 1994. *Fire Resistance Design Manual.* Gypsum Association, Washington DC.

Hadjisophocleous, G. 1996. *Extract from Report on Furnace Tests on Walls for Department of National Defence, Canada.* National Fire Laboratory, NRCC, National Research Council Canada.

Hadvig, S. 1981. *Charring of Wood in Building Fires.* Technical University of Denmark, Lyngby, Denmark, pp 9-11.

Hamerlinck, R. 1991. *The Behaviour of Fire-Exposed Composite Steel/Concrete Slabs.* Cip-Gegevens Koninklijke Bibliotheek, Den Haag.

Harmanthy, T.Z. 1988. *Properties of Building Materials.* The SFPE Handbook of Fire Protection Engineering. Section ! Chapter 6. Society of Fire Protection Engineers/National Fire Protection Association, Boston, United States.

Hibbit, Karlsson and Sorenson Inc. 1994. *ABAQUS User Manuals.* Version 5.4. Pawtucket, Rhode Island, United States.

ISO 834 1975. *Fire Resistance Tests – Elements of Building Construction.* International Organisation for Standardisation. Switzerland.

Janssens, M.L. 1994. *Physical Properties for Wood Pyrolysis Models.* Proceedings of Pacific Timber Engineering Conference. Gold Coast, Australia, pp 607-618.

Knauf Plasterboards. *Publication B1 – Diamond Drywall Systems.* January 1997, United Kingdom.

Knudson, R.M., and Schniewind, A.P. 1975. *Performance of Structural Wood Members Exposed to Fire.* Forest Products Journal, Vol 25, No 2.

Konig, J. and Walleij, L. 2000. *Timber Frame Assemblies Exposed to Standard and Parametric Fires, Part 2: A Design Model for Standard Fire Exposure.* Swedish Institute for Wood Technology Research, Report I 0001001, Sweden.

Lie, T.T. 1992. *Structural Fire Protection.* American Society of Civil Engineers, Structural Division, Manuals and Reports on Engineering Practice No. 78.

Mehaffy, J.R, Cuerrier, P, and Carisse, G. 1994. *A Model for Predicting Heat Transfer through Gypsum-Board/Wood-Stud Walls Exposed to Fire.* Fire and Materials, Vol. 18, pp. 297-305.

Magnusson, S.E and Thelandersson, S 1970. *Temperature-Time Curves of Complete Process of Fire Development.* Acta Polytechnica Scandanavica. Civil Engineering and Building Construction Series, Number 65.

Mason, J.E. 2000. *Heat Transfer Programs for the Design of Structures Exposed to Fire.* Fire Engineering Research Report 00/9. University of Canterbury, Christchurch, New Zealand.

Mikkola, E. 1990. *Charring of Wood.* Espo 1990. Valtion teknillinen tutkimuskeskus, Tutkimuksia-Statens tekniska forskningscentral, Forskningsrapporter- Technical Research Centre of Finland, Research Report 689, pp35.

NIST 1980. Thermal Properties taken from NIST website. http://fire.nist.gov/brflpubs. Original Reference: *Report 7040.* 384C Statens Provingaanstalt, Stockholm.

Rondo 1998. *Trade Literature for Cold Formed Steel Sections.* Rondo Building Services Property Ltd, Australia/New Zealand.

SAA 1990. *AS1530: Part 4: Fire Resistance Tests of Elements of Building Construction.* Standards Association of Australia. North Sydney, NSW, Australia.

SNZ 1991. MP9. *Fire Properties of Building Materials and Elements of Structure.* Miscellaneous Publication No. 9. Standards New Zealand, Wellington.

Sterner, E. and Wickstrom, U. 1990. *TASEF-Temperature Analysis of Structures Exposed to Fire.* Fire Technology SP Report 1990:05. Swedish National Testing Institute, Sweden.

Sultan, M.A. 1996. *A Model for Predicting the Heat Transfer Through Noninsulated Unloaded Steel-Stud Gypsum Board Wall Assemblies Exposed to Fire.* National Fire Laboratory, Institute for Research in Construction, National Research Council Canada, Ottawa, Ontario, Canada.

Takeda, H., and Mehaffy, J.R. 1998. *Wall2D: A Model for Predicting Heat Transfer through Wood-Stud Walls Exposed to Fire.* Fire and Materials, Vol. 22, pp 133-140.

Takeda, H. 1999. *Model to Predict Fire Resistance of Wood-Stud Walls – The Effect of Shrinkage of Gypsum Board.* Proceedings of Pacific Timber Engineering Conference PTEC99, Vol. 3, pp 21-29.

Tang, W.K. 1967. *Effect of Inorganic Salts on Pyrolysis of Wood, Alpha-Cellulose and Lignin Determined by Thermogravimetric Analysis.* US Forest Research Paper, FPL 71, Forest Products Laboratory, US Dept Agricultural Forest Service, Madison, Wisconsin, USA.

Thomas, G.C., Buchanan, A.H., Carr, A.J., Fleischmann, C.M., and Moss, P.J. 1994. *Light Timber Framed Walls Exposed to Compartment Fires.* Pacific Timber Engineering Conference, Vol. 2, pp 531-538.

Thomas, G.C., Buchanan, A.H., Carr, A.J., Fleischmann, C.M., and Moss, P.J. 1996. *Modelling Structural Fire Performance of Light Wood Frame Construction.* Proceedings of the International Wood Engineering Conference, New Orleans, Lousiana USA, Vol 2, pp 241-248.

Thomas, G.C. 1997. *Fire Resistance of Light Timber Framed Walls and Floors.* Fire Engineering Research Report 97/7. University of Canterbury, Christchurch, New Zealand.

UL 1996. *Fire Resistance Directory.* Underwriters Laboratories Inc, USA.

Westrock Heavy. Extracted from Clancy (1999) through communication with Hadjisophocleous (1996).

White, R.H., and Nordheim, E.V. 1992. Fire Technology, Vol. 28, No. 2.

Winstone Wallboards 1992b. *Gib® Board Stopping and Finishing Systems, 1992.* Winstone Wallboards Ltd. Auckland, New Zealand.

Winstone Wallboards 1997. *Gib® Fire Rated Systems, July 1997.* Winstone Wallboards Ltd. Auckland, New Zealand.

Young, S. 2000. *Structural Modelling of Plasterboard-Clad, Light Timber-Framed Walls in Fire.* Centre of Environmental Safety and Risk Engineering, Faculty of Engineering and Science, Victoria University of Technology, Victoria, Australia.

APPENDIX 1: SAFIR Input File

The input file for the 60 minute system is given below.

```
Course Section discretisation of 63 x 34 x 0.55
steel stud with one layer of 12.5 mm GIB each side

   NPTTOT        2
    NNODE  185
     NDIM    2
 NDIMMATER    1
  NDDLMAX    1
     FROM    1   TO  185 STEP    1 NDDL    1

  TEMPERAT
     TETA      0.9
  TINITIAL       20
  MAKE.TEM
 LARGEUR11     80000
 LARGEUR12      1000
   NORENUM
GIB60Z.tem
     NMAT    2
  ELEMENTS
     SOLID  140
        NG    2
     NVOID    2
FRTIERVOID   80

    NODES
      NODE    1    0.0005    0.0335
      NODE    2    0.0629    0.0335
      NODE    3    0.0571    0.0329
      NODE    4    0.0571    0.0335
      NODE    5    0.0063    0.0335
      NODE    6    0.0063    0.0329
      NODE    7    0.0005    0.0167
      NODE    8    0.0005    0.0329
      NODE    9         0    0.0005
      NODE   10         0    0.0167
      NODE   11         0    0.0329
      NODE   12   -0.0025    0.0005
      NODE   13   -0.0025    0.0167
      NODE   14   -0.0025    0.0329
      NODE   15    -0.005    0.0005
      NODE   16    -0.005    0.0167
      NODE   17    -0.005    0.0329
      NODE   18   -0.0075    0.0005
      NODE   19   -0.0075    0.0167
      NODE   20   -0.0075    0.0329
      NODE   21     -0.01    0.0005
      NODE   22     -0.01    0.0167
      NODE   23     -0.01    0.0329
      NODE   24   -0.0125    0.0005
      NODE   25   -0.0125    0.0167
      NODE   26   -0.0125    0.0329
      NODE   27         0    0.0335
      NODE   28         0    0.0901
      NODE   29         0    0.1467
      NODE   30         0    0.2033
      NODE   31         0    0.2599
      NODE   32         0    0.3165
      NODE   33         0    -0.283
      NODE   34         0   -0.2264
      NODE   35         0   -0.1698
      NODE   36         0   -0.1132
      NODE   37         0   -0.0566
      NODE   38         0         0
      NODE   39   -0.0025    0.0335
      NODE   40   -0.0025    0.0901
      NODE   41   -0.0025    0.1467
      NODE   42   -0.0025    0.2033
      NODE   43   -0.0025    0.2599
      NODE   44   -0.0025    0.3165
      NODE   45    -0.005    0.0335
      NODE   46    -0.005    0.0901
      NODE   47    -0.005    0.1467
      NODE   48    -0.005    0.2033
      NODE   49    -0.005    0.2599
      NODE   50    -0.005    0.3165
      NODE   51   -0.0075    0.0335
      NODE   52   -0.0075    0.0901
      NODE   53   -0.0075    0.1467
      NODE   54   -0.0075    0.2033
      NODE   55   -0.0075    0.2599
      NODE   56   -0.0075    0.3165
      NODE   57     -0.01    0.0335
      NODE   58     -0.01    0.0901
      NODE   59     -0.01    0.1467
      NODE   60     -0.01    0.2033
      NODE   61     -0.01    0.2599
      NODE   62     -0.01    0.3165
      NODE   63   -0.0125    0.0335
      NODE   64   -0.0125    0.0901
      NODE   65   -0.0125    0.1467
      NODE   66   -0.0125    0.2033
      NODE   67   -0.0125    0.2599
      NODE   68   -0.0125    0.3165
      NODE   69   -0.0025     -0.283
      NODE   70   -0.0025    -0.2264
      NODE   71   -0.0025    -0.1698
      NODE   72   -0.0025    -0.1132
      NODE   73   -0.0025    -0.0566
      NODE   74   -0.0025         0
      NODE   75    -0.005     -0.283
      NODE   76    -0.005    -0.2264
      NODE   77    -0.005    -0.1698
      NODE   78    -0.005    -0.1132
      NODE   79    -0.005    -0.0566
      NODE   80    -0.005         0
      NODE   81   -0.0075     -0.283
      NODE   82   -0.0075    -0.2264
      NODE   83   -0.0075    -0.1698
      NODE   84   -0.0075    -0.1132
      NODE   85   -0.0075    -0.0566
      NODE   86   -0.0075         0
      NODE   87     -0.01     -0.283
      NODE   88     -0.01    -0.2264
      NODE   89     -0.01    -0.1698
      NODE   90     -0.01    -0.1132
      NODE   91     -0.01    -0.0566
      NODE   92     -0.01         0
      NODE   93   -0.0125     -0.283
      NODE   94   -0.0125    -0.2264
      NODE   95   -0.0125    -0.1698
      NODE   96   -0.0125    -0.1132
```

```
NODE    97   -0.0125   -0.0566
NODE    98   -0.0125         0
NODE    99    0.0629         0
NODE   100    0.0473         0
NODE   101    0.0473    0.0005
NODE   102    0.0317         0
NODE   103    0.0317    0.0005
NODE   104    0.0161         0
NODE   105    0.0161    0.0005
NODE   106    0.0005         0
NODE   107    0.0005    0.0005
NODE   108    0.0629    0.0005
NODE   109    0.0629    0.0167
NODE   110    0.0629    0.0329
NODE   111    0.0676    0.0005
NODE   112    0.0676    0.0167
NODE   113    0.0676    0.0329
NODE   114    0.0635    0.0005
NODE   115    0.0635    0.0167
NODE   116    0.0635    0.0329
NODE   117    0.0676    0.0335
NODE   118    0.0676    0.0901
NODE   119    0.0676    0.1467
NODE   120    0.0676    0.2033
NODE   121    0.0676    0.2599
NODE   122    0.0676    0.3165
NODE   123    0.0635    0.0335
NODE   124    0.0635    0.0901
NODE   125    0.0635    0.1467
NODE   126    0.0635    0.2033
NODE   127    0.0635    0.2599
NODE   128    0.0635    0.3165
NODE   129    0.0676    -0.283
NODE   130    0.0676   -0.2264
NODE   131    0.0676   -0.1698
NODE   132    0.0676   -0.1132
NODE   133    0.0676   -0.0566
NODE   134    0.0676         0
NODE   135    0.0635    -0.283
NODE   136    0.0635   -0.2264
NODE   137    0.0635   -0.1698
NODE   138    0.0635   -0.1132
NODE   139    0.0635   -0.0566
NODE   140    0.0635         0
NODE   141     0.076    0.0005
NODE   142    0.0753    0.0005
NODE   143    0.0718    0.0005
NODE   144     0.076    0.0335
NODE   145    0.0753    0.0335
NODE   146    0.0718    0.0335
NODE   147     0.076    -0.283
NODE   148    0.0753    -0.283
NODE   149    0.0718    -0.283
NODE   150     0.076    0.0167
NODE   151     0.076    0.0329
NODE   152    0.0753    0.0167
NODE   153    0.0753    0.0329
NODE   154    0.0718    0.0167
NODE   155    0.0718    0.0329
NODE   156     0.076    0.0901
NODE   157    0.0753    0.0901
NODE   158    0.0718    0.0901
NODE   159     0.076    0.1467
NODE   160    0.0753    0.1467
NODE   161    0.0718    0.1467
NODE   162     0.076    0.2033
NODE   163    0.0753    0.2033
NODE   164    0.0718    0.2033
NODE   165     0.076    0.2599
NODE   166     0.076    0.3165
NODE   167    0.0753    0.2599
NODE   168    0.0753    0.3165
NODE   169    0.0718    0.2599
NODE   170    0.0718    0.3165
NODE   171     0.076   -0.2264
NODE   172    0.0753   -0.2264
NODE   173    0.0718   -0.2264
NODE   174     0.076   -0.1698
NODE   175    0.0753   -0.1698
NODE   176    0.0718   -0.1698
NODE   177     0.076   -0.1132
NODE   178    0.0753   -0.1132
NODE   179    0.0718   -0.1132
NODE   180     0.076   -0.0566
NODE   181     0.076         0
NODE   182    0.0753   -0.0566
NODE   183    0.0753         0
NODE   184    0.0718   -0.0566
NODE   185    0.0718         0
NODELINE          0.0       0.0
YC ZC             0.0       0.0
FIXATIONS

NODOFSOLID
ELEM    1    3    4    2  110    1
ELEM    2  110    2  123  116    1
ELEM    3  108  109  115  114    1
ELEM    4  169  170  168  167    2
ELEM    5  100  101  108   99    1
ELEM    6  106   38    9  107    1
ELEM    7    9   10    7  107    1
ELEM    8   11   27    1    8    1
ELEM    9    8    1    5    6    1
ELEM   10  153  145  144  151    2
ELEM   11  142  152  150  141    2
ELEM   12  183  142  141  181    2
ELEM   13   74   12    9   38    2
ELEM   14   12   13   10    9    2
ELEM   15   14   39   27   11    2
ELEM   16  145  157  156  144    2
ELEM   17  148  172  171  147    2
ELEM   18   39   40   28   27    2
ELEM   19   69   70   34   33    2
ELEM   20   80   15   12   74    2
ELEM   21   86   18   15   80    2
ELEM   22   92   21   18   86    2
ELEM   23   98   24   21   92    2
ELEM   24   15   16   13   12    2
ELEM   25   18   19   16   15    2
ELEM   26   21   22   19   18    2
ELEM   27   24   25   22   21    2
ELEM   28   17   45   39   14    2
```

```
ELEM  29  20  51  45  17  2
ELEM  30  23  57  51  20  2
ELEM  31  26  63  57  23  2
ELEM  32  45  46  40  39  2
ELEM  33  51  52  46  45  2
ELEM  34  57  58  52  51  2
ELEM  35  63  64  58  57  2
ELEM  36  75  76  70  69  2
ELEM  37  81  82  76  75  2
ELEM  38  87  88  82  81  2
ELEM  39  93  94  88  87  2
ELEM  40  10  11   8   7  1
ELEM  41  13  14  11  10  2
ELEM  42  16  17  14  13  2
ELEM  43  19  20  17  16  2
ELEM  44  22  23  20  19  2
ELEM  45  25  26  23  22  2
ELEM  46  40  41  29  28  2
ELEM  47  41  42  30  29  2
ELEM  48  42  43  31  30  2
ELEM  49  43  44  32  31  2
ELEM  50  70  71  35  34  2
ELEM  51  71  72  36  35  2
ELEM  52  72  73  37  36  2
ELEM  53  73  74  38  37  2
ELEM  54  46  47  41  40  2
ELEM  55  47  48  42  41  2
ELEM  56  48  49  43  42  2
ELEM  57  49  50  44  43  2
ELEM  58  52  53  47  46  2
ELEM  59  53  54  48  47  2
ELEM  60  54  55  49  48  2
ELEM  61  55  56  50  49  2
ELEM  62  58  59  53  52  2
ELEM  63  59  60  54  53  2
ELEM  64  60  61  55  54  2
ELEM  65  61  62  56  55  2
ELEM  66  64  65  59  58  2
ELEM  67  65  66  60  59  2
ELEM  68  66  67  61  60  2
ELEM  69  67  68  62  61  2
ELEM  70  76  77  71  70  2
ELEM  71  77  78  72  71  2
ELEM  72  78  79  73  72  2
ELEM  73  79  80  74  73  2
ELEM  74  82  83  77  76  2
ELEM  75  83  84  78  77  2
ELEM  76  84  85  79  78  2
ELEM  77  85  86  80  79  2
ELEM  78  88  89  83  82  2
ELEM  79  89  90  84  83  2
ELEM  80  90  91  85  84  2
ELEM  81  91  92  86  85  2
ELEM  82  94  95  89  88  2
ELEM  83  95  96  90  89  2
ELEM  84  96  97  91  90  2
ELEM  85  97  98  92  91  2
ELEM  86 102 103 101 100  1
ELEM  87 104 105 103 102  1
ELEM  88 106 107 105 104  1
ELEM  89 113 117 146 155  2
ELEM  90 116 123 117 113  2
ELEM  91 111 112 154 143  2
ELEM  92 114 115 112 111  2
ELEM  93 134 111 143 185  2
ELEM  94 140 114 111 134  2
ELEM  95 117 118 158 146  2
ELEM  96 123 124 118 117  2
ELEM  97 129 130 173 149  2
ELEM  98 135 136 130 129  2
ELEM  99 109 110 116 115  1
ELEM 100 152 153 151 150  2
ELEM 101 112 113 155 154  2
ELEM 102 115 116 113 112  2
ELEM 103 157 160 159 156  2
ELEM 104 160 163 162 159  2
ELEM 105 163 167 165 162  2
ELEM 106 167 168 166 165  2
ELEM 107 172 175 174 171  2
ELEM 108 175 178 177 174  2
ELEM 109 178 182 180 177  2
ELEM 110 182 183 181 180  2
ELEM 111 118 119 161 158  2
ELEM 112 119 120 164 161  2
ELEM 113 120 121 169 164  2
ELEM 114 121 122 170 169  2
ELEM 115 124 125 119 118  2
ELEM 116 125 126 120 119  2
ELEM 117 126 127 121 120  2
ELEM 118 127 128 122 121  2
ELEM 119 130 131 176 173  2
ELEM 120 131 132 179 176  2
ELEM 121 132 133 184 179  2
ELEM 122 133 134 185 184  2
ELEM 123 136 137 131 130  2
ELEM 124 137 138 132 131  2
ELEM 125 138 139 133 132  2
ELEM 126 139 140 134 133  2
ELEM 127 173 176 175 172  2
ELEM 128 149 173 172 148  2
ELEM 129 176 179 178 175  2
ELEM 130 179 184 182 178  2
ELEM 131 184 185 183 182  2
ELEM 132 143 142 183 185  2
ELEM 133 143 154 152 142  2
ELEM 134 154 155 153 152  2
ELEM 135 146 145 153 155  2
ELEM 136 146 158 157 145  2
ELEM 137 158 161 160 157  2
ELEM 138 161 164 163 160  2
ELEM 139 164 169 167 163  2
ELEM 140  99 108 114 140  1
```

```
FRONTIER
 23       FISO
 27       FISO
 31       FISO
 35       FISO
 39       FISO
 45       FISO
 66       FISO
 67       FISO
 68       FISO
 69       FISO
 82       FISO
 83       FISO
 84       FISO
 85       FISO

    VOID
    ELEM    19     3
    ELEM    50     3
    ELEM    51     3
    ELEM    52     3
    ELEM    53     3
    ELEM     6     1
    ELEM    88     4
    ELEM    87     4
    ELEM    86     4
    ELEM     5     4
    ELEM   140     4
    ELEM   126     1
    ELEM   125     1
    ELEM   124     1
    ELEM   123     1
    ELEM    98     1
ENDVOID
    VOID
    ELEM   118     1
    ELEM   117     1
    ELEM   116     1
    ELEM   115     1
    ELEM    96     1
    ELEM     2     2
    ELEM     1     2
    ELEM     1     1
    ELEM     1     4
    ELEM    99     1
    ELEM     3     1
    ELEM     5     2
    ELEM    86     2
    ELEM    87     2
    ELEM    88     2
    ELEM     7     3
    ELEM    40     3
    ELEM     9     4
    ELEM     9     3
    ELEM     9     2
    ELEM     8     2
    ELEM    18     3
    ELEM    46     3
    ELEM    47     3
    ELEM    48     3
    ELEM    49     3
```

```
ENDVOID
SYMMETRY
ENDSYM
PRECISION   0.0001
MATERIALS
STEELEC2
                                                    12  12
  USER1  15
     0      0.3      900      747     5  12
   100      0.3      900      747
   105      0.3    36000      747
   125     0.12    36000      725
   140     0.12     2000      710
   150     0.12     2000      702
   200     0.12     1000      702
   205     0.12     9000      702
   215     0.12     9000      702
   220     0.12      900      702
   400     0.12      900      680
   600     0.15      900      680
   700      0.6      900      680
  1000      0.8      900      680
  1200      1.0      900      680
  TIME
          0.01      500
          0.05     2000
           0.1     2800
           0.5     3900
ENDTIME
IMPRESSION
TIMEPRINT     60
```

APPENDIX 2: Observations from Furnace Testing

Observations from furnace testing conducted at BRANZ testing facilities are given below.

Time	Observations (FP2879)
1:15	Paper on exposed face beginning to burn, paper discolours
2:00	Thin layer of paper begins to peel and fall to bottom of furnace
5:00	Furnace filled with smoke, excess fuel within furnace producing large quantities of smoke
6:45	Smoke is forced out from the side of the furnace
8:00	Smoke begins to clear and specimen is again visible, plaster is fully exposed (all paper has been burnt off).
9:00	Small narrow cracking (crazing) is observed on the fire exposed face
10:00	Smoke begins to fill furnace again
16:30	Sounds of plaster falling to the bottom of the furnace
17:00	Specimen is visible, fire exposed face is falling off exposing studs and outer panel
18:00	Steam can be seen exiting from the outer panel
20:00	Areas near screws and joints in panel begin to go black, panel has deflected in towards furnace.
21:00	Large cracking in the bottom 1/3 of the panel is observed from the fire side of the panel, and the lines of cracking can also be seen on the outer face of the panel
21:30	Panel begins to straighten as steel studs begin to expand on the outer flange
22:00	Panel in cavity region begins to bow out
25:00	Large cracks begin to form over entire face of panel
27:00	Paper at top of panel begins to change colour and burn
30:00	Burning front of paper moves down panel from top of furnace
34:00	Panel loses contact with studs, bows out and allows flames to propagate from furnace
35:00	Test stopped

Time	Observations (FP2880)
1:00	Paper on exposed face beginning to discolour, difficulty maintaining low furnace Temperatures, burners going out due to low fuel feed.
3- 5.00	Still having difficulty maintaining low furnace temperatures
6:00	Plaster stopping starting to discolour
6:30	Paper face burning off at bottom of furnace
7:00	Paper face peeling off near burner
10:00	All paper surface of exposed face is burning
12:00	Small narrow cracking (crazing) is observed on the fire exposed face
19:30	Small horizontal cracking beginning to appear on exposed face
21:30	Thin slices of gypsum can be seen peeling off exposed face at top of furnace
30:00	Horizontal cracks stemming from joint in plaster face, localised cracking around screws into stud at joint
33:00	Horizontal cracking in stud beginning to open up considerably 3-4mm wide
34:00	Significant cracking on exposed face can be seen
36:00	Sections of panel formed by the cracking of the exposed face begin to fall into the furnace leaving studs and other panel exposed
40:30	Larger sections of the exposed panel are beginning to fall off and fall into the furnace.
50:00	Integrity failure at top of unexposed panel. Flange of top channel buckled due to thermal expansion, pushing unexposed panel away from stud and allowing the passage of hot gases
53.00	Test terminated
	It is obvious that the degree of deformation of the assembly is much less than that of the more severe fire. The frame tended to deflect less due to the much slower heating and more uniform elongation of the studs. After test the fallen gypsum can be seen to have broken down into much finer particles than that of the more severe test.

Time	Observations (FP2881)
1:00	Paper on exposed face beginning to burn, paper discolours
1:30	Peeling of paper
2:00	Paper falling off
4:15	All paper has burnt off exposing plaster
6:30	Very thin small (5 mm in dia) peelings of plaster begin to peel off face "ablate" and fall to the floor of furnace.
8:00	Slight deflection of wall assembly into furnace, vermiculite in board is quite prominent.
9:20	Surface still ablating but more vigorously.
11:00	Furnace beginning to fill with smoke
16:00	Wall has bow (deflected) quite severely towards furnace
20:00	Somewhere between 20-23 minutes the exposed panel fell off exposing internal studs, significant pulsing of unexposed face can be noticed
26:00	Paper on ambient side of unexposed panel is beginning to discolour in cavity region between studs.
27:00	Significant heat is concentrated in region between studs, paper beginning to burn on ambient side of unexposed face
28:00	Flame has burnt through the mid-section of the unexposed panel, integrity failure has occurred, flaming begins to extend from most of the cavity between the studs.
29:30	Test terminated.
	Due to the rapid temperature rise physical and chemical changes within the lining are occurring rapidly, compared to FP2882 the lining degraded very quickly, due to mass movement and near explosive physical forces of air and water escaping the lining causing the lining to degrade quickly. Steel sections were buckled significantly due to the much faster temperature rise. Exposed lining was lost quite quickly.

Time	Observations (FP2882)
2:00	Paper on exposed face beginning to discolour
5:00	Paper burnt off exposed face at top section of panel
8:00	All paper is burnt off and gypsum core is exposed to furnace
18:00	Ablation and crazing of surface, vermiculite is clearly identifiable
	Exposed panel remains unchanged for the remainder of the test
1:00:00	Bowing in towards furnace , pulsing of unexposed panel.
1:22:00	Insulation failure of ambient side of unexposed panel, from average of thermocouples in between studs on unexposed face. In conjunction with discolouring of unexposed face
1:25:00	Decay stage of fire curve is initiated
1:35:00	Discolouring of plaster and paper around screws of unexposed face
1:50:00	Unexposed panel opened up on joint line allowing escape of heat, no flames extend from opening due to exposed panel still remaining in place.
2:05:00	Test terminated, integrity failure not reached
	Due to the slow temperature rise, the physical and chemical changes within the board were occurring much slower, once the paper of the exposed panel was burnt off exposing the gypsum core ablation of the surface began, however loss of material ceased and the gypsum continued to lose its moisture but remain in one piece. It formed a blanket which prevented the internal components of the assembly from being exposed to the full furnace temperatures. There was very little distortion to the studs and channels, with no buckling of the studs and a small amount of deflection remained in the studs.

Time	Observations (FP2922)
2:00	Paper on exposed face beginning to burn, paper discolours
3:00	Thin layer of paper begins to peel and fall to bottom of furnace
5:00	Small narrow horizontal cracking (crazing) is observed on the fire exposed face
7:30	Horizontal cracking beginning to widen (0.2mm)
9:00	Horizontal cracking is widening (0.5mm) especially in region around cavity concentrated near joint in lining.
13:00	Horizontal cracking approximately 0.8mm – lost plaster over joint, slight bowing of specimen into furnace.
15:30	Cracking opened to about 1 mm
18:30	Large cracking approximately 5 mm with vertical cracking linking horizontal cracks
20:00	Sections of plaster beginning to "curl" in towards furnace, large horizontal crack at mid height of system allowing passage of gas approximately 8-10 mm.
22:00	Large cracking interlinking forming sections of plaster, frame deflected into furnace, deflection is not as prominent as the fast fire.
25:00	Vertical joint has opened up considerably
26:00	Sections of lining falling into furnace
28:00	Deflection of furnace begins to reduce as studs are heated uniformly.
31:00	Large area of frame and cavity is exposed directly to the furnace, large sections of board falling into furnace.
35:00	Discolour of unexposed face indicating burning through, buckling of top channel has caused unexposed lining to be pushed out.
38:00	Test terminated. Flames extended from top of board and through central cavity.

FIRE ENGINEERING RESEARCH REPORTS

95/1	Full Residential Scale Backdraft	I B Bolliger
95/2	A Study of Full Scale Room Fire Experiments	P A Enright
95/3	Design of Load-bearing Light Steel Frame Walls for Fire Resistance	J T Gerlich
95/4	Full Scale Limited Ventilation Fire Experiments	D J Millar
95/5	An Analysis of Domestic Sprinkler Systems for Use in New Zealand	F Rahmanian
96/1	The Influence of Non-Uniform Electric Fields on Combustion Processes	M A Belsham
96/2	Mixing in Fire Induced Doorway Flows	J M Clements
96/3	Fire Design of Single Storey Industrial Buildings	B W Cosgrove
96/4	Modelling Smoke Flow Using Computational Fluid Dynamics	T N Kardos
96/5	Under-Ventilated Compartment Fires - A Precursor to Smoke Explosions	A R Parkes
96/6	An Investigation of the Effects of Sprinklers on Compartment Fires	M W Radford
97/1	Sprinkler Trade Off Clauses in the Approved Documents	G J Barnes
97/2	Risk Ranking of Buildings for Life Safety	J W Boyes
97/3	Improving the Waking Effectiveness of Fire Alarms in Residential Areas	T Grace
97/4	Study of Evacuation Movement through Different Building Components	P Holmberg
97/5	Domestic Fire Hazard in New Zealand	KDJ Irwin
97/6	An Appraisal of Existing Room-Corner Fire Models	D C Robertson
97/7	Fire Resistance of Light Timber Framed Walls and Floors	G C Thomas
97/8	Uncertainty Analysis of Zone Fire Models	A M Walker
97/9	New Zealand Building Regulations Five Years Later	T M Pastore
98/1	The Impact of Post-Earthquake Fire on the Built Urban Environment	R Botting
98/2	Full Scale Testing of Fire Suppression Agents on Unshielded Fires	M J Dunn
98/3	Full Scale Testing of Fire Suppression Agents on Shielded Fires	N Gravestock
98/4	Predicting Ignition Time Under Transient Heat Flux Using Results from Constant Flux Experiments	A Henderson
98/5	Comparison Studies of Zone and CFD Fire Simulations	A Lovatt
98/6	Bench Scale Testing of Light Timber Frame Walls	P Olsson
98/7	Exploratory Salt Water Experiments of Balcony Spill Plume Using Laser Induced Fluorescence Technique	E Y Yii
99/1	Fire Safety and Security in Schools	R A Carter

99/2	A Review of the Building Separation Requirements of the New Zealand Building Code Acceptable Solutions	J M Clarke
99/3	Effect of Safety Factors in Timed Human Egress Simulations	K M Crawford
99/4	Fire Response of HVAC Systems in Multistorey Buildings: An Examination of the NZBC Acceptable Solutions	M Dixon
99/5	The Effectiveness of the Domestic Smoke Alarm Signal	C Duncan
99/6	Post-flashover Design Fires	R Feasey
99/7	An Analysis of Furniture Heat Release Rates by the Nordtest	J Firestone
99/8	Design for Escape from Fire	I J Garrett
99/9	Class A Foam Water Sprinkler Systems	D B Hipkins
99/10	Review of the New Zealand Standard for Concrete Structures (NZS 3101) for High Strength and Lightweight Concrete Exposed to Fire	M J Inwood
99/12	An Analytical Model for Vertical Flame Spread on Solids: An Initial Investigation	G A North
99/13	Should Bedroom Doors be Open or Closed While People are Sleeping? - A Probabilistic Risk Assessment	D L Palmer
99/14	Peoples Awareness of Fire	S J Rusbridge
99/15	Smoke Explosions	B J Sutherland
99/16	Reliability of Structural Fire Design	JKS Wong
99/17	Heat Release from New Zealand Upholstered Furniture	T Enright
00/1	Fire Spread on Exterior Walls	FNP Bong
00/2	Fire Resistance of Lightweight Framed Construction	PCR Collier
00/3	Fire Fighting Water: A Review of Fire Fighting Water Requirements (A New Zealand Perspective)	S Davis
00/4	The Combustion Behaviour of Upholstered Furniture Materials in New Zealand	H Denize
00/5	Full-Scale Compartment Fire Experiments on Upholstered Furniture	N Girgis
00/6	Fire Rated Seismic Joints	M James
00/7	Fire Design of Steel Members	K R Lewis
00/8	Stability of Precast Concrete Tilt Panels in Fire	L Lim
00/9	Heat Transfer Program for the Design of Structures Exposed to Fire	J Mason
00/10	An Analysis of Pre-Flashover Fire Experiments with Field Modelling Comparisons	C Nielsen
00/11	Fire Engineering Design Problems at Building Consent Stage	P Teo
00/12	A Comparison of Data Reduction Techniques for Zone Model Validation	S Weaver
00/13	Effect of Surface Area and Thickness on Fire Loads	H W Yii
00/14	Home Fire Safety Strategies	P Byrne
00/15	Accounting for Sprinkler Effectiveness in Performance Based Design of Steel Buildings in Fire	M Feeney

00/16	**A Guideline for the Fire Design of Shopping Centres**	**J M McMillan**
01/1	**Flamability of Upholstered Furniture Using the Cone Calorimeter**	**A Coles**
01/2	**Radiant Ignition of New Zealand Upholstered Furniture Composites**	**F Chen**
01/3	**Statistical Analysis of Hospitality Industry Fire Experience**	**T Y A Chen**
01/4	**Performance of Gypsum Plasterboard Assemblies Exposed to Real Building Fires**	**B H Jones**
01/5	**Ignition Properties of New Zealand Timber**	**C K Ngu**
01/6	**Effect of Support Conditions on Steel Beams Exposed of Fire**	**J Seputro**
01/7	**Validation of an Evacuation Model Currently Under Development**	**A Teo**
01/8	**2-D Analysis of Composite Steel - Concrete Beams in Fire**	**R Welsh**
01/9	**Contribution of Upholstered Furniture to Residential Fire Fatalities in New Zealand**	**C R Wong**
01/10	**The Fire Safety Design of Apartment Buildings**	**S Wu**

School of Engineering
University of Canterbury
Private Bag 4800, Christchurch, New Zealand

Phone 643 364-2250
Fax 643 364-2758